IDENTIFICATION OF THE ROLE OF A NOVEL CELL ADHESION MOLECULE, UNZIPPED, IN MEDIATING NEURON-GLIA INTERACTIONS IN DROSOPHILA

by

Selen Zülbahar

B.S., Molecular Biology and Genetics, Middle East Technical University, 2010

Submitted to the Institute for Graduate Studies in

Science and Engineering in partial fulfillment of

the requirements for the degree of

Master of Science

Graduate Program in Molecular Biology and Genetics

Boğaziçi University

IDENTIFICATION OF THE ROLE OF A NOVEL CELL ADHESION MOLECULE, UNZIPPED, IN MEDIATING NEURON-GLIA INTERACTIONS IN DROSOPHILA

APPROVED BY:

Assoc. Prof. Arzu Çelik …….
(Thesis Supervisor)

Prof. Thomas Hummel …….

Prof. Kuyaş Buğra ……..

DATE OF APPROVAL: 04.10.2012

To my family…

ACKNOWLEDGEMENTS

First of all, I would like to send my special thanks to my thesis supervisor Assoc. Prof. Arzu Çelik, for her great supervision, guidance and encouragement. I'm also grateful to her for her trust in me. Her continuous support in bad and good times let me keep my motivation.

I wish to express my sincere thanks to Prof. Thomas Hummel for hosting me in his lab to conduct many of these experiments there. I'm grateful to him for his support, excellent guidance and creative discussions during this project. It is his encouragement and valuable suggestions that gave me the motivation to continue my scientific research.

I would like to thank also Prof. Dietmar Schmucker for giving me the chance to prepare my constructs in his lab. And I thank Prof. Kuyaş Buğra for spending her valuable time on evaluating this thesis.

My very specific thanks go to *Leo*, who was always there for me, making the distances shorter. And for many many other things that cannot be listed here... His encouragement and constant support, together with his endless patience, I was able to overcome many difficulties.

The huge thanks go to the fly lab members. Especially Bahar Şahin, for being much more than a lab-mate, for being a sister to me… and Çağrı Çevrim…and Ece Terzioğlu Kara… I would like to thank also Duygu Koldere, Gamze Akgün, Xalid Bayramlı, Mustafa Talay, Sercan Sayın and Güner Kaçmaz.

I would like to send a huge bunch of thanks to my dear friends for making my time amazing during my masters: Alperen, Yıldız, Özden, Kaya, Kerem, Merve K., Burçak, Ulduz… and Rashmit. I'll miss you guys!

And last but not least, I would like to thank my family for the unconditional love and support throughout my life. Without them, nothing would be possible.

Finally, I am very grateful to TUBITAK-BIDEB for the financial support throughout my undergraduate and master studies.

This project was supported by funds provided by EMBO Project No. 1656 and Bogazici University Research Fund Project No. BAP6644 and TÜBİTAK Project 111T446.

ABSTRACT

IDENTIFICATION OF THE ROLE OF A NOVEL CELL ADHESION MOLECULE, UNZIPPED, IN MEDIATING NEURON-GLIA INTERACTIONS IN DROSOPHILA

The intricate but still precise pattern of brain circuitry is unquestionably the most complex feature of both vertebrates and invertebrates. How that complex circuitry develops has been the subject of intense study for over a century. Neurons, being the excitable residents of the nervous system, are guided to their destinations in a tightly regulated manner, in order to conduct the sensory inputs to the correct targets. Growth cones of the neurons experience many different trans-cellular cues in their journey to their final target, which can be attractive or repellent. Glial cells constitute one class of cells that promote axonal outgrowth, either through cell-cell adhesion or by secreting diffusible signals. Olfactory system of *Drosophila* represents an ideal system for the study of axonal guidance. There are about 1500 olfactory receptor neurons (ORNs), which are subdivided into 50 classes according to the olfactory receptor they express. Olfactory receptor neurons, expressing the same olfactory receptor converge into the same synaptic subunit on brain, which are called glomeruli. There are many mechanisms identified in the formation of this accurate pattern of olfactory system, but still many steps remain unknown. Towards this end, the recently identified cell adhesion molecule *Unzipped* was found to be expressed by a subset of ORNs and glia in the *Drosophila* olfactory system. Results of this study implicate that, Unzipped is necessary for midline crossing of all olfactory receptor neurons, and also for proper targeting of some ORNs to the brain. Therefore, it is claimed that Unzipped is an important factor in mediating neuron-glia interaction in the olfactory system of *Drosophila*.

ÖZET

YENİ HÜCRE ADHEZYON MOLEKÜLÜ UNZIPPED'İN *DROSOPHILA*'DA NÖRON GLİA ETKİLEŞİMLERİNDEKİ ARACILIK ROLÜNÜN BELİRLENMESİ

Beynin devre sistemi girift fakat kesin yapısıyla omurgalı ve omurgasızların şüphesiz ki en karmaşık özelliğidir. Bu karmaşık devre sisteminin nasıl geliştiği yüzyıllardan beridir yoğun bir araştırma konusu olmuştur. Nöronlar, sinir sisteminin uyarılabilen üyeleri olmaları itibariyle, duysal girdileri doğru hedeflere aktarmak amacıyla, hedeflerine sıkı düzenlenmiş bir yolla yönlendirilmektedir. Nöronların büyüme konileri nihai hedeflerine yolculukta çekici veya itici çok farklı transselüler işaretlere maruz kalmaktadır. Glia hücreleri hücre-hücre yapışması ya da yayılır sinyallerin salgılanması ile aksonal büyümeyi teşvik eden bir hücre sınıfıdır. *Drosophila* koku alma sistemi aksonal rehberlik çalışmak için ideal bir sistemi temsil etmektedir. İfade ettikleri koku reseptörüne göre 50 sınıfa ayrılan yaklaşık 1500 koku reseptör nöronu (KRN) vardır. Aynı koku reseptörünü ifade eden koku reseptör nöronları beyinde glomeruli olarak adlandırılan aynı sinaptik altbirimde birleşmektedir. Koku alma sisteminin bu kesin yapısının oluşumunda birçok mekanizma belirlenmiştir fakat birçok aşama hala bilinmemektedir. Bu amaçla, yeni tanımlanmış hücre yapışma molekülü Unzipped'in *Drosophila* koku alma sisteminde KRN ve gliaların bir alt kümesinde ifade edildiği bulunmuştur. Bu çalışmanın sonuçları Unzipped'in tüm koku reseptörü nöronlarının ortahat geçişi ve bazı KRNlerin beyine düzgün yönlendirilmesi için gerekli olduğunu önermektedir. Bu sebeple, Unzipped'in *Drosophila* koku alma sisteminde nöron-glia etkileşiminde önemli bir faktör olduğu iddia edilmektedir.

TABLE OF CONTENTS

ACKNOWLEDGEMENTS iv
ABSTRACT v
ÖZET vi
LIST OF FIGURES xi
LIST OF TABLES. xvi
LIST OF ACRONYMS/ ABBREVIATIONS. xvii
1. INTRODUCTION. 1
1.1. Neuron-Glia Interactions 1
1.1.1. Roles of Glia in the Nervous System. 1
1.1.2. Glial Cells in *Drosophila* vs. Vertebrates. 2
1.1.3. Roles of Glia in Axon Guidance. 3
1.2. The Olfactory System as a Model for Studying Neuron-Glia Interactions. 6
1.2.1. The Olfactory System of *Drosophila*. 6
1.2.2. Development of the *Drosophila* Olfactory System. 8
1.2.3. The Mechanisms of ORN Targeting. 9
1.2.4. Role of Glial Cell in the Olfactory System. 10
1.3. The Novel Cell Adhesion Molecule, Unzipped 12
1.4. The Gal4/ UAS Binary System. 13
1.5. BAC Transgenesis. 15
2. PURPOSE 19
3. MATERIALS AND METHODS. 20
3.1. Biological Material. 20
3.2. Chemicals and Supplies 22
3.2.1. Enzymes. 22
3.2.2. Chemical Supplies. 22
3.2.3. Solutions and Buffers 22
3.2.4. Oligonucleotide Primers 25
3.2.5. Antibodies 27
3.2.6. Embedding Media 28
3.2.7. Disposable Labware 28
3.2.8. Equipment 29

3.3. Molecular Biological Techniques. 30
3.3.1. Isolation of DNA. 30
3.3.1.1. Copy Number Induction of P[acman] Plasmids. 30
3.3.1.2. Isolation of P[acman] Plasmid DNA. 30
3.3.2. Transformation of P[acman] Plasmids into SW105 Cells. 31
3.3.3. Gradient PCR 31
3.3.4. Conventional PCR 32
3.3.5. DpnI Digestion. 32
3.3.6. PCR Purification. 33
3.3.7. Agarose Gel Electrophoresis. 33
3.3.8. Gel Extraction of DNA. 33
3.3.9. Sequencing Analysis. 33
3.3.10. BAC Recombination. 34
3.3.11. Colony PCR 34
3.4. Biochemical Methods. 35
3.4.1. Protein Extraction. 35
3.4.2. SDS-PAGE. 35
3.4.3. Western Blot. 35
3.5. Histological Methods. 36
3.5.1. Preparation of Drosophila Tissues for Immunohistochemistry. 36
3.5.1.1. Preparation of adult brains. 36
3.5.1.2. Preparation of pupal brains and eye disc. 36
3.5.1.3. Preparation of larval brains and eye imaginal disc. 36
3.5.2. Immunohistochemistry. 36
3.5.2.1. Antibody staining of adult brain. 37
3.5.2.2. Antibody staining of pupal eye disc and brain. 37
3.5.2.3. Antibody staining of larval eye imaginal discs. 37
3.5.2.4. Antibody staining of Flag::HA::Uzip transgenic flies. . . . 37
3.6. Experiments for Expression Analysis. 38

3.6.1. Expression Analysis of Unzipped Enhancer Trap Line (AC783-*Gal4*). 38

3.6.2. Expression Analysis of Flag and HA Tagged Unzipped Transgenic Lines. 39
3.7. Experiments for Functional Analysis. 40
3.7.1. Loss of Function Experiments: Unzipped Deficiency. 40
3.7.2. Loss of Function Experiments: RNA Interference. 42
3.7.3. Loss of Function Experiments: Clonal Analysis. 43
3.7.3.1. Generation of Uzip Deficiency Lines Recombined to an FRT site. 44
3.7.3.2. Generation of Mitotic clones. 46
3.7.4. Gain of Function Experiments: Misexpression. 46
3.7.5. Gain of Function Experiments: Tissue Specific Rescue. 47
3.7.6. Gain of Function Experiments: Nonspecific Rescue. 47
4. RESULTS. 49
4.1. Expression of Uzip Determined by an Enhancer Trap Insertion. 49
4.1.1. *Uzip* is Expressed in the Eye Imaginal Disc in the 3rd Instar Larval Stage. 49
4.1.2. *Uzip* is Expressed in the Visual and Olfactory Systems During Pupal Development. 51
4.1.3. *Uzip* Expression in the Adult Stage 54
4.2. Generation of Uzip Transgenic Lines tagged with Flag HA and eGFP. . . . 57
4.2.1. Generation of Flag::HA tagged *Uzip* Transgenic Construct. 58
4.2.2. Generation of Flag::HA::GFP tagged *Uzip* Transgenic Construct. . 60
4.2.3. Analysis of the Flag::HA::Uzip Transgenic Construct. 61
4.3. Functional Analysis of *Uzip* in the *Drosophila* Olfactory System. 64
4.3.1. Experiments for the Analysis of *Uzip* Expression in the Olfactory System. 64
4.3.2. Identification of the Antennal ORN Subtype Expressing Uzip. . . . 69
4.3.3. Loss of Function Experiments: Mutant Analysis. 71
4.3.4. Loss of Function Experiments: RNA Interference. 74
4.3.5. Loss of Function Experiments: Clonal Analysis. 76
4.3.6. Gain of Function Experiments: Misexpression. 78
4.3.7. Gain of Function Experiments: Rescue. 78
5. DISCUSSION 80

5.1. Uzip is an R8-Specific Protein in the *Drosophila* Visual System 81
5.2. Uzip is Expressed in the *Drosophila* Olfactory System During Development 83
5.3. Problems with Finding the Uzip Expressing Antennal ORN Class 85
5.4. Uzip is Necessary for Midline Crossing of ORNs 86
5.5. Problems with the Knock-Down Experiments 88
5.6. Misexpression of Uzip in Glial Cells does not Result in any Defect 89
5.7. Cell-Specific Rescue of Uzip may Unravel its Role 89
5.8. Uzip is not necessary in ORNs to cross the midline 89
5.9. Problems with the tagged Uzip Transgene 90
5.10. Which Subsets of Glial Cells Express Uzip? 91
REFERENCES 94

LIST OF FIGURES

Figure 1.1. Model of growth cone guidance to reach the final targets. …… 4

Figure 1.2. Representation of glial migration into the eye imaginal disc. ……..…. 5

Figure 1.3. Schematic representation of the structural organization of olfactory organs and olfactory processing centers. ..……..…. 7

Figure 1.4. Projection of ORNs to the antennal lobe. …..…….. 8

Figure 1.5. Developmental chart of *Drosophila* olfactory receptor neurons. ……... 9

Figure 1.6. Representation of the structure of Uzip protein. ..……... 13

Figure 1.7. Schematic representation of the principle of the Gal4 / UAS binary system. ..……. 15

Figure 1.8. Schematic representation of the phiC31-mediated transgenesis of transgenic constructs into the fly genome. ...……..... 17

Figure 1.9. Overview of the P[acman] transgenesis method. ….…….. 18

Figure 3.1. Set up of crosses for the analysis of *Uzip* expression pattern. ..…….. 39

Figure 3.2. Crosses for the generation of *Uzip* deficient flies on which single classes of ORN's are labeled with membrane-localized GFP reporter. …… 41

Figure 3.3. Crosses for the analysis of the projection of single class ORNs in *Uzip* hypomorphs. …… 42

Figure 3.4. Crosses for down-regulation of *Uzip* protein levels specifically in Glia. 42

Figure 3.5. Crosses for down-regulation of *Uzip* protein levels specifically in neurons. …… 43

Figure 3.6. Crosses for the generation of UzipD43 allele recombined to FRT42 site. …… 45

Figure 3.7. Crosses for the generation of MARCM clones of ORNs homozygote for *Uzip* deficiency (UzipD43). …… 46

Figure 3.8. Crosses for misexpression of *Uzip* protein specifically in glia. ..……. 47

Figure 3.9. Crosses for the glial-rescue of *Uzip* in the background of *Uzip* mutation. …… 47

Figure 3.10. Crosses for the non-specific rescue of Uzip in the background of *Uzip* mutation. ……..... 48

Figure 4.1. *Uzip* expression in the eye imaginal disc of third instar larva. …..…… 50

Figure 4.2. *Uzip* expression in the pupal retina of *Drosophila*. ….…….. 52

Figure 4.3. Expression of *Uzip* during the late pupal stage. …….. 53

Figure 4.4. *Uzip* expression co-labeled with the glial cell marker repo. ...……..... 53

Figure 4.5. *Uzip* is expressed by a subset of glial cells in the adult brain. …..…….. 55

Figure 4.6. *Uzip* expression labeled by membrane-localized GFP in the adult brain. 56

Figure 4.7. *Uzip* expression visualization by pre-synaptic GFP in the adult brain. 56

Figure 4.8. Map of the P[acman] plasmid. ….…….. 58

Figure 4.9. Scheme of the preparation of recombination fragment for the generation of Flag;;HA tagged Uzip construct. ….……..... 59

Figure 4.10. Gel photos of the Flag::HA tagged *Uzip* construct. …… 59

Figure 4.11. Scheme of the preparation of recombination fragment for the generation of Flag-HA-GFP tagged *Uzip* construct. …… 60

Figure 4.12. Gel photos of Flag-HA-GFP tagged *Uzip* construct. ……. 61

Figure 4.13. Western blot of Flag-HA-Uzip constructs. ...……. 62

Figure 4.14. Expression analysis of Flag-HA tagged Uzip constructs using antibody against the HA polypeptide. …… 63

Figure 4.15. *Uzip* expression in the mid-pupal antennal lobes. ……..…… 65

Figure 4.16. Uzip is expressed in the antenna at ~50h of pupal development. ……..… 66

Figure 4.17. Differential labeling of *Uzip* expression in ORNs and glia using flip-out technique. …….. 67

Figure 4.18. Uzip expression in the adult antenna and maxillary palp. ……..…… 67

Figure 4.19. Uzip expression in the maxillary palp co-localizes with some of the ORNs. ……..…….. 68

Figure 4.20. Determination of the position of Uzip expressing ORN glomeruli. …….. 69

Figure 4.21. Comparison of *Uzip* expression to OR19a expression in the brain and the antenna. ……..…… 70

Figure 4.22. Comparison of *Uzip* expression to OR56a expression in the brain and the antenna. ……...…… 71

Figure 4.23. Projection of antennal ORNs to the antennal lobe in Uzip mutant background. …….. 72

Figure 4.24. Projection of maxillary palp ORNs to the antennal lobe in the background of Uzip loss-of-function. …….…….... 73

Figure 4.25. Projection of ORNs to the antennal lobe in Uzip hypomorphs. ……... 74

Figure 4.26. Downregulation of Uzip protein levels specifically in neurons. ……... 75

Figure 4.27. Downregulation of *Uzip* protein levels specifically in glia. ……... 76

Figure 4.28. MARCM clones of *Uzip* loss of function allele UzipD43. ……... 77

Figure 4.29. Misexpression of *Uzip* in glia does not have an effect on the projection of ORNs. ……..……. 78

Figure 4.30. Rescue of Uzip loss-of-function phenotype by transgenic Flag-HA Uzip allele. …..……... 79

Figure 5.1. Projection of photoreceptor cells to their respective layers in the optic lobe. ……..…… 81

Figure 5.2. Co-expression of Uzip with the glial cell marker repo in the eye imaginal disc. ……..…… 81

Figure 5.3. Molecular organization of the *Drosophila* olfactory system. ……. 85

Figure 5.4. Proposed model of the mechanism of Uzip function. …..…… 87

LIST OF TABLES

Table 1.1. Comparison of vertebrate and Drosophila glial subtypes. ……..... 3

Table 3.1. Drosophila melanogaster lines used in the course of study. ……..... 20

Table 3.2. Suppliers of the chemicals used in the course of study. ……. 22

Table 3.3. Solutions and Buffers. ….…….. 22

Table 3.4. Primers used in the course of the study. ….……... 25

Table 3.5. Antibodies used in the course of the study. ……..……. 27

Table 3.6. Suppliers of the disposable labware used in the course of study. …….. 28

Table 3.7. Suppliers of the laboratory equipment used in the course of study. …… 29

LIST OF ACRONYMS/ABBREVIATIONS

AL	Antennal lobe
APF	After Puparium Formation
BAC	Bacterial Artificial Chromosome
bp	Base Pairs
cDNA	Complementary DNA
CNS	Central Nervous System
DNA	Deoxyribonucleic Acid
Dscam	Down Syndrome Cell Adhesion Molecule
Flp	Flippase enzyme
FRT	Flip Recombinase Targets
GFP	Green Fluorescent Protein
HRP	Horse Radish Peroxidase
IR	Ionotropic Receptor
LH	Lateral Horn
LN	Local Interneuron
MARCM	Mosaic Analysis with a Repressible Cell Marker
MB	Mushroom Body
NDS	Normal Donkey Serum
NGS	Normal Goat Serum
OR	Olfactory Receptor
ORN	Olfactory Receptor Neuron
PBS	Phosphate Buffered Saline
PCR	Polymerase Chain Reaction
PFA	Paraformaldehyde
pH	Power of Hydrogen
PN	Projection Neuron
PR	Photoreceptor
RFP	Red Fluorescent Protein
RNA	Ribonucleic Acid
RNAi	RNA Interference
RT-PCR	Real Time PCR
UAS	Upstream Activating Sequence
Uzip	Unzipped protein

1. INTRODUCTION

The nervous system is composed of two broad categories of cell types: neurons and glia. In comparison to their excitable neighbors, the neurons, glial cells have not been studied very well. In contrast to the common opinion, glia outnumber neurons in the brain. About 90% of our brain is composed of glial cells, which have been long thought to be only simple supporting cells. However, work done over the last two decades uncovered many striking features of glia.

1.1. Neuron-Glia Interactions

1.1.1. Roles of Glia in the Nervous System

From ancient knowledge of the cellular basis of the nervous system, neurons are the main cells in the nervous system. Their ability to transfer and process information, since they extend towards the sensory organs, muscles and glands, and their electrically excitable identity make them key players of nervous system function. On the other hand, glial cells were long considered to have only a simple supportive role, since they lack long processes connecting sensory organs to the effector organs.

With the recent developments of the methods for studying glial function, the role of glia has been better understood and intimate functional connections between glia and neurons were partially resolved. However, because of the lack of molecular markers marking all glial subtypes and the inability to attack or manipulate glia, many questions remain to be answered.

Glial cells have diverse roles in nervous system function, varying from neuronal survival to synapse formation. Astrocytes for example, being the most common cell type in the vertebrate nervous system, can promote synaptogenesis in the CNS (Song *et al*., 2002). A number of *in vitro* studies also showed that Schwann cells, which are the ensheating cells of PNS neurons, take role in synaptogenesis (Ullian *et al*., 2004; Peng *et al*., 2003, Reddy *et al*., 2003). In addition to participating in important regulatory events at the synapse, glial cells also affect the electrical properties of neurons. Oligodendrocytes, being a subtype of

glial cells, up-regulate the electrical conduction of axons by forming myelin sheath. Neuronal survival is also linked to glial function, since many studies have shown that neurons eventually die when the signalling from glia is blocked (Bao *et al*., 2002; Jessen and Mirsky, 2002). Glial cells also have a role in the regulation of neuronal excitability by the uptake of K^+ ions when these accumulate in the extracellular environment (Walz *et al*., 2002). In addition, microglia are the resident immune cells of the CNS (Peters *et al*., 1991). Besides all these regulatory roles of many aspects in neuronal conduction, glia are also known as the regulators of growth cone guidance and proper establishment of neuronal circuitry, which will be discussed in detail in Section 1.2.3.

1.1.2. Glial Cells in *Drosophila* vs. Vertebrates

In contrast to the vertebrate nervous system that comprises 90% of glia, *Drosophila* has a rather small repertoire of glial cells, accounting only for 10% of the cells in the nervous system. Extensive enhancer-trap screens (Klämbt *et al*., 1991) and glial gene expression studies (Freemann *et al*., 2003) in the past decades have led to the identification and characterization of many diverse molecular subclasses of glia in the *Drosophila* embryonic CNS.

Surprisingly, the morphological diversity of the glial cells in *Drosophila* is enormous. Only in the visual system of the adult *Drosophila*, there are at least seven distinct morphological subtypes of neuropil glia (Kretzschmar *et al*., 2002). Although fewer glial markers are available for the analysis of molecular diversity of mammalian glia, a similar level of diversity is very likely. In the CNS of *Drosophila*, the main subtypes of glial cells are cortex glia, surface glia, peripheral glia and neuropil glia, which show many functional and morphological similarities to their vertebrate counterparts (Table 1.1). Cortex glia also called cell body-associated glia, are very similar to astrocytes. They form a network of processes around the cell bodies of neurons (Pereanu *et al*., 2005). Neuropil glial cells on the other hand, resemble oligodendrocytes and ensheath axonal tracts (Klämbt *et al*., 1991). Finally, periperal nerves are ensheated and supported by the CNS-derived peripheral glia. Like the Schwann cells of vertebrates in the PNS, these CNS-derived peripheral glia ensheath and support peripheral nerves containing motor and sensory axons (Leiserson *et*

al., 2000). Although there is no equivalent of microglia of vertebrates in *Drosophila*, all glia seem competent to perform immune-like functions (Sonnenfeld *et al*., 1995).

Table 1.1. Comparison of vertebrate and *Drosophila* glial subtypes. (adapted from Freeman & Doherty, 2006). Almost all types of vertebrate glia have counterparts in *Drosophila*, making it a good model organism to study glia function.

Vertebrate glial subtype	**Primary Functions**	**Distribution**	**Comparable *Drosophila* glial subtype**
Astrocytes	- trophic support to neurons - modulation of synapses	Embedded in CNS cell cortex, ensheathing synapses, CNS surface	Cortex glia (and a subset of surface glia)
Oligodendrocytes	- neuronal ensheathment - trophic support to neurons - myelination	Ensheathing axons in CNS	Neuropil glia
Microglia	- Immune surveillance - macrophage function	Throughout CNS	Cortex, surface and neuropil glia
Schwann cells	- ensheathment and support of peripheral nerves - myelination	Ensheathing PNS nerves	Peripheral glia

1.1.3. Roles of Glia in Axon Guidance

During the establishment of neural circuits, axons travel long distances before they eventually stop to form synapses. Along their way to the correct target region, axons make numerous pathway choices and these decisions are made in a sterotyped manner with very few errors. Cell-cell interactions with the intermediate targets and the attractive or repellent molecular cues from the environment play an important role for the establishment of the intricate pattern of neuronal wiring (Cook *et al*., 1998; Colamarino *et al*., 1995; Stoeckli *et al*., 1998; Tessier-Lavigne *et al*., 1991). Glia function as intermediate targets in the axonal pathfinding, secreting guidance cues or expressing cellular cues on their surface that guide

axonal outgrowth (Figure 1.1). This functon of glia is conserved between vertebrate and invertebrate nervous systems. There are a number of well-studied examples of neuron-glia interaction in mediating axon guidance.

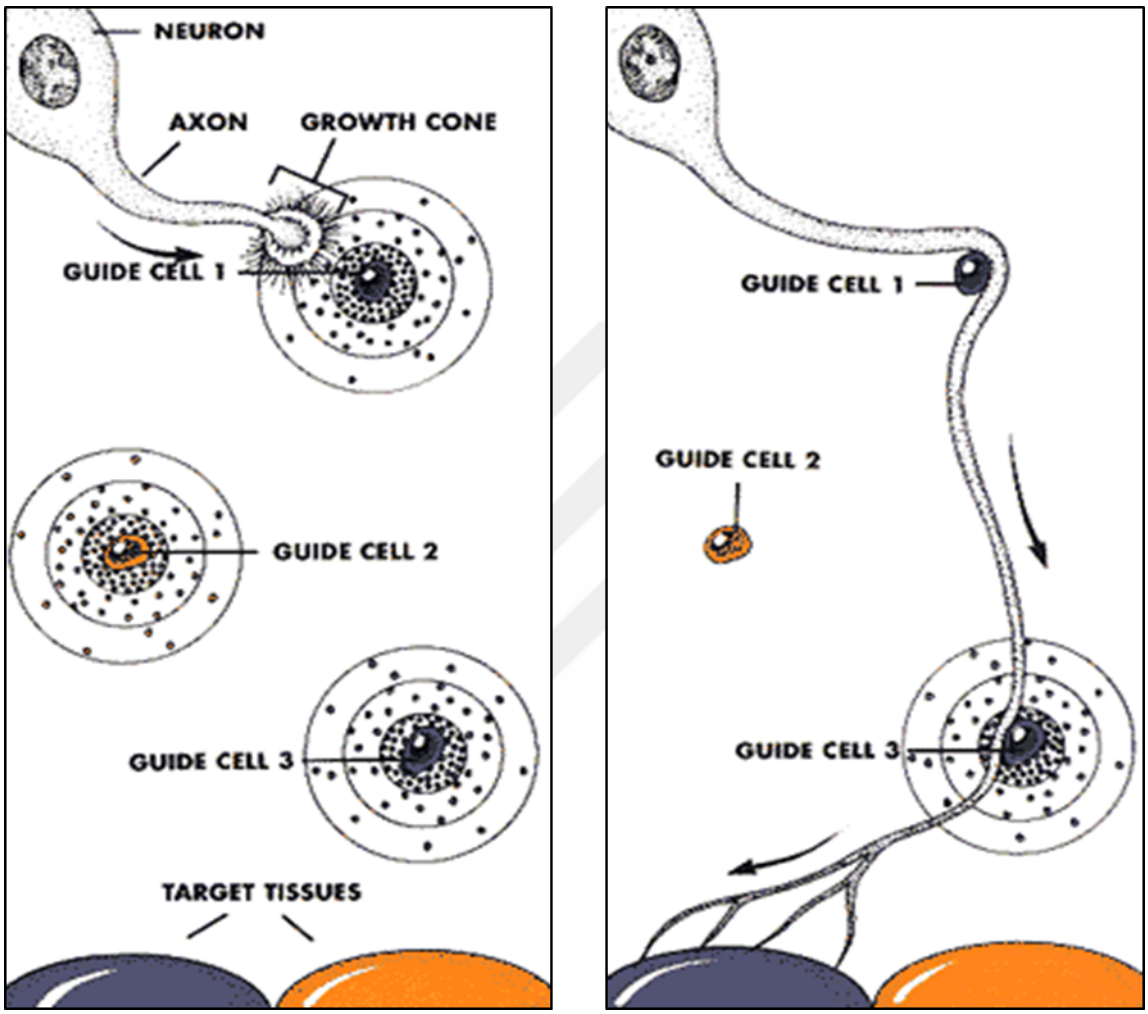

Figure 1.1. Model of growth cone guidance to reach the final targets. Axonal trajectories receive cues from the guide cells that act both positively or negatively to attract or repel the growth cone. Growth cones are guided to the correct targets upon response to the attraction or repulsion from the guide cells (adapted from Barallobre *et al*., 2005).

The *Drosophila* embryonic ventral nerve cord constitutes a good example of glia, function as guidepost cells. While some axons project to the contralateral sites of the ventral nerve cord, some exclusively remain at the ipsilateral site. During this process, the three pairs of midline glia, also called longitudinal glia (LG), and the midline neurons interact with each other for the decision of crossing the midline (Hummel *et al*., 1999).

Another example is the *Drosophila* visual system, where tightly regulated glial development is crucial for axonal pathfinding (Figure 1.2). During larval stages of development, photoreceptor cells (R1-R8) within the eye imaginal disc start to differentiate in a wave of morphogenesis, progressing from posterior to anterior. Developing R-cells project into the optic lobe in the brain passing through the optic stalk. Meanwhile, retinal glial cells originate in the optic stalk and migrate into the eye disc up to an area where youngest R-cells are found. When glial migration into the eye disc is prevented, R-cell axons cannot extend to the optic stalk properly (Rangarajan *et al.*, 1999). Moreover, when the glia enter the eye imaginal disc prematurely, before the onset of R-cell differentiation, growing R-cell axons follow the ectopic glia instead of extending towards the optic stalk (Hummel *et al.*, 2002).

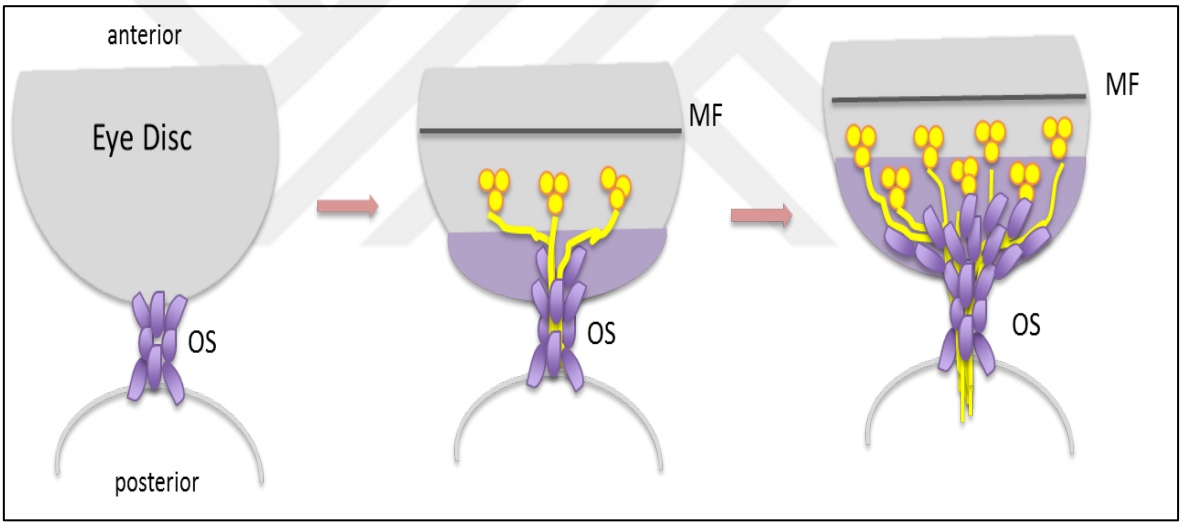

Figure 1.2. Representation of glial migration into the eye imaginal disc. During larval stage, photoreceptor cells differentiate in a wave of morphogenesis, which progresses from posterior to anterior. Differentiated photoreceptor neurons (in yellow) project towards the brain passing through the optic stalk (OS). The retial basal glia (in purple), which are born in the optic stalk migrate opposite to the axons, towards the eye imaginal disc**.**

1.2. The Olfactory System as a Model for Studying Neuron-Glia Interactions

1.2.1. The Olfactory System of *Drosophila*

The Drosophila olfactory system exhibits a high degree of synaptic specificity with a very similar organization to that of vertebrates, but with a less complex pattern. Both peripheral and central nervous systems function in the processing of olfactory stimuli. In *Drosophila*, odors are detected by the olfactory receptor neurons (ORNs) in the peripheral olfactory organs and the information is sent to the CNS, to the synaptic subunits in the brain, called glomeruli (Hildebrand *et al*., 1997).

ORNs are located in two olfactory organs, antenna and maxillary palp. There are about 1200 ORNs located in each antenna and about 120 ORNs in the maxillary palp. These are the homologues to the nasal cavity in the mouse, which contains ~10 million ORNs. These organs are covered with hair-like structures, called sensilla. ORN cell bodies are housed in these organs together with some non-neuronal cells (Shanbhag *et al*., 2000; Hallem and Carlson, 2004). There are three morphologically different classes of sensilla, known as basiconic, trichoid and coeloconic sensilla. The antenna houses all three types of the sensilla whereas maxillary palps contain only the basiconic type (Vosshall *et al*., 1999). Each sensillum houses usually two ORNs although there are some antennal sensilla housing three or four ORNs (Hallem and Carlson, 2004).

ORNs, expressing the same olfactory receptor (OR) gene among ~60 different OR classes, project their axons to the same synaptic subunit on the antennal lobe (Ressler *et al*., 1993; Vassar *et al*., 1993; Laissue *et al*., 1999; Couto *et al*., 2005). The antennal lobe (AL) is a bilateral structure, located centrally in the *Drosophila* brain, and represents the first olfactory processing center. It is the homologue to the olfactory bulb in mice (Mombaerts, 2001). Once ORNs reach the antennal lobe glomeruli, they make synapses with the dendrites of higher order neurons which are local interneurons (LNs) and projection neurons (PNs). Higher order neurons send their axons to the higher olfactory processing centers in the brain, which are mushroom bodies (MB) and the lateral horn (LH) (Hallem and Carlson, 2004) (summarized in Figure 1.3).

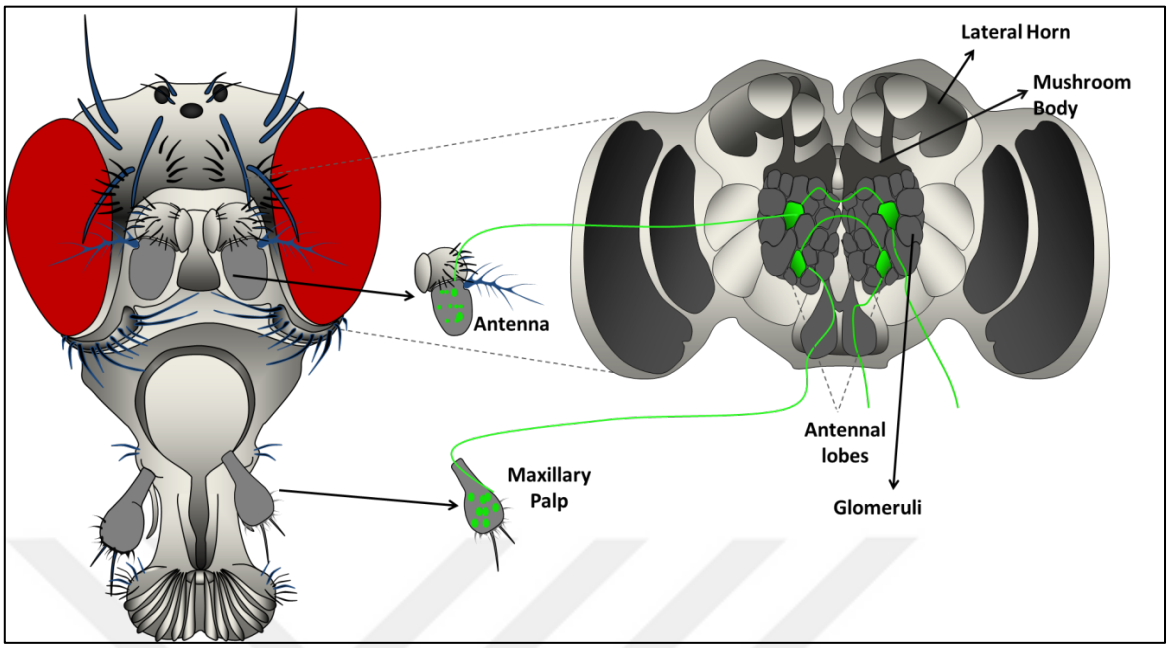

Figure 1.3. Schematic representation of the structural organization of olfactory organs and olfactory processing centers. Antenna and maxillary palp house the ORN cell bodies. ORN axons are sent to the distinct synaptic subunits (glomeruli) on the primary olfactory processing center (antennal lobes) to make synapses with the higher order neurons, which project their axons to the mushroom bodies and the lateral horn.

All ORNs of the antenna project together to the antennal lobe through the antennal nerve. Once they reach the periphery of the antennal lobe, they are sorted out into distinct glomeruli according to the olfactory receptor gene they express. All ORNs expressing the same receptor converge into the same glomeruli. Glomeruli receiving input from different subclasses of ORNs are easily distinguishable by their characteristic size, shape and position in the antennal lobe. Maxillary palp ORNs on the other hand, project to the antennal lobe through the labial nerve, passing across the suboesophageal ganglion (SOG). They are sorted out at the periphery like in the case of antennal ORNs. Once ORNs reach the corresponding glomeruli on the antennal lobe, they extend a branch to the same region on the contralateral side across the commissure. On both sides of the antennal lobe, ORNs make synapses with the higher order neurons within the glomeruli (Stocker *et al*., 1990) (summarized in Figure 1.4). Throughout these processes, many molecular and cellular interactions play a role to direct each ORN to the antennal lobe and then to the correct glomerulus. This property of

the olfactory system constitutes one of the best examples of tightly regulated axonal projection and pathfinding mechanisms in the nervous system.

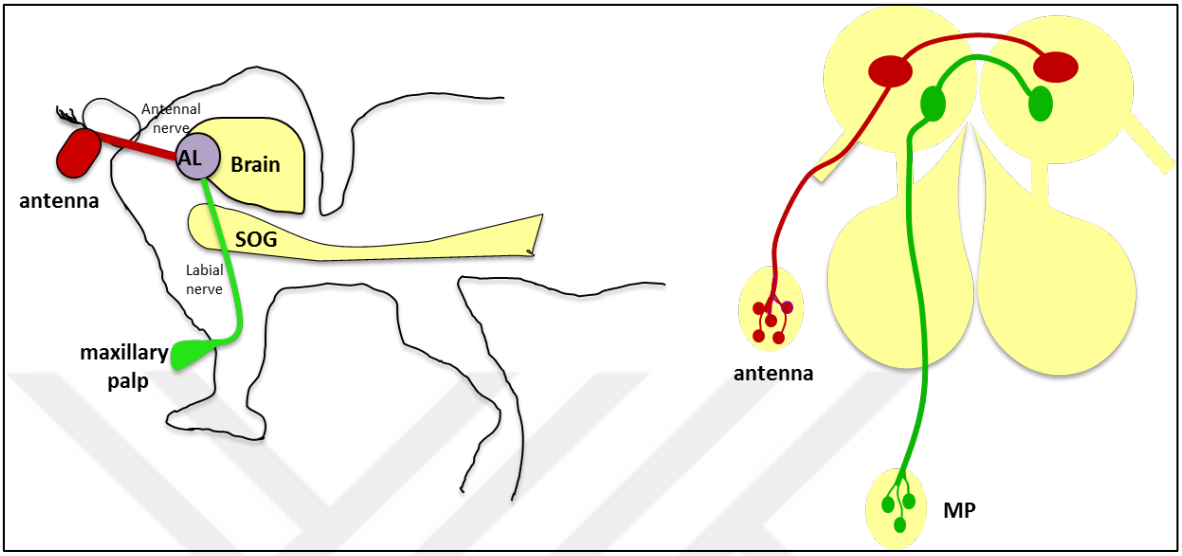

Figure 1.4. Projection of ORNs to the antennal lobe. ORNs of antenna and maxillary palp follow different paths to reach the antennal lobe. Antennal lobe neurons fasciculate into the antennal nerve whereas maxillary palp neurons fasciculate into the labial nerve and have to cross the SOG before reaching the antennal lobe. ORNs also project to the contralateral glomeruli crossing the midline (adapted from Hummel *et al*., 2003)

1.2.2. Development of the *Drosophila* Olfactory System

Development of the *Drosophila* olfactory system takes place mainly during pupal stages. ORNs start to form at 10 h after puparium formation (APF) in the antenna (Ray and Rodrigues, 1995). Developing ORNs form three distinct fascicles in the antenna, and they start to project their axons to the antennal lobe at around 15-20 h APF. Once they reach the respective regions, they form protoglomeruli and also project to the contralateral site across the commissure (Jhaveri *et al*., 2000, Jefferis *et al*., 2004). Axons of the maxillary ORN classes arrive later and reach the AL at about 30 h APF. These early-arriving axons of antennal olfactory ORNs are required for the proper targeting of late-arriving maxillary palp ORN axons. Semaphorin-1a signaling is necessary for this mechanism. It is required for targeting of all maxillary palp, but only half of the antennal ORN classes (Sweeney *et al*., 2007). Once they reach their correct targets, ORNs become responsive to the odorants at

around 50 h APF (Dubin and Harris, 1997). They start to express olfactory receptors. This process starts after the first ORNs reach the antennal lobe, and continues until around 80-90 h APF (Clyne *et al*., 1999). Time course of developmental events in Drosophila olfactory system is summarized in Figure 1.5. It is also important to note that, in contrast to vertebrates, expression of receptors take place very late in *Drosophila*, excluding an intructive role of these genes in the extablishment of synaptic specifity (Jefferis *et al*., 2004).

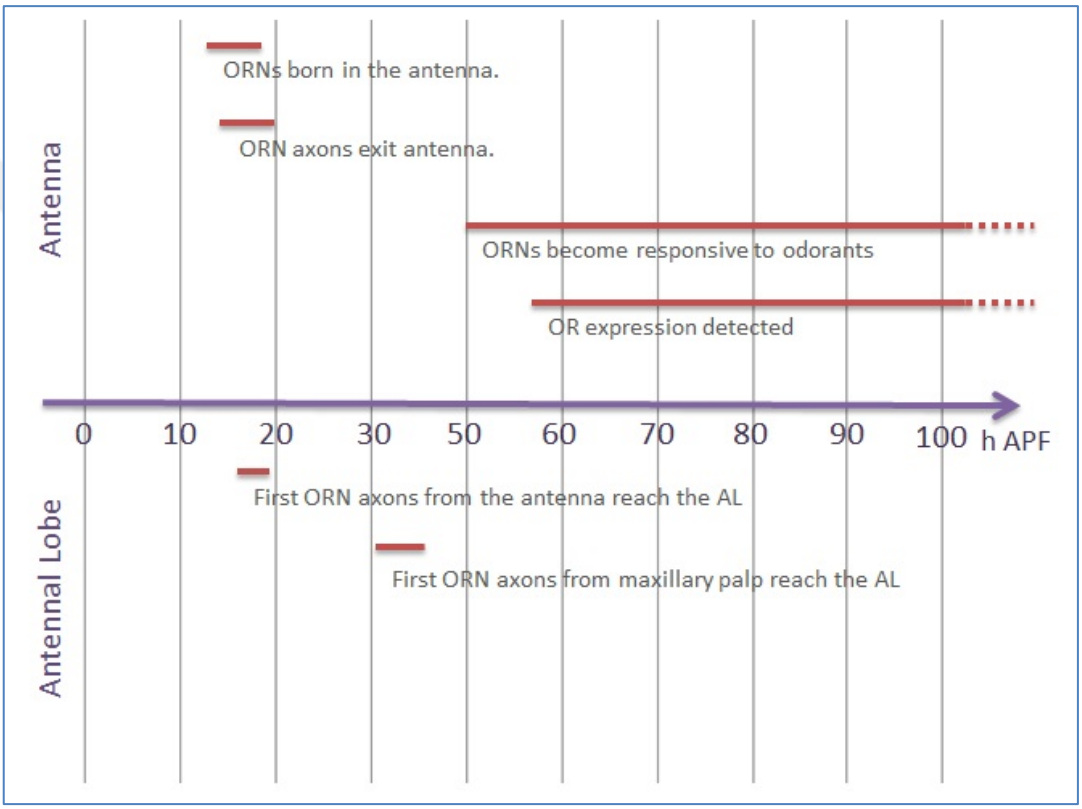

Figure 1.5. Developmental chart of *Drosophila* olfactory receptor neurons. Data are collected from Ray and Rodrigues (1995), Dubin and Harris (1997), Clyne *et al* (1999), Jhaveri *et al*. (2000), Jefferis *et al*. (2004) and Sweeney *et al*. (2007).

1.2.3. The mechanisms of ORN targeting

Unlike the mammalian olfactory system, olfactory receptor expression starts after the convergence of ORNs into distinct glomeruli. This excludes the possibility of a role of OR choice in the pathfinding of ORNs in *Drosophila* (Jefferis *et al*., 2004) as is the case for vertebrates. Several axon guidance molecules have been identified that function through

neuron-neuron or neuron-glia interactions and direct the ingrowing axons to the correct target glomeruli.

One of these molecules is the Down syndrome cell adhesion molecule (Dscam) that functions in the targeting of ORN axons through cell-cell adhesion. ORN axons, deficient for Dscam are not able to find the correct targets and mistarget to ectopic glomeruli (Hummel *et al*., 2003). N-Cadherin (Ncad) is another example of such a cell adhesion molecule, which is required for the formation of protoglomeruli during pupal development. In NCad deficient *Drosophila*, ORNs cannot enter the antennal lobe, but stay at the periphery instead (Hummel and Zipursky, 2004).

Another means of targeting mechanism is observed through neuron-glia interactions, as in the case of the cell signaling molecule Wnt5, and its receptor Derailed (Drl). Wnt5 functions in ORNs to regulate the glomerular organization. Drl is introduced by glia and antagonizes Wnt5 signaling. When Drl is mutated, Wnt5 accumulates at the midline. Loss of Drl function results in loss of commissure formation along the midline. Drl2, on the other hand, is another receptor for Wnt5 which is introduced by a subset of ORNs and positively regulates Wnt5 signaling. These two receptors cooperate by carrying out antagonistic roles, and help the establishment of the olfactory circuitry through Wnt5 signaling. This study thus demonstrates perhaps the first example of a role for glia in the patterning of olfactory map (Yao *et al*., 2007; Sakurai *et al*., 2009).

1.2.4. Role of Glial Cell in the Olfactory System

Studies in the moth *Manduca* have described three distinct types of glia in the developing olfactory system; (i) the peripheral glia that are born in the antenna and ensheath the ORNs in the antenna (Tucker *et al*., 2003); (ii) the neuropil glia that is born in the antennal lobe periphery and that project into the antennal lobe to surround and stabilize olfactory glomeruli (Oland *et al*., 1988; Baumann *et al*., 1996); (iii) and the sorting zone glia which are centrally born but migrate towards the antenna through the antennal nerve and function to segregate the axons to their corresponding glomeruli (Rössler *et al.*, 1999; Tucker *et al*., 2004). *Drosophila* has the equivalents of peripheral and neuropil glia whereas the actual homologue of sorting zone glia is not present in *Drosophila*.

The *Drosophila* antennal lobe neuropil is divided into compartments, called glomeruli, where ORN axons make synapses with the dendrites of local interneurons and projection neurons, which are the equivalents of mitral cells in the vertebrate olfactory bulb (Hildebrand and Shepherd, 1997). Each glomerulus is ensheated by the processes of glial cells that arrange in net-like structures (Oland *et al*., 2008). These glial cells resemble the periperal glia in *Manduca*. The cell bodies of the net-like glial trajectories are always found at the periphery, and are never seen within the synaptic glomerular neuropil (Hähnlein and Bicker, 1996; Oland *et al*., 1999).

In the third segment of the antenna, which houses the cell bodies of ORNs, another type of glia was found to be of the Ato lineage of sensory precursors. These glia migrate over the antenna and associate with the developing axons of ORNs. This glial subtype is suspected to have a role in the fasciculation of sensory neurons into three distinct fascicles before leaving the antenna, and also within the antennal nerve (Jhaveri *et al.*, 2000). But, unlike the case of *Manduca,* this fasciculation is not OR choice-dependent, since ORNs expressesing different receptors were found also in different fascicles (Bhalerao *et al*., 2003).

There is no discrete sorting zone made of glial cells at the periphery, which directs the subclasses of ORNs to the corresponding glomeruli, like it is the case for Manduca (Bhalerao *et al*., 2003; Sen *et al*., 2005). Instead, axonal sorting at the periphery largely depends on axonal cues (Hummel and Zipursky, 2004), some of which may be lineage-specific (Endo *et al*., 2007). Thus, glial cells in *Drosophila* appear to have no significant role in the sorting of olfactory receptor axons at the base of the antennal nerve or in the nerve layer. But the other way around, neuron-glia interaction are important for the branching of glial processes within the neuropil (Jhaveri and Rodrigues, 2002).

In addition to these three types of glial cells in *Drosophila*, a recently identified class of glia seems to play many striking roles in the glomerular organization and midline crossing of ORNs. The transient interhemispheric fibrous ring (TIFR) was depicted to have a role in ORN wiring, which is comprised of glial cells of repo-negative lineage. TIFR prefigures the midline during the pupal stage, prior to the arrival of ORN axons to the antennal lobe. It also shows cell-cell interactions with the ORN axons in the midline. Moreover, the targeted ablation of the TIFR glia blocks the antennal lobe commissure

formation, which indicates that TIFR glia are necessary for ORN axon midline crossing. It was also proposed that TIFR glia may be secreting some guidance cues for directing ORN axons to the midline, acting as guidepost cells (Chen and Hing, 2008). In the adult stage, although TIFR has disappeared, the antennal commissure is still found as tightly enwrapped by glial processes (Stocker *et al*., 1990), indicating that TIFR could be replaced by a sheath of some other glial cells. In an independent study, it was also shown that Drl, expressed by TIFR glia, has a role in the regulation of Wnt5 signaling for proper organization of glomeruli and midline commissure formation (Yao *et al*., 2007).

1.3. The Novel Cell Adhesion Molecule, Unzipped

The recently identified Drosophila *Unzipped* gene encodes a protein which is determined to be a novel cell adhesion molecule (Ding *et al*., 2011).

The full-length protein Unzipped (Uzip,) is a 488 aa long protein with a Serine/Threonine-rich domain between amino acids 380-400. Although the full-length protein is only 55 kD, endogenous Uzip in wild type fly extracts is present in two forms: 80 kD and 65 kD. After further investigation, it was discovered that Uzip is modified by posttranslational mechanisms, mainly by glycosylation (Figure 1.5). The 65 kD form is the secreted form that is lacking the C-terminus and 80 kD form is the membrane bound form which is anchored by GPI. Moreover, only the membrane-attached form is able to bind cells together and cause aggregation.

Uzip has no identical cell adhesion molecule domain and no homolog in vertebrates. But it is highly conserved within the insects up to an identity level of about 94%. Within insects, the most conserved domain of the Uzip protein was found to be the region between amino acids 42-379, which is suspected to be the functional domain. The region between amino acids 401-450 on the other hand, shows a lower identity among insects, and upon deletion of this region, Uzip transfected cells are still able to form aggregates, excluding the functional importance of this region.

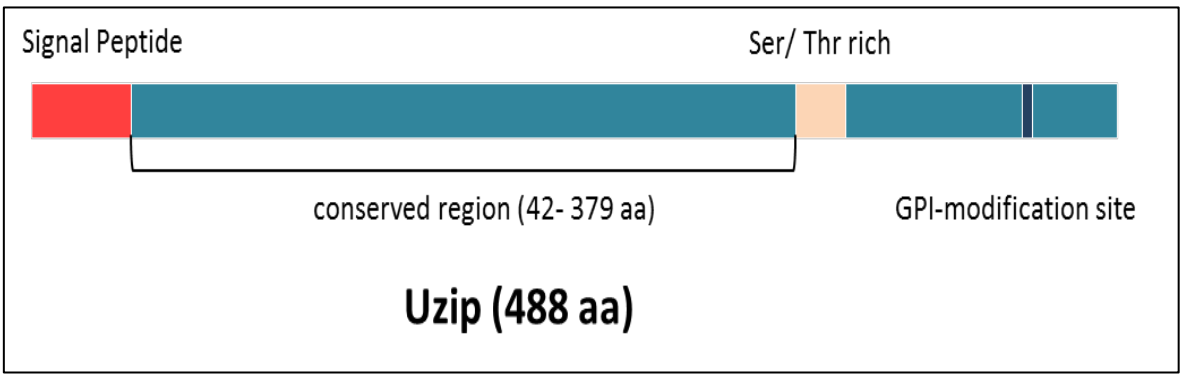

Figure 1.6. Representation of the structure of *Uzip* protein.

(adapted from Ding *et al*., 2011)

When the expression pattern of *Uzip* was studied in *Drosophila* embryos, *Uzip* mRNA was found to be dominantly present in the ventral nerve cord (VNC) and especially enriched in the two most dorsal stripes, where longitudinal glia (LG) are located. It is also expressed by axons, but to a very low extent. Although there is no obvious phenotypic defect seen in Uzip null mutants in the axonal tracts, Uzip mutation increases the severity of defects seen in NCad and Wnt5 mutants (Ding *et al.*, 2011).

1.4. The Gal4/ UAS Binary System

Drosophila melanogaster is one of the best model organisms to do functional genomics. Due to a large number of avaiable genetic tools, the manipulation, alteration and modification of the genetic background is very straightforward.

Within the available tools for *Drosophila* genetics, the Gal4/UAS binary system is the most commonly used one (Duffy *et al*., 2002). It enables targeted tissue-, cell- and time-specific expression of the gene of interest, leading to detailed analysis of gene function. The Gal4 gene, which was identified in the yeast *Saccharomyces cerevisiae*, encodes a protein of 881 amino acid length. The Gal4 protein is a transcription factor with both DNA binding and transcriptional activation functions. It acts through binding to the specific DNA sequences, called upstream activating sequence (UAS). The binding domain of the Gal4 protein is necessary for binding to the DNA and the activating sequence is necessary for the

activation of the transcription of downstream genes (Webster *et al*., 1988). The Gal4 protein sequence showed some artifacts in cloning due to its highly acidic binding region, which was replaced by a shorter amphipathic sequence in order to optimize it for use in *Drosophila*, and this modification showed no deleterious effect in flies (Fischer *et al*., 1988). This improvement leaded to a new era in *Drosophila* genetics. Through the publication of the landmark article by Brand and Perrimon (1993), describing the use of the Gal4-UAS binary system for targeted gene expression, Gal4-UAS system became one of the most commonly used tools in *Drosophila* genetics.

In order to make use of this system in *Drosophila*, a tissue promoter or enhancer with a minimal promoter is cloned to the upstream of the Gal4 gene. This Gal4, termed "driver", then expresses a particular pattern that resembles the functional activity of the cloned upstream region. When this driver line is crossed to a line bearing an UAS sequence, expression of the targeted gene that bears the UAS sequence is observed in the offspring in the pattern of the driver line (reviewed in Duffy *et al*., 2002) (Figure 1.7a).

Moreover, the Gal4/UAS binary system is a repressible system (Lee and Luo, 1999). The Gal80 protein is the repressor of the Gal4 protein, which binds to the activator domain of Gal4 and inhibits its function. When Gal80 is introduced to the genetic background of Gal4 and UAS containing flies, the system is repressed (Figure 1.7b). This feature of the Gal4/UAS system is applied in many approaches like lineage tracing and clonal analysis (Lee and Luo, 1999 and 2001).

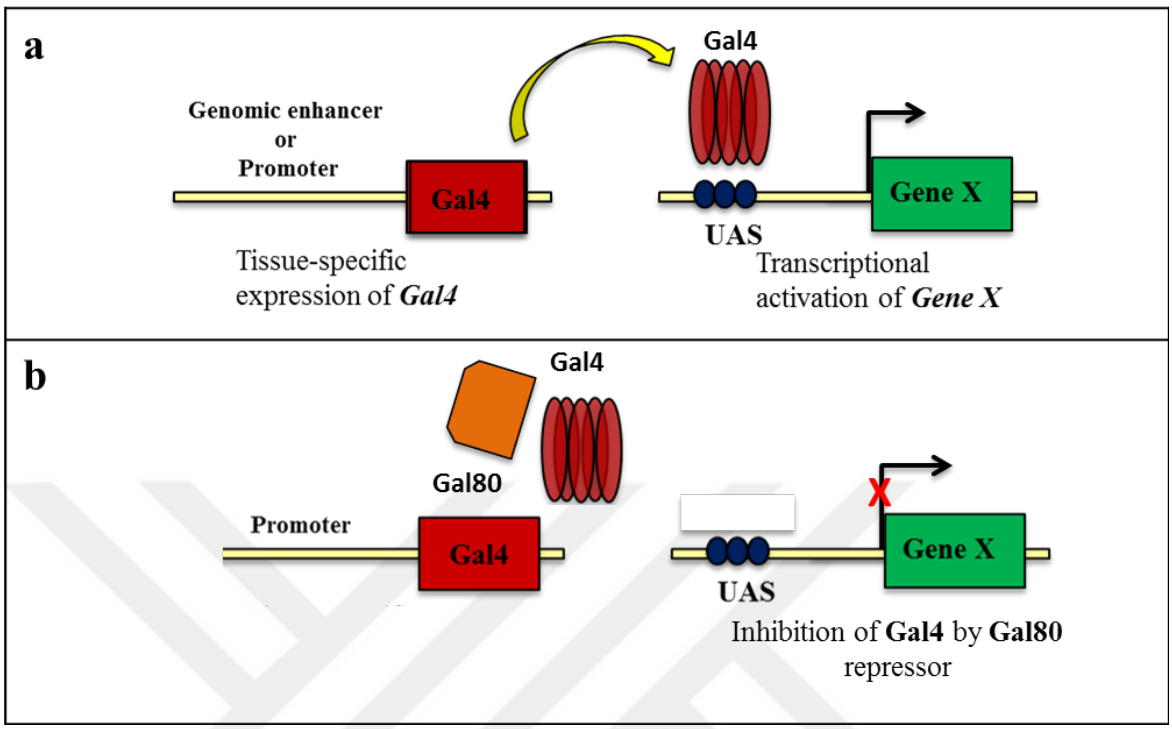

Figure 1.7. Schematic representation of the principle of the Gal4 / UAS binary system. (a) Gal4 protein, expressed from a genomic enhancer or promoter, binds to the UAS sequence and turns on the transcription of the target gene, which is located downstream of the UAS sequence. (b) Whenever Gal80 protein is present, it binds to Gal4, inhibiting its function. Transcription of the target gene is prevented.

1.5. BAC Transgenesis

Biological model organisms such as *Drosophila melanogaster* are powerful tools for the study of biological processes due to various aspects like short life cycle, easy culturing and handling, readily obtainable mutant strains, and a wide array of genetic tools. A major advance in the concept of genetic tools was the development of the P-element mediated transformation system in *Drosophila* to create transgenic flies (Rubin *et al.*, 1982). By using P-element transformation recombinant flies with the desired genetic background are readily obtained after successful integration of the recombinant DNA fragments into the genome through injection of plasmids into *Drosophila* embryos. Several P-element vectors are available that have been engineered for numerous applications (Ryder *et al.*, 2003).

Although the use of P-element-mediated transgenesis enables the generation of a wide range of recombinant flies, it has also some limitations. With the available P-element vectors, it has been problematic to clone large DNA fragments, manipulate them and transfer them into the fly genome. Moreover, targeting specific genome regions is not possible since P-element vectors insert into the genome randomly. There is always a risk to be inserted into the regulatory or coding sequences of the genes, disrupting the gene function, hence complicating phenotypic analysis due to position effects.

Towards this end, an alternative method was developed that makes use of a phage integrase, which enables targeted insertion into the genome (Groth *et al*., 2000). This method involves the injection of mRNA for phiC31-integrase together with P-element vectors. The site-specific integrase from phiC31 was previously shown to be functional at a high frequency in mice and human, which mediates recombination between two sites, attB and attP (Groth *et al*., 2000; Thyagarajan *et al*., 2001; Olivares *et al*., 2002).

Later, it was established that phiC31 functions well even in *Drosophila*. The *Drosophila* genome contains some pseudo-attP sites with 23-41% identity to the minimal 39-bp WT attP. However, these sites are inefficient in mediating precise recombination events. Therefore, attP sites are engineered into the fly genome through P-element transposition that have different efficiency and viability frequencies (Groth *et al*., 2000, Groth *et al*., 2004) (Figure 1.8).

P-element vectors, carrying a w+ marker, recognize the artificially inserted attP sites within the genome. Activity of the transposase enzyme drives the attachment of AttB site on the vector and attP site within the genome and the subsequent transposition. attB-attP attachment occurs between the vector and the genome. Recombinant flies are selected through the expression of w^+ marker in flies with w^- background.

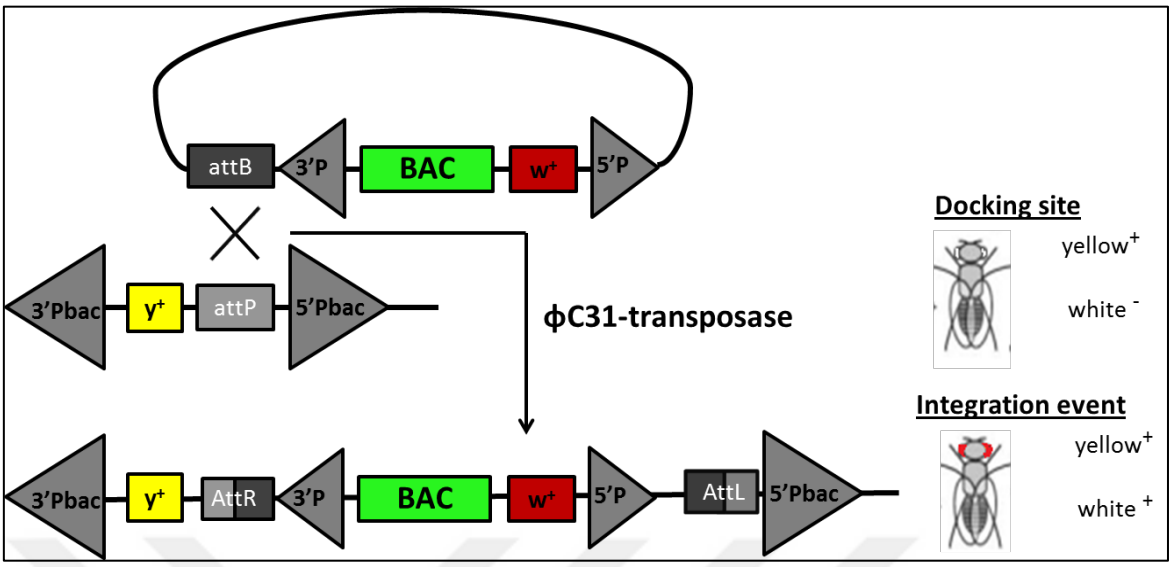

Figure 1.8. Schematic representation of the phiC31-mediated transgenesis of transgenic constructs into the fly genome. P-element vectors, carrying a w+ marker, recognize the artificially inserted attP sites within the genome. Through the activity of transposase, attB-attP attachment occurs between the vector and the genome. Recombinant flies are selected through the expression of w^+ marker in flies with w^- background.

However, discovery of p-mediated transgenesis didn't overcome the size limitation problem of integrating large DNA fragments. High-copy number plasmids such as P-element vectors are inefficient in stabilizing large DNA fragments >40 kb. On the other hand, high-copy number propagation is advantageous for the manipulation and injection steps which require high amount of DNA. An elegant solution to this problem came with the construction of P[acman] (P/phiC31 artificial chromosome for manipulation) vectors, which are conditionally amplifiable. In addition to P1 and BAC clones, P[acman] vectors have two origins of replication, OriS for low-copy propagation and OriV for high-copy propagation. Moreover, the P[acman] system makes use of homologous recombination, which has many advantages over conventional methods that rely on restriction digestion and DNA ligation. Hence, recombination and stabilization of large DNA fragments is established efficiently with low-copy number plasmids, which are easily switched to high-copy number for manipulation and injection. Thus, the P[acman] system enables the modification of cloned fragments through recombineering and site-specific germline transformation of DNA fragments up to 133 kb (Venken *et al*., 2006, Venken *et al*., 2009). P[acman] transgenesis method is summarized in Figure 1.9).

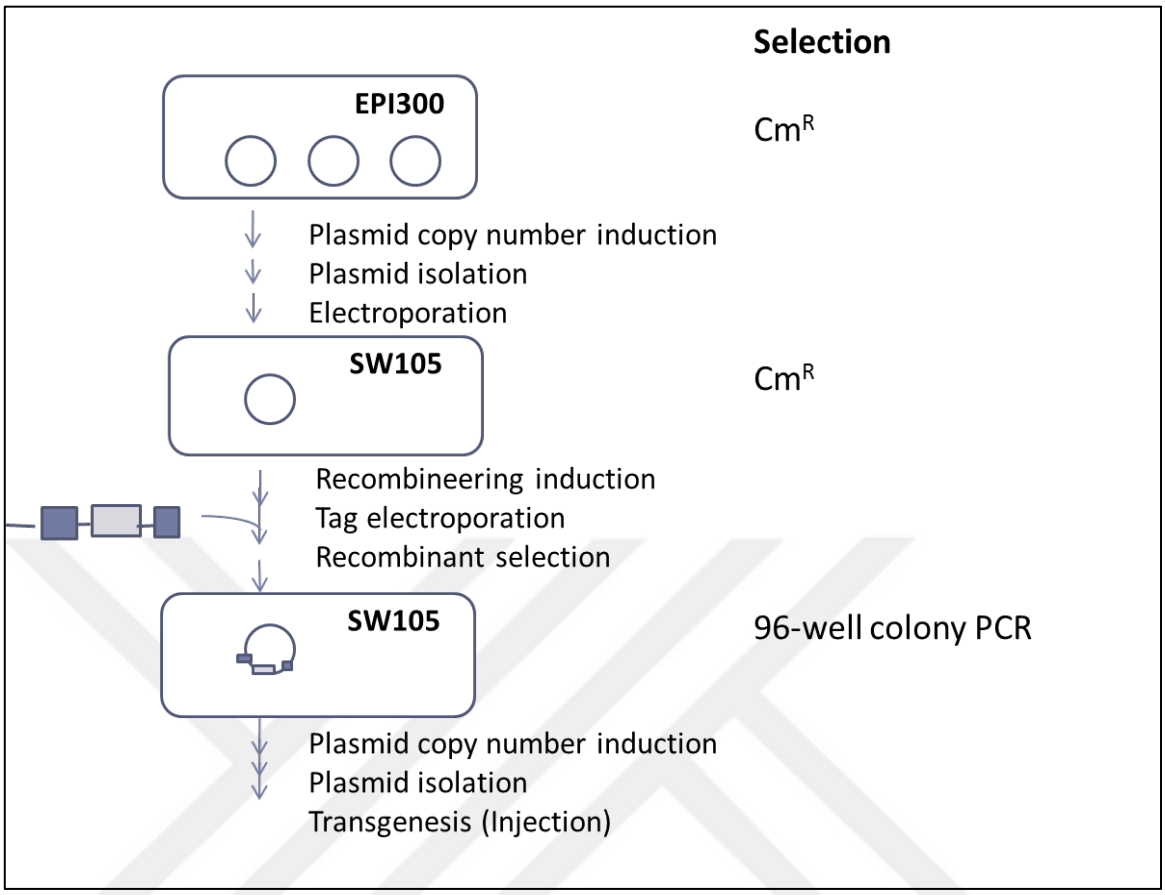

Figure 1.9. Overview of the P[acman] transgenesis method.

2. PURPOSE

Glial cells are known to be functioning in many developmental stages of the nervous system. They take role in many processes during the formation of neuronal circuits, varying from cell survival to guidance.

The role of glia in axonal guidance has been a hot topic for the last two decades. Glial membranes express or secrete cellular guidance cues, which can function either as attractants or repellents in axonal pathfinding. Identification of these guidance cues in more detail will bring new insights into our understanding of neuronal development.

The recently identified cell adhesion molecule, Unzipped, is a new candidate for these guidance cues, through its expression profile both in neurons and glia.

The olfactory system of *Drosophila*, on the other hand, constitutes a good example of the tightly regulated formation of complex neuronal circuits. It has been in the center of interest since many years how the complex pattern of olfactory system is arranged in a precise manner. How the olfactory sensory neurons of the same subset find each other and converge into the same synaptic centers.

The aim of this study was:

- to generate tools for the study of Uzip function,
- to perform a detailed analysis of *Uzip* expression in the nervous system, which will help in defining its function in nervous system development,
- to elucidate the function of Uzip specifically in the *Drosophila* olfactory system, in order to gain insight into the neuron-glia interactions in the olfactory system.

3. MATERIALS AND METHODS

3.1. Biological Material

Unless stated otherwise, all fly stocks were kept at 25°C in the incubators with a 12:12 day: night cycle and 80% humidity. Flies were raised in the commercially available fly medium (Nutri-Fly^{TM} Bloomington Formulation). 4.8 ml of propionic acid was added per liter of the medium.

For crosses, virgin females were collected 0-4h after eclosion and crossed to males of various ages.

Table 3.1. *Drosophila melanogaster* lines used in the course of study.

Name of Line	Chr. No	Description
General Stocks		
ey-FLP	I	Expresses FLP-recombinase (Flippase) under the control of the eyeless promoter
FH::Uzip	III	Uzip transgenic construct with Flag and HA tags at the N-terminal
FRT42	II	Allows FLP-mediated site specific recombination on the chromosome arm 3R
FRT42, GMR-hid	II	Expresses eye-specific cell-death gene, *hid*, which is recombined to an FRT42 site
FRT42, Gal80	II	Expresses Gal80 ubiquitously, from a locus recombined to FRT42 site
FRT42, UzipD43	II	*Uzip* null mutant allele recombined to FRT42 site
UzipD43	II	Null mutant allele of *Uzip*
UzipD23	II	Hypomorphic allele of *Uzip*
Bl	II	Phenotypic marker
CyO	II	Balancer chromosome
TM2	III	Balancer chromosome
TM6B	III	Balancer chromosome

Table 3.1. Drosophila *melanogaster* lines used in the course of study (continued).

Name of Line	***Chr. No***	***Description***
UAS constructs		
UAS-mCD8::GFP	III	UAS fused to membrane targeted GFP cDNA
UAS-syt::GFP	III	UAS fused to the pre-synaptic protein synaptotagmin protein which is also fused to GFP cDNA at the C-terminal
UAS-mRFP	II	UAS fused to membrane targeted RFP cDNA
UAS>CD2>mCD8::GFP	III	Flip-out cassette which carries a stop codon after the cDNA of CD2 that is located between two FRT sites
UAS-nlsGFP	III	UAS fused to cDNA of GFP with a nuclear localization signal
Gal4 Drivers		
elav-Gal4	I	Expresses Gal4 in post-mitotic neurons under the control of *elav*
Repo-Gal4	III	Expresses Gal4 in all glial cells, except the midline glia, under the control of *repo*
PrOR22a-Gal4	III	Expresses Gal4 under the control of OR22a promoter
PrOR46a-Gal4	III	Expresses Gal4 under the control of OR46a promoter
PrOR47a-Gal4	III	Expresses Gal4 under the control of OR47a promoter
PrOR47b-Gal4	III	Expresses Gal4 under the control of OR47b promoter
PrOR56a-Gal4	III	Expresses Gal4 under the control of OR56a promoter
PrOR59c-Gal4	III	Expresses Gal4 under the control of OR59c promoter
AC783-Gal4 (Uzip-Gal4)	II	The enhancer trap line in which Gal4 is inserted into the second intron of *Uzip*
OR markers		
PrOR19a-mCD8::GFP	III	Expresses cell surface GFP under the control of OR19a promoter
PrOR22a-mCD8::GFP	III	Expresses cell surface GFP under the control of OR22a promoter
PrOR46a-mCD8::GFP	III	Expresses cell surface GFP under the control of OR46a promoter
PrOR47a-mCD8::GFP	III	Expresses cell surface GFP under the control of OR47a promoter
PrOR47b-mCD8::GFP	III	Expresses cell surface GFP under the control of OR47b promoter
PrOR59c-mCD8::GFP	III	Expresses cell surface GFP under the control of OR59c promoter

3.2 Chemicals and Supplies

All chemicals used in this study were from Fisher Scientific, Molecular Probes, Sigma or Roche unless stated otherwise.

3.2.1. Enzymes

KOD Hot Start DNA Polymerase Master mix was used from EMD Milipore Chemicals. Taq Polymerase was used from Fermentas.

3.2.2. Chemical Supplies

Table 3.2. Suppliers of the chemicals used in the course of study.

Chemical	Supplier
1 kb Marker	NEB, USA (N3232L)
Bovine Serum Albumin (BSA)	Sigma-Aldrich, USA (A9647)
Donkey Serum	Milipore
Ethidium Bromide solution	Sigma Life Sciences, USA (E1510)
Goat Serum	Milipore
Paraformaldehyde	Sigma-Aldrich, USA (P6148)
SeaKem LE agarose	Biomax (104514PR)
Triton X-100	AppliChem, USA (A4975)
Tween 20	Roche, USA (11332465001)

3.2.3. Solutions and Buffers

Table 3.3. Solutions and Buffers.

Buffer/ Solution	Content
EB (Elution Buffer)	10 mM Tris-Cl, pH 8.5
BNT Solution	PBS (1X) 0.3% Triton X-100 1% BSA 250mM NaCl

Table 3.3. Solutions and Buffers (continued).

Buffer/ Solution	Content
Donkey Serum Blocking Solution	10% NDS in PBX3 solution
Embryo Lysis Buffer	50 mM NaCl 50nM Tris-Cl pH 7.5 10% Glycerol 320 mM sucrose 1% Triton-X 100 0.5% NP-40 05.% Na-DOC 1X Roche Protease Inhibitor Cocktail®
Goat Serum Blocking Solution	10% NGS in PBX3 solution
Laemmli	50 mM Tris-Cl pH 7.5 2% SDS 10% glycerol 0.1% bromophenol blue 100 mM DTT
LB Broth	5 g/l NaCl 10 g/l Tryptone 5 g/l Yeast extract
LB Agar	5 g/l NaCl 10 g/l Tryptone 5 g/l Yeast extract 14 g/l Agar
Loading Buffer (10X)	50% Glycerol 0,0005% Bromophenol Blue
P1(Resuspension Buffer)	50 mM Tris-Cl, p H 8.0 10 mM EDTA 100 µg/ml RNase A
P2 (Lysis Buffer)	200 mM NaOH 1% SDS (w/v)
P3 (Neutralization Buffer)	3.0 M Potassium Acetate, pH 5.5

Table 3.3. Solutions and Buffers (continued).

Buffer/ Solution	Content
16% Paraformaldehyde	8g paraformaldehyde powder 500 mL of distilled water Add 1M NaOH dropwise until solution becomes transparent
PBS (1X)	137mM NaCl 2.7 mM KCl 10mM Na_2HPO_4 1.8mM KH_2PO_4
PBX3	1X PBS 0.3% Triton X-100
Resolving Gel (5 ml)	1.7 ml ddH_2O 1.875 ml, pH 8.8 Tris-Cl 1.35 ml Acrylamide-Bisacrylamide 29%-1% 25 µl SDS 20% 50 µl APS 10% 3 µl TEMED
Stacking Gel (3 ml)	2.175 ml ddH_2O 375 µl, pH 6.8 Tris-Cl 397.5 µl Acrylamide-Bisacrylamide 29%-1% 15 µl SDS 20% 30 µl APS 10% 7.5 µl TEMED
Buffer QBT (Equilibrium Buffer)	750mM NaCl 50mM MOPS, pH7.0 15% isopropanol 0.15% Triton X-100
Buffer QC (Wash Buffer)	1.0M NaCl 50mM MOPS, pH 7.0 15% isopropanol
Buffer QF (Elution Buffer)	1.25M NaCl 50mM Tris-Cl, pH 8.5 15% isopropanol

Table 3.3. Solutions and Buffers (continued).

Buffer/ Solution	Content
Running Buffer	25 mM Tris Base 190 mM glycine 0.1% SDS pH adjusted to 8.3 with HCl
1X TAE Buffer	40 mM Tris.HCl 1 mM Ethylenediaminetetraacetic acid (EDTA) 0.1% Acetic acid
TBS-T	2 mM Tris base 15 mM NaCl 0.1% Tween-20 pH adjusted to 8.3 with HCl
Transfer Buffer	25 mM Tris bas 190 mM glycine 20% ethanol pH adjusted to 8.3 with HCl

3.2.4. Oligonucleotide Primers

Primers were diluted with distilled sterile water to obtain a final concentration of 100pmol/µl. Diluted primers were stored at -20°C.

Table 3.4. Primers used in the course of the study.

Primer Name	Primer Sequence (5'→3')	T_m°C
Uzip-FH_overlap_R	gtatcctccagcggccgacttgtcatcgtcgtccttgtagtcCGCAGCCTTTGCTGGAGC	60
Uzip-FH_F	GTTACGTATACGCCGTGTGTC	57
Uzip-FH_overlap_F	GacaagtcggccgctggaggatacccctacgacgtgcccgactacgccggcagcggcGAGCACTCAGTGTTCACCCAC	59
Uzip-FH_R	CCGTCGTCGTAGTACTTCTCACG	58

Table 3.4. Primers used in the course of the study (continued).

Primer Name	Primer Sequence (5'→ 3')	T_m°C
Uzip-FH-GFP-overlap_R	ctccagtgaaaagttcttctcctttactcatgccgctgccGGCGTAGTC	65
Spacer-Uzip_F	gattacacatggcatggatgaactatacaaaggcagcggcGAGCACTC AGTGTTCACCC	56
GFP_F	ATGAGTAAAGGAGAAGAACTTTTC	52
GFP_R	TTTGTATAGTTCATCCATGCCATG	55
FH-Uzip-scr_F	CAGTCTAGGCCTTCTCCTGGT	59
FH_Uzip-scr_R	CCCATACTAGGGTACTCGAGG	55
FH-Uzip_scr_F	GACAAGTCGGCCGCTGGAGGATAC	65
FH-Uzip_scr_R	GGTAAACCACGAGCAACACCCTCG	63
FH-GFP-Uzip_F1	GGGCACAAACTGGATTGAC	55
FH-GFP-Uzip_F2	GCCCGAAGGTTATGTCCAGG	59
FH-GFP-Uzip_F3	CCCACAAAAACGCATCATCG	56
FH-Uzip_R1	GTCGTCCTTGTAGTCCGCAG	58
FH-GFP-Uzip_R2	CAATTGACCCAAGACCGATG	55
FH-GFP-Uzip_scr_F	GAGGCAAATGGTCTGGGTTC	57
FH-GFP-Uzip_scr_R	CTTCACCCTCTCCACTGAC	55
FH-Uzip_WTctrl_F	CAAAGGCTGCGGAGCACTC	60

* lowercases indicate the regions in the primers that do not anneal to the template, but include the Flag::HA tags or used to generate the overlapping arms for the overlapping PCR.

3.2.5. Antibodies

Antibodies used during experiments and their dilution ratios are listed in Table 3.4.

Table 3.5. Antibodies used in the course of the study

Name	Antigen	Species	Dilution	Source
Primary Antibodies				
Anti-CD2	CD2	mouse	1:1000	Invitrogen
Anti-elav	Elav	rat	1:50	DSHB
Anti-GFP	GFP	rabbit	1:1000	Invitrogen
Anti-HA	HA	rat	1:500	Roche
Anti-Nc82	bruchpilot	mouse	1:100	DSHB
Anti-Ncad	N-Cadherin	rat	1:20	DSHB
Anti- repo	Repo	mouse	1:20	DSHB
Secondary Antibodies				
Alexa 488	rabbit	donkey	1:800	Invitrogen
Alexa 488	sheep	donkey	1:800	Invitrogen
Alexa 546	rat	goat	1:300	Invitrogen
Alexa 555	mouse	goat	1:800	Invitrogen
Alexa 647	rat	donkey	1:800	Invitrogen
Alexa 647	mouse	goat	1:500	Invitrogen
Toto3	-	-	1:5000	Molecular Probes

3.2.6. Embedding Media

Vectashield Embedding Medium (Vector Laboratories, Inc) was used as the embedding medium for the tissues that were processed with fluorescent immunohistochemistry in the course of this study.

3.2.7. Disposable Labware

Table 3.6. Suppliers of the disposable labware used in the course of study.

Disposable Labware	Supplier
Culture tubes, 14 ml	Greiner Bio-One, Belgium
Culture plates (96 well)	Bio-Rad, USA
Filter tips	Greiner Bio-One, Belgium
Microscope cover glass	Fisher Scientific, UK
Microscope slides	Fisher Scientific, UK
Microseal PCR sealers	Bio-Rad, USA
PCR tubes (200 µl)	Bio-Rad, USA
PCR plates (96 well)	Bio- Rad, USA
Petri dish	Greiner Bio-One, Belgium
Pipette tips	VWR, USA
Syringe (1 cc)	Becton, Dickinson and Company, USA
Test tubes, 0.5 ml	Citotest Labware Manufacturing, China
Test tubes, 1.5 ml	Citotest Labware Manufacturing, China
Test tubes, 2 ml	Citotest Labware Manufacturing, China
Test tubes, 15 ml	Becton, Dickinson and Company, USA
Test tubes, 50 ml	Becton, Dickinson and Company, USA

3.2.8. Equipment

Table 3.7. Suppliers of the laboratory equipment used in the course of study.

Equipment	Supplier
Autoclave	Astell Scientific Ltd., UK
Centrifuges	Eppendorf, Germany (Centrifuge 5424, 5417R)
Cold Room	Birikim Elektrik Soğutma, Turkey
Confocal Microscope	Leica Microsystems, USA (TCS SP5)
Electrophoresis Equipment	Bio-Rad Labs, USA (ReadySub-Cell GT Cells)
Environmental Test Chamber	Sanyo, Japan (MLR 351H)
Fluorescence Stereomicroscope	Leica Microsystems, USA (MZ16FA)
Freezers	Arçelik, Thermo Electron Corp., USA (Thermo Forma 723)
Gel Documentation System	Bio-Rad Labs, USA (Gel Doc XR)
Heating Block	Fisher Scientific, France (Dry-bath incubator)
Heating magnetic stirrer	IKA, China (RCT Basic)
Incubator	Weiss Gallenkamp, USA (Incubator Plus Series)
Inverted Microscope	Zeiss, USA (Axio Observer, Z1)
Laboratory Bottles	Isolab, Germany
Micropipettes	Eppendorf, Germany
Microwave oven	Vestel, Turkey
pH meter	WTW, Germany (Ph330i)
Refrigerators	Arçelik, Turkey
Stereo Microscope	Olympus, USA (SZ61)
Thermal Cycler	Bio-Rad Labs, USA (C1000 Thermal Cycler)
Vortex Mixer	Scientific Industries, USA (Vortex Genie2)
Water Bath	Grant Instruments, UK (JB Aqua 12)

3.3. Molecular Biological Techniques

3.3.1. Isolation of DNA

3.3.1.1. Copy Number Induction of P[acman] Plasmids. P[acman] plasmid, including the corresponding BAC clone was received from the BACPAC company in EPI300 cell-line. For the induction of plasmid copy number, 6 µl/ml of Epicentre BAC Autoinduction Solution was added into the LB including 12.5 µg/mL of Chloramphenicol and cells were cultured overnight at 30°C by vigorous shaking.

3.3.1.2. Isolation of P[acman] Plasmid DNA. To extract DNA from the P[acman] plasmids, QIAprep Spin Miniprep Kit (QIAGEN) was used according to the manufacturer's instructions. Briefly, a starter culture of 5 ml copy number induced EPI300 cells were incubated overnight at 30°C by vigorous shaking. The starter culture was diluted 1/500 into 50 ml Chloramphenicol containing LB medium, and incubated 12-16 h at 30°C by vigorous shaking. Cells were harvested by centrifugation at 3500 rpm for 10 min at 4°C. The supernatant was discarded and the pellet was resuspended in 6 ml of P1 Buffer. Then, 6 ml of P2 Buffer was added and mixed by inverting the tube a few times, and incubated at room temperature for 5 min. 6 ml of chilled P3 Buffer was added and the tube mixed thoroughly by inverting the tube several times. The mixture was incubated on ice for 15 min and centrifuged for 30 min at 3500 rpm at 4°C. The supernatant was transferred. The supernatant containing the plasmid was filtered through a compress and the filtrate was recovered in a 50 ml Falcon tube. A QIAGEN-tip 100 was equilibrated by applying 4 ml Buffer QBT, and the column was allowed to empty by gravity flow. The supernatant was applied to the QIAGEN-tip and allowed to enter the resin by gravity flow. The QIAGEN-tip was washed two times with 10 ml Buffer QC. After washing, DNA was eluted with 5 ml of Buffer QF. The DNA was precipitated by adding 3.5 ml (0.7 volumes) of room-temperature isopropanol to the eluted DNA. Eluted DNA was mixed and centrifuged immediately at ≥15,000 g for 30 min at 4°C. The supernatant was carefully decanted. The DNA pellet was washed with 2 ml of room-temperature 70% ethanol, and centrifuged at ≥15,000 g for 10 min. The supernatant was carefully decanted without disturbing the pellet. The pellet was air-dried for 5–10 min, and the DNA was dissolved in 100 µl of water.

3.3.2. Transformation of P[acman] Plasmids into SW105 Cells

A starter culture of 3 ml SW105 cells were grown in low salt LB, overnight at 30°C by vigorous shaking**.** The starter culture was diluted 1:50 to a total volume of 25 ml and grown 3-4 hours at 30°C until the density reached an OD of ≈0.6. Cells were incubated at least 30 min on ice-water bath. (From now on, it was critical to keep the cells always cold.) Then, the cells were transferred into pre-cooled 50 ml falcon tubes and spinned down at 4000 rpm, 0°C for 5 min. The supernatant was gently discarded and the pellet was resuspended in 30 ml of pre-cooled H_2O for washing. The wash step was repeated two more times at 4000 rpm, 0°C for 5 min, after discarding the supernatant and resuspending the pellet in 29 ml of pre-cooled H_2O each time. In the fourth step of washing, resuspended cells were transferred into 1.5 ml eppendorf tubes and spinned down. The supernatant was resuspended in 30µL H_2O. 15µl of the cells were mixed with 750ng - 1µg of plasmid DNA and transferred to plastic cuvettes. Electroporation was conducted at 1.75 kV with a time constant of 4.0. Cells were transferred to a 15 ml falcon tube by the addition of 1 ml of LB. Then, they were left to recover for 1h on a rotator at room temperature. Recovered cells were streaked out on the LB agar plates containing chloramphenicol. The transformed cells were selected by chloramphenicol resistance.

3.3.3. Gradient PCR

Gradient PCR was performed prior to all PCR steps to optimize the annealing temperature for each oligonucleotide primer couple. The following conditions were used with the varying annealing temperature according to the primer couple to be used. The interval of the annealing temperature was generally started at 5°C lower than the T_m of the primer with lower T_m value and increased up to 15°C higher than the lower limit.

PCR mixture:

Template DNA	100 ng
KOD Polymerase Master Mix	7.5 µl
Forward Primer (10µM)	0.9 µl
Revese Primer (10µM)	0.9 µl
Sterile H_2O	to the final volume of 15 µl

Cycling conditions:

(i)	Initial denaturation	95 °C	2 min

(ii)	Denaturation	95 °C	10 sec
(iii)	Annealing	50-65 °C (variable)	10 sec
(iv)	Extension	72 °C	20 sec/kb
		Repeat the steps 2-4 30x	
(v)	Final extension	72 °C	10 min
(vi)	Cooling	12 °C	as needed

3.3.4. Conventional PCR

For the amplification of BAC recombination fragments, KOD Hot Start DNA Polymerase Master Mix was used which amplifies the DNA with blunt ends that is suitable for cloning. Briefly, 100 ng of template plasmid DNA and 1.5 µl of each primer (10 pmol/ µl) was mixed with 25 µl of KOD DNA Polymerase Master Mix, and distilled water was added to a total volume of 50 µl. Every PCR step was optimized by a prior gradient PCR step to determine the annealing temperature. Cycling conditions were used as the following:

(i)	Initial denaturation	95 °C	2 min
(ii)	Denaturation	95 °C	10 sec
(iii)	Annealing	X °C(variable)	10 sec
(iv)	Extension	72 °C	20 sec/kb
		Repeat the steps 2-4	30x
(v)	Final extension	72 °C	10 min
(vi)	Cooling	12 °C	as needed

3.3.5. DpnI Digestion

Whenever the P[acman] plasmid or another plasmid was used as a template for the amplification of recombination fragments, DpnI digestion was performed following the PCR reaction, in order to get rid of the template DNA. Briefly, 1µl of DpnI enzyme was added to the PCR reaction tube after the PCR reaction was completed. PCR products were incubated with DpnI 1 h at 37°C.

3.3.6. PCR Purification

In order to get a pure PCR products, which is critical for the homologous recombination event to take place, and to get rid of the template DNA and nonspecific products, PCR purification was performed. The PCR Purification kit from QIAGEN was used according to the manufacturer's instructions.

3.3.7. Agarose Gel Electrophoresis

All the PCR products were run on a 1% agarose gel (w/v), which was prepared with 1X TAE buffer and 30 ng/ml ethidium bromide solution. Prior to running, PCR products were mixed with 6X Loading Buffer from Fermentas to the final loading dye concentration of 1X. As size marker, Gene Ruler 1kb DNA Marker from Fermentas was used. The gels were run at different voltages varying between 90V- 220V, according to the width of the gel and the length of the PCR product. A transilluminator from Bio-Rad was used to visualize the gels under UV.

3.3.8. Gel Extraction of DNA

The desired DNA fragment was excised from the agarose gel with a clean razor blade. In order to extract the DNA, QIAquick Gel Extraction Kit (QIAGEN) was used according to the manufacturer's instructions.

3.3.9. Sequencing Analysis

Purified DNA samples were directly subjected to sequencing for the verification of correct sequences. Sequencing reactions were performed at Macrogen Inc. (Korea) and sequencing results were analyzed by using MacVector or Ape softwares.

3.3.10. BAC Recombination

Recombination fragments, which were obtained by overlapping PCR reactions and whose sequence was verified by sequencing analysis, were transformed into SW105 cells,

which were previously transformed with the P[acman] vector including our desired BAC clone. The same protocol as the transformation of BAC clones into SW105 cells was used with only minor differences. After the OD of cells reached 0.6, prior to the incubation in an ice-water bath, the cells were induced at 42°C for 15 min by gentle swirling. This activates the recombinase enzyme in cells, which drives the homologous recombination between the recombination fragment and the BAC clone. The second difference was that, electroporated cells were recovered for 3 h at room temperature instead of 1 h and smaller volumes of the cells were plated on the agar plate since there was no selection marker this time.

3.3.11. Colony PCR

For the selection of recombinant colonies, 96-well colony PCR was performed. Selection was done by two rounds of 96-well PCR. Prior to starting, a PCR master mix and LB broth including chloramphenicol at the appropriate concentration were distributed to the 96-well PCR tubes and 96-well culture plates, respectively. In the first round of selection, 8-10 colonies were picked with a pipette tip from the agar plates that were plated with the electroporated cells of BAC recombination procedure. The colonies were first dipped into the PCR master mix and then into the LB culture to make the replica culture of each PCR mixture.

Once the recombination-positive culture was detected by agarose gel electrophoresis, it was plated on chloramphenicol LB agar in order to use for the second round of selection. For the second round of selection, single colonies were picked each time and the same procedure was followed as in the first round of selection.

3.4. Biochemical Methods

3.4.1. Protein Extraction

The total protein was extracted from young adult *Drosophila*. Crude protein extract was obtained from the whole fly. From each genotype 5 flies were smashed in 100 µl embryo lysis buffer. The flies were thoroughly smashed using a pestle and kept on ice for 30 min to let the tissues dissolve. They were centrifuged at 4°C, for 10 min at 10000 rpm. Avoiding the pellet of hard tissue debris and the upper layer rich in lipids, the 80 µl supernatant was taken into a clean tube. 40 µl of 3X Laemmli's buffer was added. To reduce and denature the proteins, they were heated at 95°C for 6 min.

3.4.2. SDS-PAGE

A polyacrylamide gel was poured in conventional way. To be able to separate 80 kD from 65 kD, an 8% gel was preferred. First, the resolving gel was poured. After it polymerized, a stacking gel was poured on the polymerized resolving gel. A ready-to-use protein ladder and each protein extract were loaded as 4 µl and 30 µl, respectively. The gel was run in 1X running buffer under 30 mA constant current.

3.4.3. Western Blot

The PVDF membrane was activated in Ethanol for 1 min and equilibrated in 1X transfer buffer. The gel was transferred to the membrane, under 200 mA constant current for 2 hours, in cold 1X transfer buffer. The completion of the transfer was confirmed with reversible Ponceau's Red staining. It was destained in TBS-T. The membrane was blocked in 5% non-fat dry milk dissolved in TBS-T for 1 hour at room temperature. The primary antibody rat α-HA was dissolved in 1% milk 1:1000 and incubated with the membrane overnight at 4°C by shaking. The following day, it was washed with TBS-T 3 times, 10 min each. The secondary antibody α-mouse-HRP was dissolved in 1% milk 1:1000 and incubated with the membrane 2h at room temperature. It was washed similarly. On the platform, the membrane was incubated with HRP revealing kit 20X LumiGlo® diluted to 1X in ddH_2O for 3 min. The emission was recorded for 30 min with the Stella system. The image was processed with Photoshop using conventional methods

3.5. Histological Methods

3.5.1. Preparation of *Drosophila* Tissues for Immunohistochemistry

3.5.1.1. Preparation of adult brains. 10-15 flies from the desired genotype were anesthetized with CO_2 and transferred into 70% ethanol to kill the flies. The dead flies were washed three times with 1X PBS and dissected on silicon plates in a drop of PBS. Dissection was performed briefly as follows: The proboscis was removed with the aid of forceps. This leaves a hole, which was used to grab the head exoskeleton. The exoskeleton was removed by holding the brain with forceps from both sides, and removing the first and the second halves of the exoskeleton one by one. After cleaning out the residual tracheae, the brain was detached from the body and transferred into PBS on ice.

3.5.1.2. Preparation of pupal brains and eye disc. Pupae of the desired stage were carefully removed from the vials and transferred onto double-sided adhesive tape. The operculum was grabbed and the puparium was removed carefully. Then, the pupa was transferred onto a second stripe of tape and covered with PBS. A little hole was pinched in the anterior and enlarged carefully to take out the eye-brain complex and the tissue was transferred into PBS on ice.

3.5.1.3. Preparation of larval brains and eye imaginal disc. Larvae from the desired genotype were dipped into PBS. With one pair of forceps, carefully holding the mouth hook, a hole was made on the body with the second pair of forceps right below the third-most anterior segment of the larval body. Then, pulling from the mouth hook, the eye- antennal disc attached to the brain were taken out and transferred into PBS on ice.

3.5.2. Immunohistochemistry

The following procedure was used for all the immunohistochemistry experiments, except those in which anti-HA antibody was used, with only minor differences which are stated below for each type of tissue. Blocking solutions used were either normal goat serum (NGS) or normal donkey serum (NDS).

- Tissues were fixed in 2% or 4% PFA in PBS with the duration varying according to the tissue.
- Tissues were washed three times for 20 min PBX3.
- Tissues were blocked in the corresponding blocking solution for 1h at room temperature.

- Tissues were incubated with primary antibodies overnight at 4°C. Primary antibodies were diluted in the same solution which was used for blocking.
- Tissues were washed three times for 20 min in PBX3.
- Secondary antibody incubation was performed at room temperature for 2-3 h. Dilution of the secondary antibodies was made with the solution used for blocking.
- Final washing step was performed three times for 20 min in PBX3.
- Tissues were mounted in Vectashield embedding medium, and stored at 4°C in dark.
- Visualization of the samples was perfomed using confocal microscopy.

3.5.2.1. Antibody staining of the adult brain. Fixation was performed in 2% PFA for 90 min. For the whole brain and antennal lobe visualization, brains were mounted with an anterior view. For blocking, either NGS or NDS was used.

3.5.2.2. Antibody staining of the pupal eye disc and brain. Dissected tissues were collected in 2% PFA on ice until the end of dissection. Fixation of the pupal tissue was performed in 2% PFA for 1 h. For blocking, either NGS or NDS was used. For the visualization of eye discs, eye discs were carefully detached from the brain after the staining and mounted carefully. Brains were mounted with the anterior view.

3.5.2.3. Antibody staining of larval eye imaginal discs. Fixation of the larval tissue was performed in 4% PFA for 20 min. For blocking, BNT solution was used.

3.5.2.4. Antibody staining of Flag::HA_Uzip transgenic flies. Since immunohistochemistry with the antibody against HA polypeptide may require some modifications to commonly used antibody staining protocols, the following protocol was followed to detect HA expression which was inserted to the N-terminal of *Unzipped* protein.

Adult brains were dissected in PBS and fixed in 4% PFA in PBS for 2 h at 4°C. 10% NGS in PBX3 was used for blocking. Both the primary and the secondary antibody incubation was performed overnight at 4°C.

3.6. Experiments for Expression Analysis

The expression profile of *Unzipped* protein was analyzed by two main strategies. In the first strategy, the enhancer trap line AC783-Gal4, where Gal4 is inserted in the second intron of Unzipped, was used to label the endogenous *Unzipped* expression by a GFP reporter using different GFP-reporter lines. In the second strategy, transgenic *Unzipped* lines, which were tagged with HA and Flag polypeptides through BAC recombination, were used.

3.6.1. Expression Analysis of Unzipped Enhancer Trap Line (AC783-Gal4)

For the analysis of endogenous *Unzipped* expression, crosses in the Figure 3.1. were set up to generate the stocks of the desired genotypes. Stocks were used for the analysis of the *Unzipped* expression pattern.

Stocks of AC783-Gal4 driver line were generated with three different GFP-reporter lines. NuclearGFP, membraneGFP and synaptotagminGFP were used to trace the endogenous *Uzip* expression. AC783-Gal4, being the enhancer trap line of *Uzip*, should drive the expression of the GFP reporters in a manner showing the endogenous expression pattern of Uzip.

In parallel, a flip-out cassete was used to generate stock for the analysis of *Uzip* expression differentially in neuons and glia.

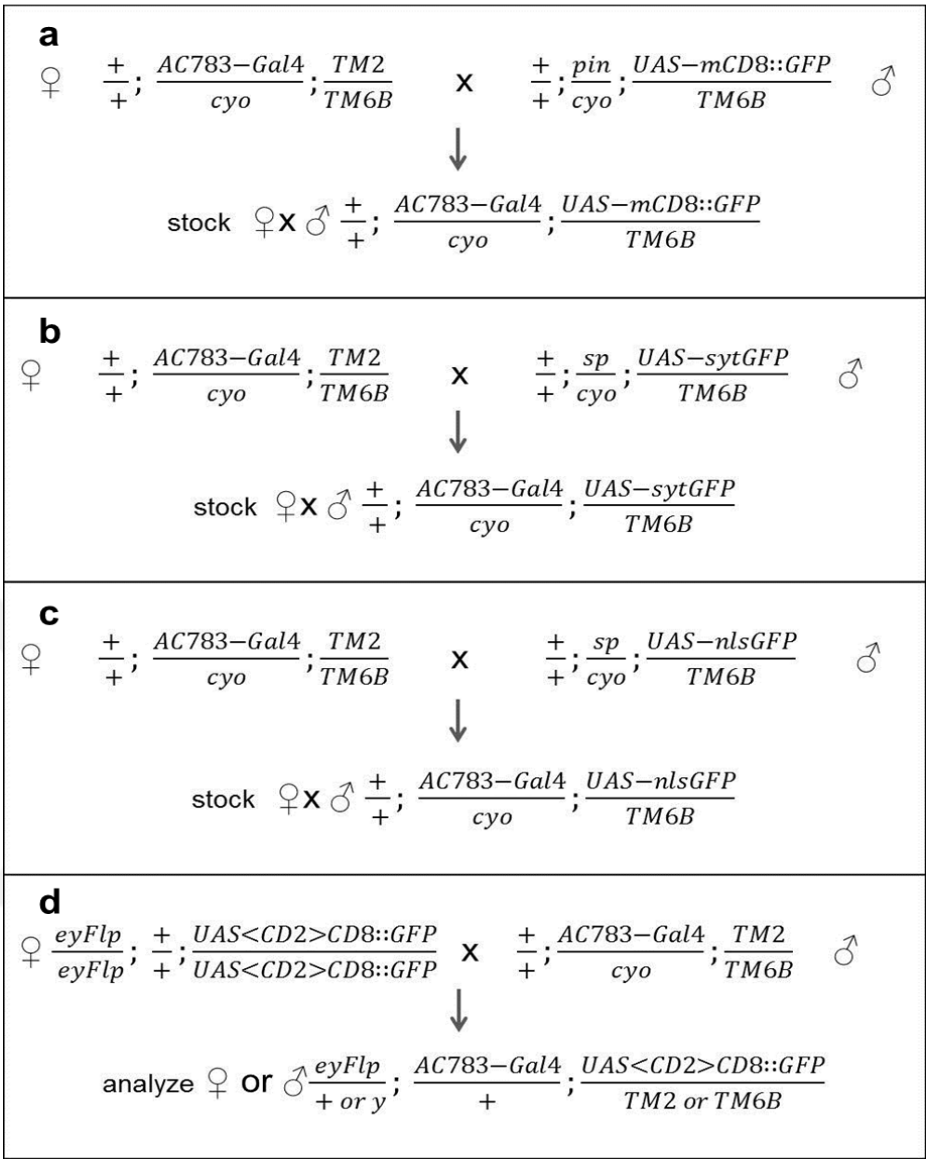

Figure 3.1. Set up of crosses for the analysis of *Uzip* expression pattern. (a) Labeling *Uzip* expression with the membrane localized GFP reporter. (b) Labeling *Uzip* expression with presynaptic GFP reporter. (c) Labeling *Uzip* expression with a nuclear localized GFP reporter. (d) Labeling *Uzip* expression differentially in neurons and glia by a flip-out cassette.

3.6.2. Expression Analysis of Flag and HA Tagged Unzipped Transgenic Lines

After injection, recombinant flies were selected through w^+ marker expression which was present on the P[acman] plasmid, and gives red eye color to the flies in an otherwise white-eyed background. The integrity of the eye color depends on the genome region that the plasmid was inserted in. The color may vary from yellow to dark-red.

In the course of this study, three transformant flies were separately used to generate stocks of Flag::HA::Unzipped genotyped flies. These flies were directly used to analyze the expression pattern of the transgene by immunohistochemistry, using a monoclonal antibody against HA polypeptide.

3.7. Experiments for Functional Analysis

3.7.1. Loss of Function Experiments: Unzipped Deficiency

The *Uzip* deficiency lines UzipD43 and UzipD23 (Ding *et al*., 2011) were used for the loss of function analyses. Deficiency alleles were brought together with the ORXX- Gal4 or ORXX::mCD8GFP lines on the same fly and the projection pattern of the single OR classes were visualized in the background of *Uzip* deficiency.

The following crosses seen in Figure 3.2 and Figure 3.3 were set up to obtain the desired genotype of the flies. Flies, homozygous for UzipD43 allele were used for the loss-of-function experiments of null mutants in order to observe the consequences of Uzip loss-of-function. Flies heterozygous for UzipD43 allele were used as controls.

For the analysis of the effect of the hypomorphic allele, trans-heterozygous flies having both UzipD23 and Uzip D43 alleles were used. Therefore, a decrease in the Uzip protein level was guaranteed by putting the null allele in trans to the hypomorphic allele. As control, heterozygous flies for UzipD43 allele were used.

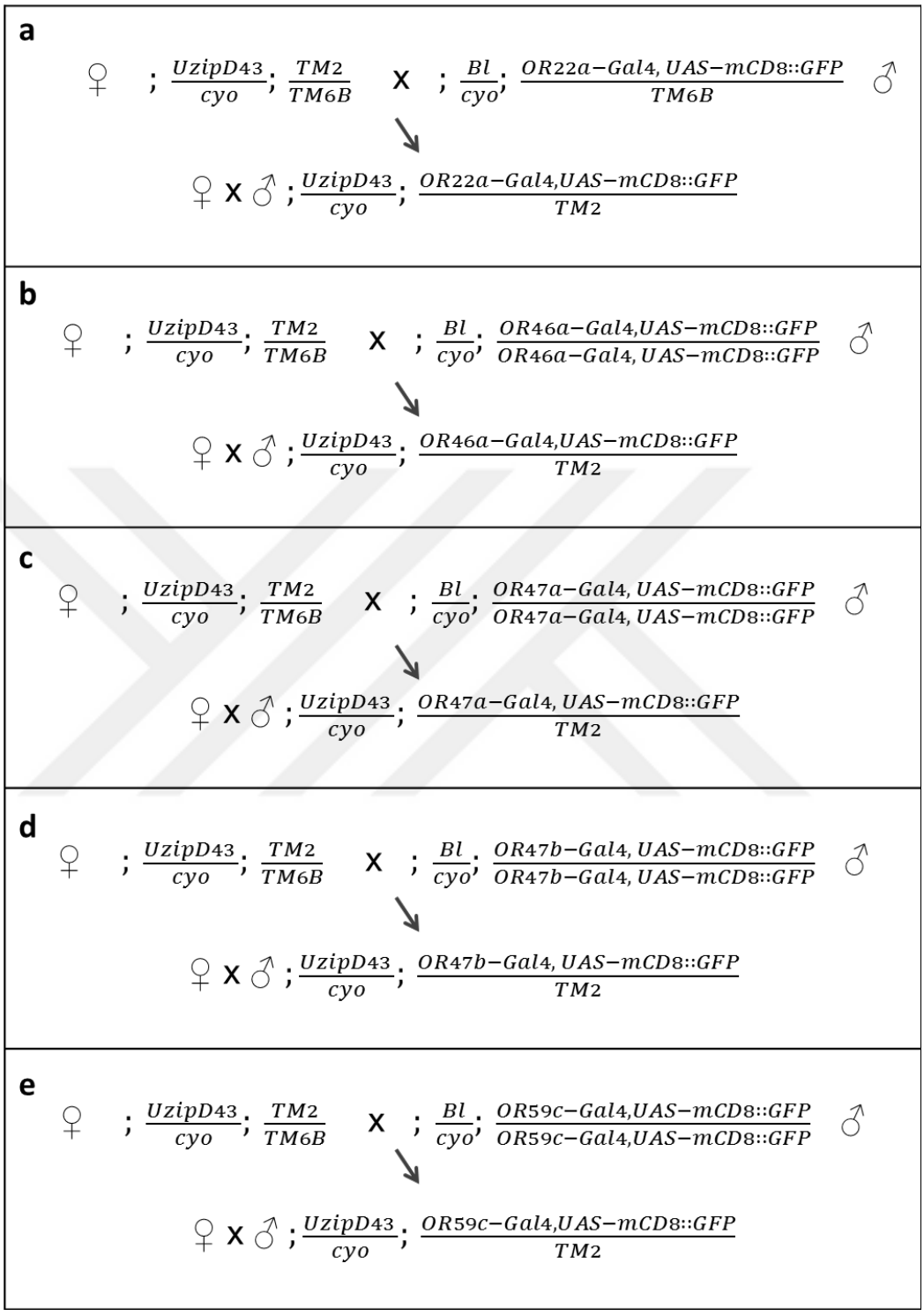

Figure 3.2. Crosses for the generation of *Uzip* deficient flies on which single classes of ORN's are labeled with membrane-localized GFP reporter. (a) Generation of *Uzip* deficient fly stocks using membrane-localized GFP reporter fused to OR promoters. (b) Generation of Uzip deficient fly stocks using membrane-localized GFP reporter driven by OR drivers.

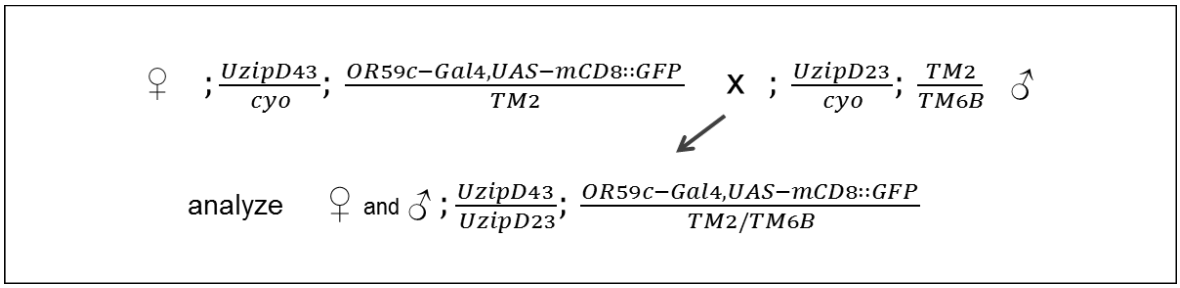

Figure 3.3. Crosses for the analysis of the projection of single class ORNs in *Uzip* hypomorphs.

3.7.2. Loss of Function Experiments: RNA Interference

Publicly available UAS-RNAi lines for Uzip gene were ordered from Vienna Drosophila Stock Center (VDRC). They were balanced w^-; sp/CyO; MKRS/TM2 flies and used for the subsequent experiments. Crosses shown on the figures 3.4 and 3.5 were set up to obtain the desired genotype for the downregulation of *Uzip* expression levels. Projection pattern of single ORN classes were analyzed upon the downregulation of *Uzip* expression.

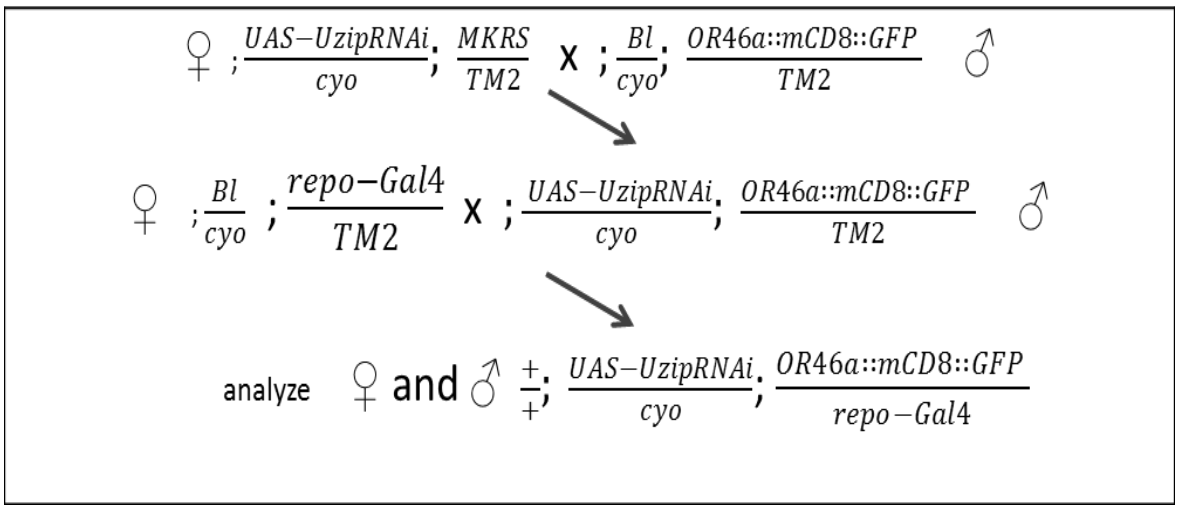

Figure 3.4. Crosses for down-regulation of *Uzip* protein levels specifically in glia.

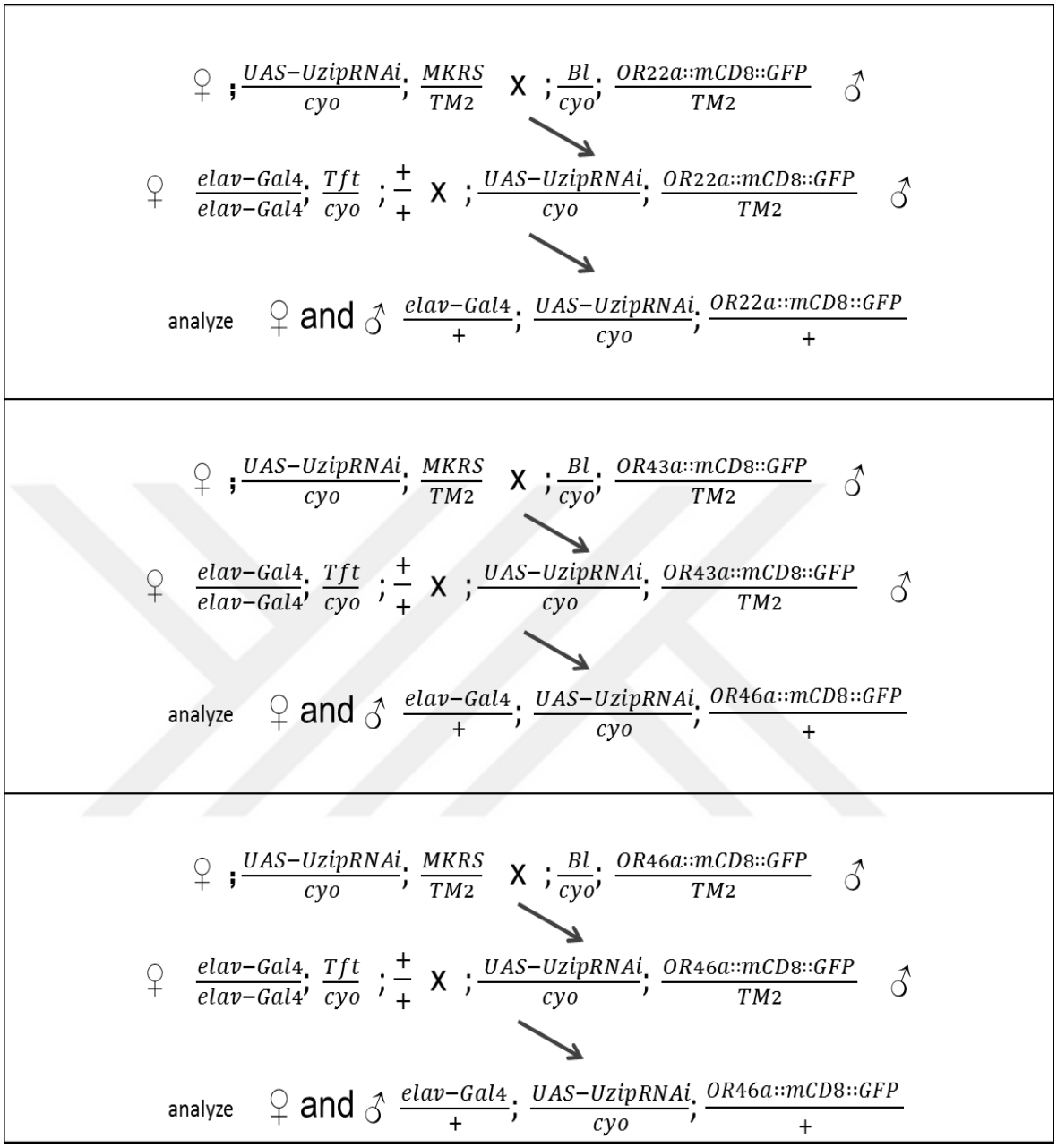

Figure 3.5. Crosses for down-regulation of *Uzip* protein levels specifically in neurons.

3.7.3. Loss of Function Experiments: Clonal Analysis

FLP/ FRT system is commonly used in *Drosophila* genetics to circumvent the lethality of the alleles and allow the examination of homozygous clones in an otherwise heterozygous animal (Xu and Rubin, 1993). Mosaic Analysis with a Repressible Cell Marker (MARCM) technique allows the tissue specific induction of mitotic clones. In addition, introducing a Gal80 element that suppresses Gal4, allows visualizing homozygous mutant

cells in a heterozygous or homozygous wild type background (Lee and Luo, 1999). In our case, we generated clones of single ORN classes which are homozygous for *Uzip* deficiency in an animal heterozygous for *Uzip* deficiency. We expressed the Flippase enzyme under the control of eyeless promoter (eyFlp) (Newsome, Asling and Dickson, 2000). Therefore, we generated the clones of Uzip deficiency specifically in ORNs in the olfactory system.

3.7.3.1. Generation of Uzip Deficiency Lines Recombined to an FRT site. The mutant allele (UzipD43) (Ding *et al*., 2011) was crossed to a wild type chromosome with an FRT42 insertion. Virgin flies carrying the mutant chromosome in trans to the wild type chromosome were crossed against a balancer stock. Colored-eye males were picked up since UzipD43 allele carries a w^+ marker and re-crossed against the balancer to generate stocks. After the females laid eggs, males were taken out of the vial and crossed to eyFlp/eyFlp; FRT42, GMR-hid/CyO flies for the complementation test of the FRT42 site. GMR-hid is a dominant photoreceptor cell lethal transgene. This transgene kills the photoreceptor cells because of eye-specific expression of the cell death gene "hid" during metamorphosis (Grether *et al*., 1995). By using the GMR-hid allele on the second chromosome as homolog to our UzipD43 allele, we induced mitotic recombination through the eyFlp. We insured that only cells having an FRT site recombined to UzipD43 allele will undergo complementation and show a wild type eye phenotype. The stocks of the crosses with an eye complementation were our desired recombinant flies, having a recombinant allele as FRT42, UzipD43 on the second chromosome. The strategy is summarized in Figure 3.6.

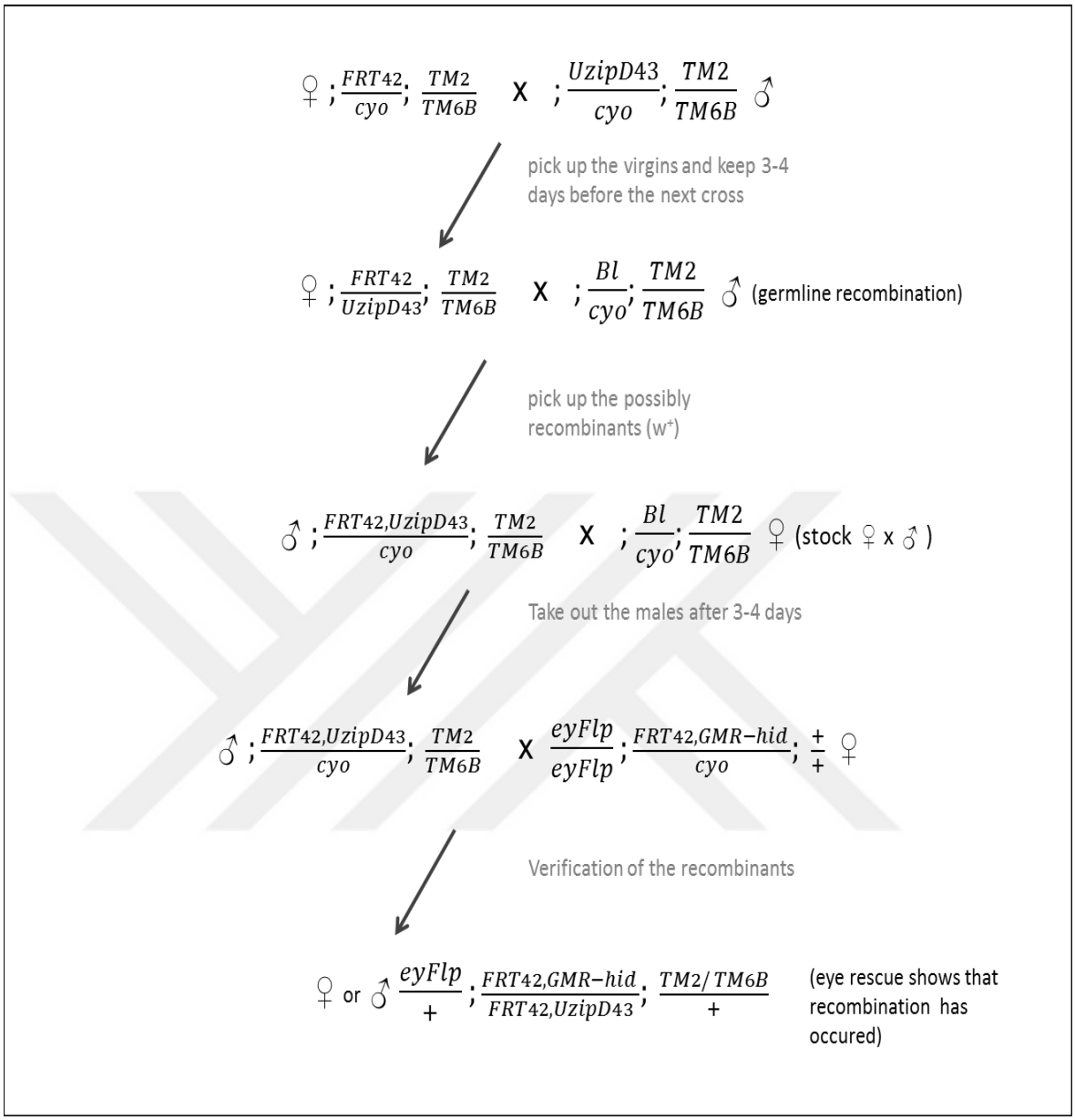

Figure 3.6. Crosses for the generation of UzipD43 allele recombination to a FRT42 site. Recombination was carried out in four subsequent crosses. The correct recombinants were tested by using the cell-death gene *hid.*

3.7.3.2. Generation of Mitotic clones. Mitotic clones were generated through the crosses shown in Figure 3.7.

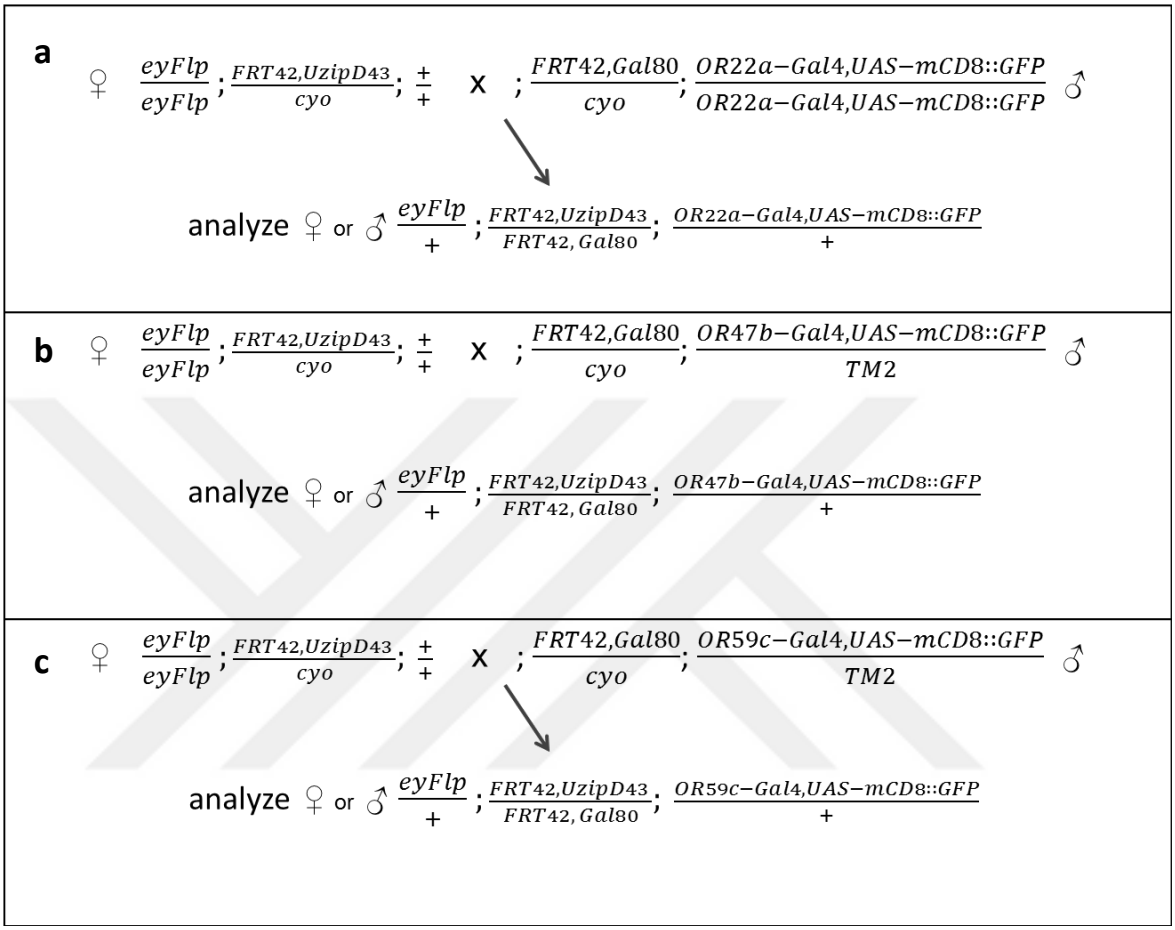

Figure 3.7. Crosses for the generation of MARCM clones of ORNs homozygote for *Uzip* deficiency (UzipD43).

3.7.4. Gain of Function Experiments: Misexpression

For tissue-specific mis-expression studies, a repo-Gal4 driver was used to over-express the Uzip protein specificially in glial cells. Crosses to generate the desired genotype for mis-expression studies are listed below in Figure 3.8.

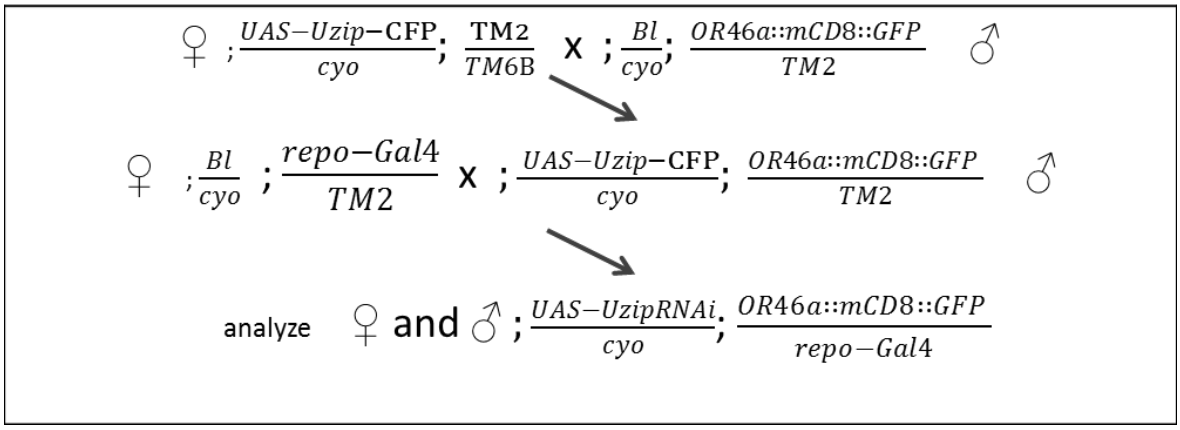

Figure 3.8. Crosses for misexpression of *Uzip* protein specifically in glial cells.

3.7.5. Gain of Function Experiments: Tissue Specific Rescue

To verify the role of Uzip in midline crossing of olfactory receptor neurons, we performed tissue specific rescue experiments. In the background of *Uzip* deficient allele UzipD43, we expressed an UAS-*Uzip* transgene under the control of glial driver repo-Gal4 and traced the axonal trajectories of ORNs by using an anti-HRP monoclonal antibody. Crosses set up in order to generate the desired genotype are listed below in Figue 3.9.

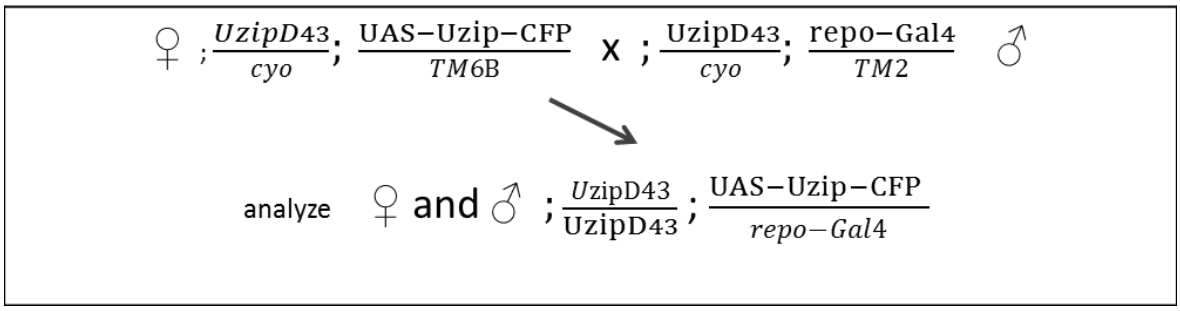

Figure 3.9. Crosses for the glial-rescue of *Uzip* in the background of the *Uzip* mutation.

3.7.6. Gain of Function Experiments: Nonspecific Rescue

In the last round of gain of function experiments, we added Flag::HA::Uzip transgene to the background of *Uzip* deficient flies and checked the projection of single ORN classes. Crosses set up to generate the desired genotypes are listed below in Figure 3.10.

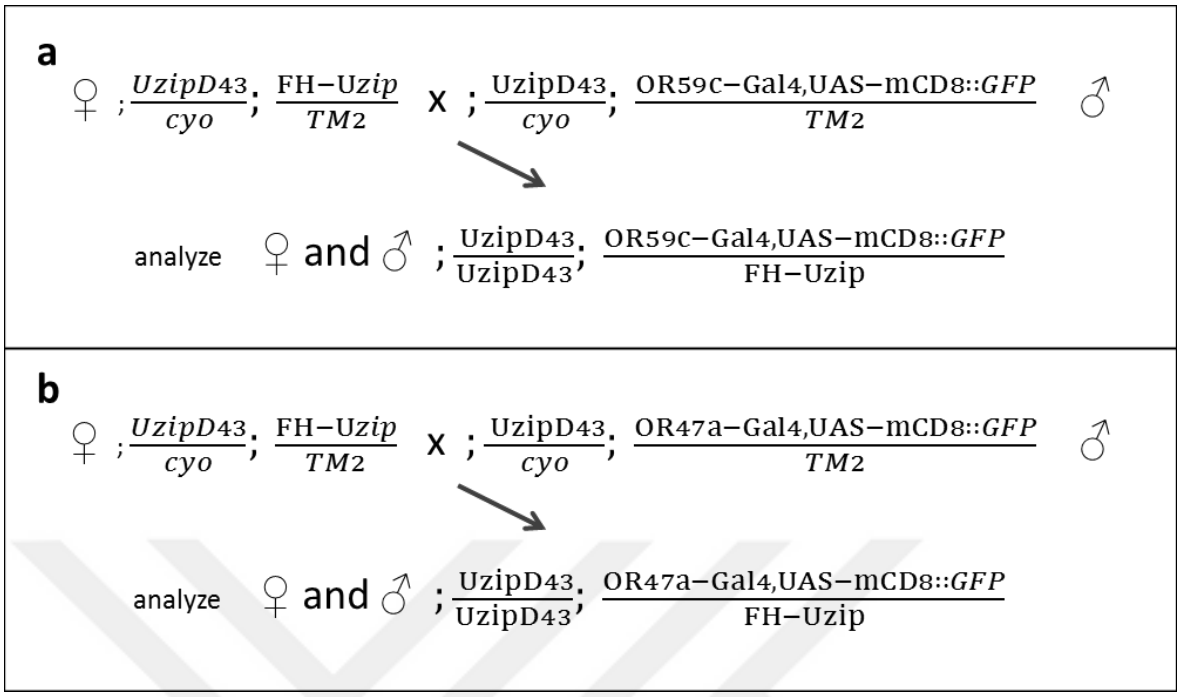

Figure 3.10. Crosses for the non-specific rescue of Uzip in the background of Uzip mutation.

4. RESULTS

The recently identified protein Unzipped is a novel cell adhesion molecule, which is expressed in longitudinal glial (LG) cells in the embryonic stage of *Drosophila*, and has a role in axonal targeting. It is a 488 amino acid GPI anchored protein, which triggers cell adhesion by homophilic binding. Endogenously two forms of unzipped are expressed; the 65kD secreted form and the 80 kD membrane-bound form (Ding *et al*., 2011). The goal of this project was to make a detailed analysis of unzipped expression profile and characterize the specific roles of unzipped during the sensory system development of *Drosophila.*

4.1. Expression of *Uzip* determined by an Enhancer Trap insertion

4.1.1. *Uzip* is Expressed in the Eye Imaginal Disc in the 3rd Instar Larval Stage

In order to determine the expression pattern of *Uzip*, we made use of the enhancer trap line (AC783-Gal4) generated in our laboratory. This line carries a PiggyBac[Gal4] insertion in the first intron of *Uzip* gene, therefore expected to reflect the endogenous expression of *Uzip*.

The enhancer trap line was crossed to different GFP reporter lines and the expression pattern was analyzed. The analysis was started in third instar larva, where the sensory organ precursors are found as a monolayer epithelium called imaginal discs. Strong expression of *Uzip* was observed in the eye imaginal disc (Figure 4.1).

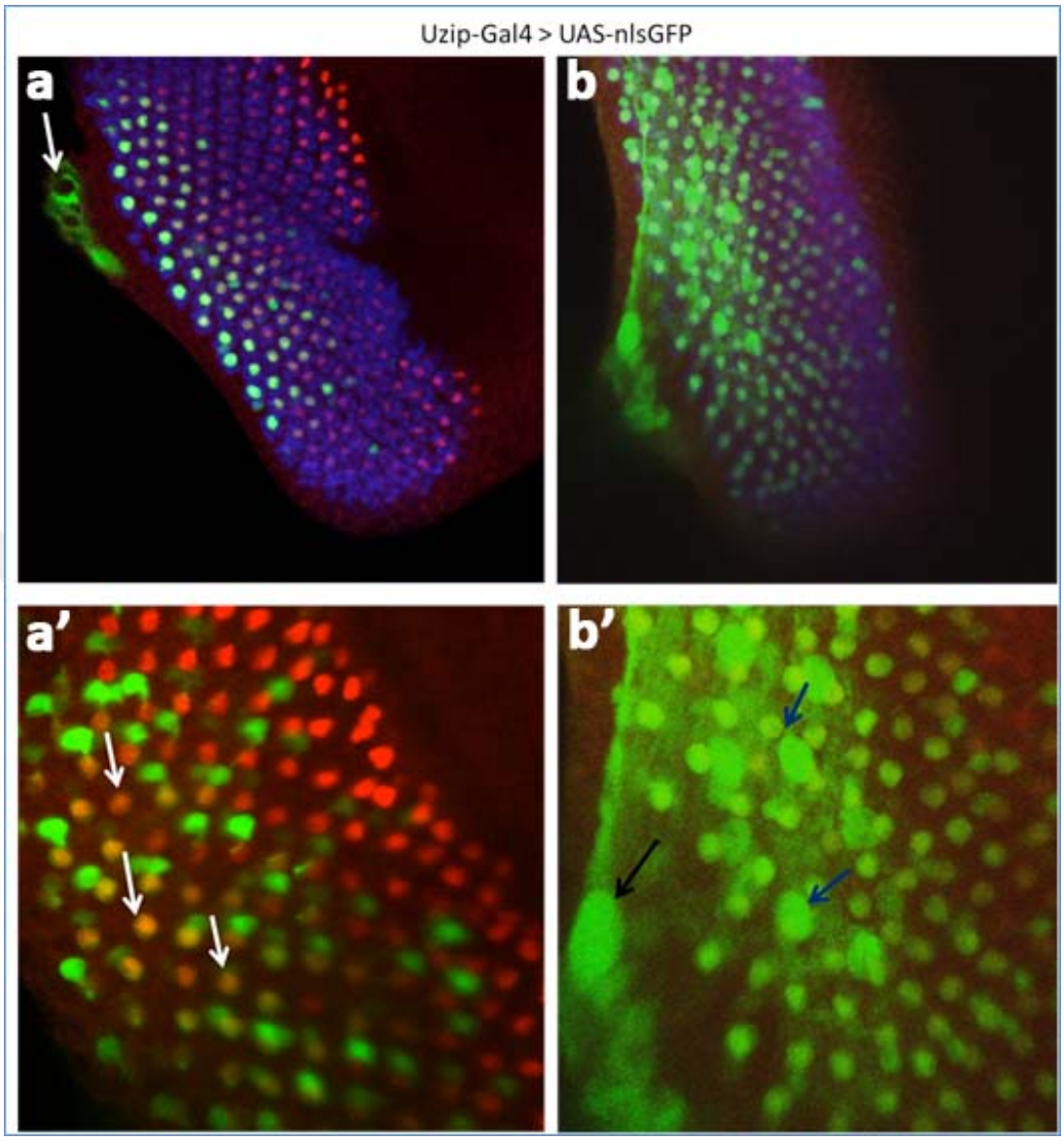

Figure 4.1. *Uzip* expression in the eye imaginal disc of third instar larva. Following antibodies were used: α-senseless (red), α-GFP (green), α-elav (blue) and images were acquired with a confocal microscope. Anterior is to the right.

Uzip is expressed at the posterior of the eye imaginal disc where the early-born photoreceptor neurons are found. Expression is also seen in the optic stalk (see the white arrow in Figure 4.1a) where the photoreceptor neurons fasciculate and project to the brain. Some of the *Uzip* expressing cells, specifically the ones very close to the optic stalk, colocalize with the R8 marker senseless indicating that R8 is a source of some of the *Uzip* protein, but not all (Figure 4.1a'). In the whole stack of the eye imaginal disc (Figure 4.1b),

superficial expression of *Uzip* shows a glia-like pattern (see figure 5.2 in the discussion). *Uzip* is expressed by at least two types of glial cells (Figure 4.1b') in the eye imaginal disc (see the arrows), the first one being carpet glia (black arrow).

Uzip is co-expressed with the pan-neural marker *elav* in the eye imaginal disc, and also with the R8 marker *senseless*. But R8 is not the only source of Uzip in the eye imaginal disc. An additional and much stronger expression not co-localizing with either Elav or senseless was observed, indicating that there is at least one more type of cell expressing *Uzip* in the eye imaginal disc, which is not a photoreceptor cell. This idea became apparent with the more superficial images taken from the eye imaginal discs. There is *Uzip* expression on the surface of the eye imaginal discs, which resembles a glial pattern. Especially the comparatively bigger nucleus that expresses *Uzip* near the optic stalk (see the blacks arrow in Figure 4.1b') may be the carpet glia membrane, which extends around the stalk and separates outer perineurial glia from inner glia (Sillies *et al*., 2007). The rather smaller nucleus near the optic stalk (see the blue arrow in Figure 4.1b') and the other nuclei distributed over the eye imaginal disc that do not co-localize with the neuronal marker *elav,* may belong to the perineural glia and the wrapping glia, respectively.

4.1.2. *Uzip* is Expressed in the Visual and Olfactory Systems During Pupal Development

Expression of *Uzip* was further analyzed at pupal stages where photoreceptors start to acquire their differentiated state. Again, the nuclear-GFP reporter was used to visualize *Uzip* expression, *senseless* for labelling R8 cells and *elav* for labelling all photoreceptor neurons (see Figure 4.2). Uzip shows co-localization with R8 cells in the pupal retina, similar to the expression in photoreceptor neurons in the eye imaginal disc during larval development. Additional *Uzip* expression not co-localizing with the neuronal Elav marker was also observed. Towards the end of pupal development, *Uzip* expression gets weaker in R8 cells and it becomes difficult to detect its expression especially in R8 (Figure 4.2b). No expression of *Uzip* was observed in adult retinas (data not shown).

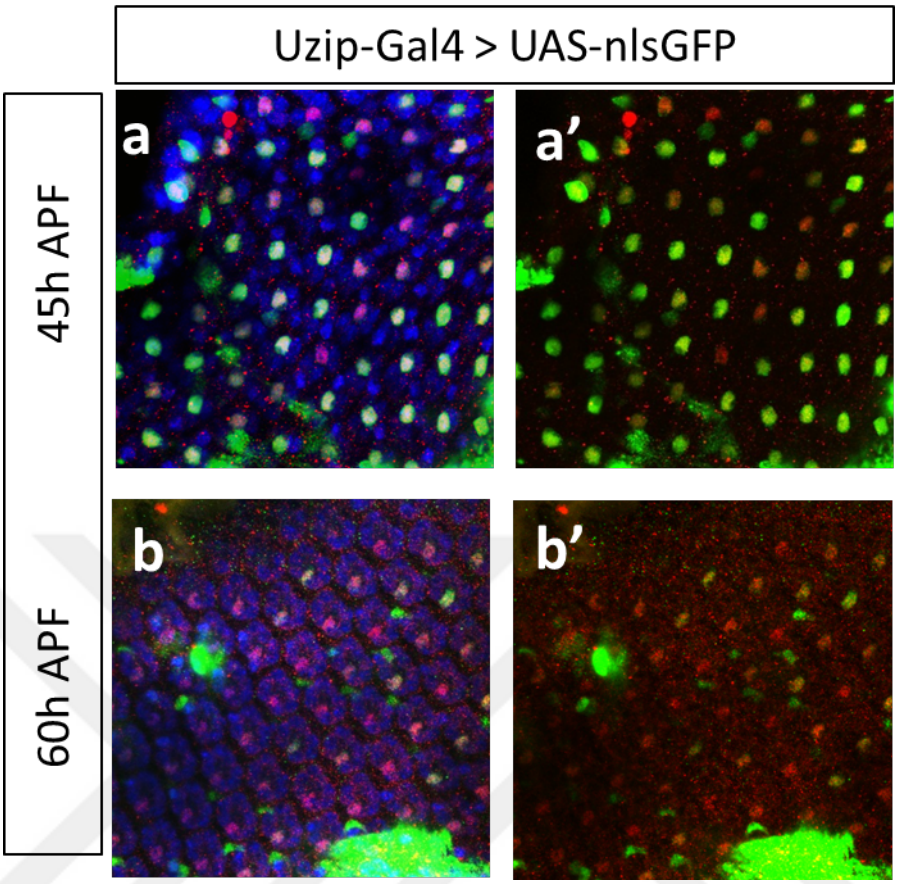

Figure 4.2. *Uzip* expression in the pupal retina of *Drosophila*. (a, a') 45 h pupal retina to label *Uzip* expression by driving the expression of nuclear-localized GFP reporter with the *Uzip* enhancer trap line (AC783-Gal4). (b, b') *Uzip* expression at 60 h APF shows the same R8 co-localized and a non-neural expression pattern, but the GFP reporter expression gets weaker, especially in R8. α-Elav (blue), α-sens (red), α-GFP (green).

In the next round of experiments, Uzip expression was detected by antibody staining in whole mount pupal *Drosophila* brains using a membrane-localized GFP reporter (UAS-mCD8::GFP). Uzip expression dominates around the midbrain, especially in the antennal lobes. It is also strongly expressed in the retina and also in the lamina, medulla and lobula in the optic lobes as well as the SOG (Figure 4.3). The samples were co-stained also with the glial cell marker repo, to see whether Uzip is expressed by glia or not (Figure 4.4).

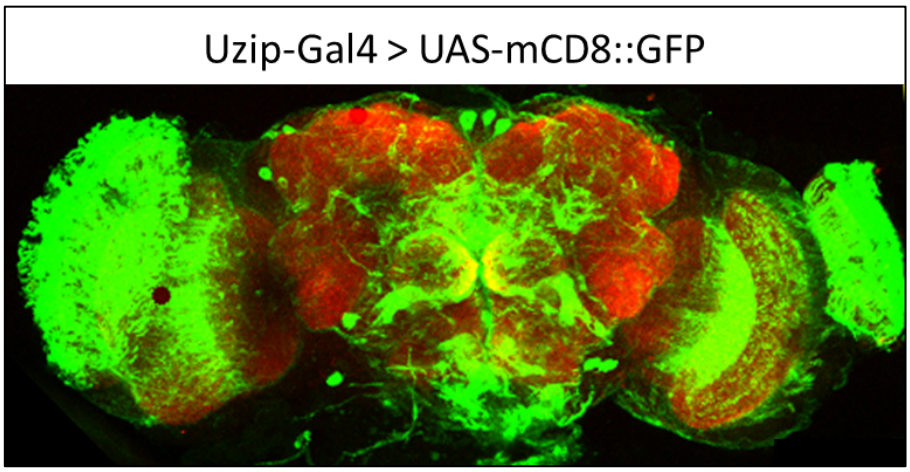

Figure 4.3. Expression of *Uzip* during the late pupal stage (around 72 h APF). Membrane-localized GFP reporter was expressed under the control of the enhancer trap line AC783 and *Uzip* expression was visualized in the whole mount pupal brain by using antibody against GFP (green). Brains were co-stained with NCad (red) to visualize the neuropil.

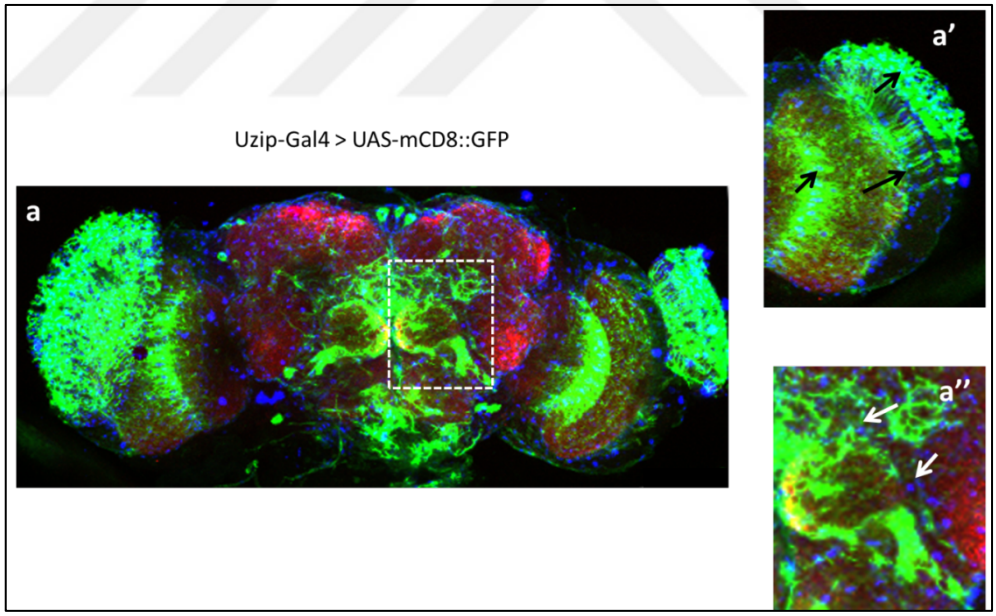

Figure 4.4. *Uzip* expression co-labeled with the glial cell marker *repo*. (a) Whole mount 72 h hour pupal Drosophila brain showing the glial cell nuclei marked by *repo*. (a') magnified image of optic lobe, showing strong *Uzip* expression on retina, medulla and lobula, which co-localizes with the glial nuclei. α-repo (blue), α-GFP (green), α-NCad (red).

Despite the fact that the GFP reporter was localized to the membranes and repo antibody detects only the nuclei of the glial cells, some co-localization was observed on the optic lobes (see the black arrows in Figure 4.4a'). On the other hand, Uzip on the antennal lobes doesn't co-localize with the glial nuclei (Figure 4.4a'').

4.1.3. *Uzip* Expression in the Adult Stage

As the next step, *Uzip* expression was analyzed in the adult *Drosophila* brain, in order to complete the expressional analysis of *Uzip* during development and come up with a conclusion about the possible role of *Uzip* during the development of *Drosophila* sensory systems.

The adult expression pattern analysis was performed by making use of three different GFP reporter lines. First, the nuclear GFP reporter line UAS-nlsGFP was employed and the co-localization of *Uzip* with glial cell nuclei was observed (Figure 4.5).

Then, the membrane-localized GFP reporter line UAS-mCD8::GFP was used in order to determine the whole expression pattern (Figure 4.6). In this way, membranes of the *Uzip* expressing cells could be visualized to get an idea about the possible role of Uzip protein.

Lastly, the pre-synaptic GFP reporter line UAS-sytGFP was used to probe for neuronal expression of *Uzip* (Figure 4.7).

It was observed that the UAS-nlsGFP reporter colocalizes with a subset of glial cells (Figure 4.5). Expression dominates on the optic lobe, antennal lobes and the mushroom bodies (Figure 4.6). And there was a very specific expression observed on the antennal lobes mimicking that of a single class ORN expression (Figure 4.7).

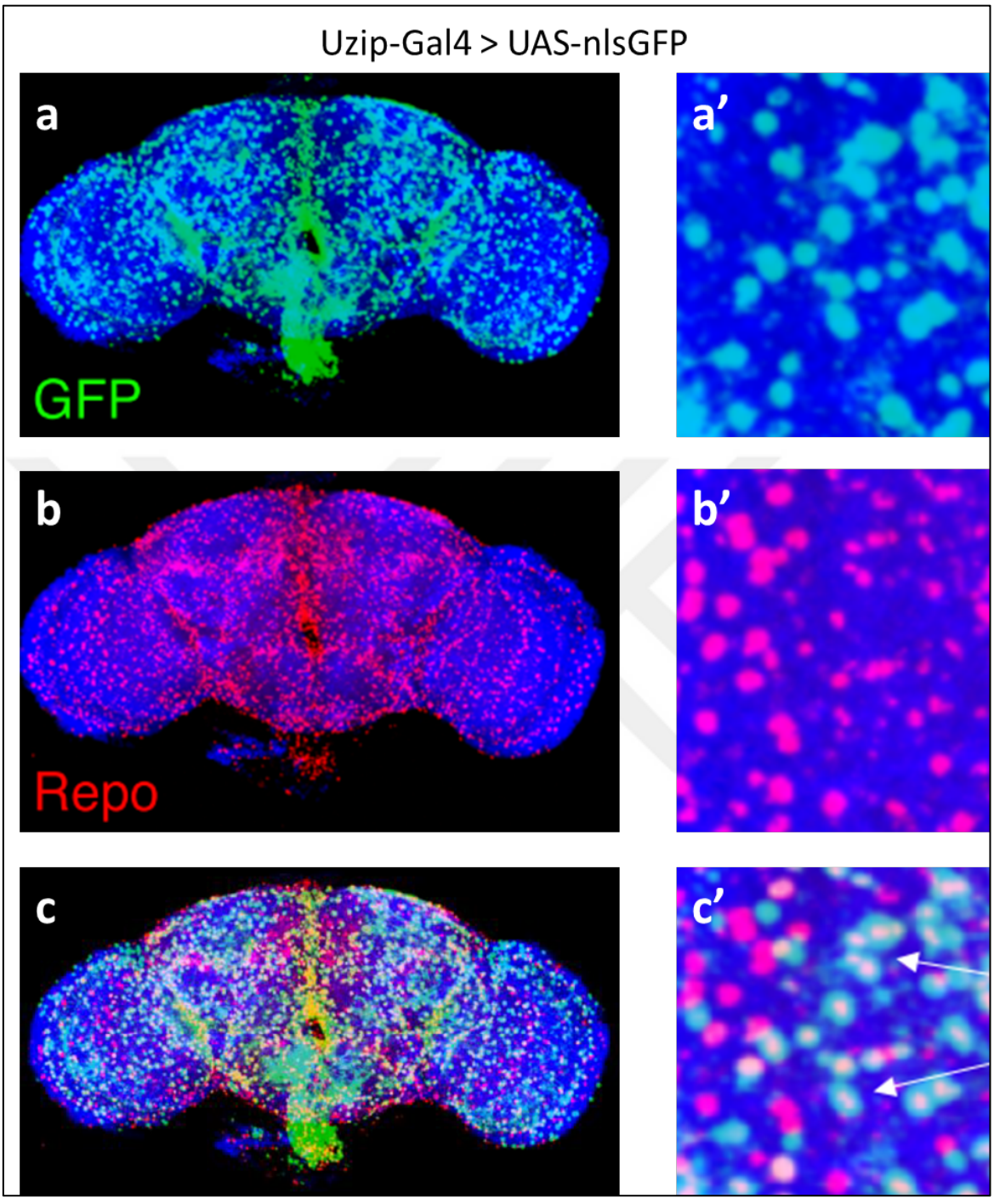

Figure 4.5. *Uzip* is expressed by a subset of glial cells in the adult brain. (a-a') *Uzip* expressing cell nuclei are distributed all over the brain and dominate around the midline. (b-b') Glial cell nuclei, marked by *repo.* (c-c') *Uzip* expression co-localizes with a subset of glial cells. α-NCad (blue), α-GFP (green), α-repo (red).

Figure 4.6. *Uzip* expression labeled by membrane-localized GFP in the adult brain (AC783-Gal4>UAS-mCD8GFP). (a) Uzip expression dominates on the mushroom bodies (a') and on the antennal lobes (a''), which are the olfactory processing centers in the brain. α-NCad (red), α-GFP (green).

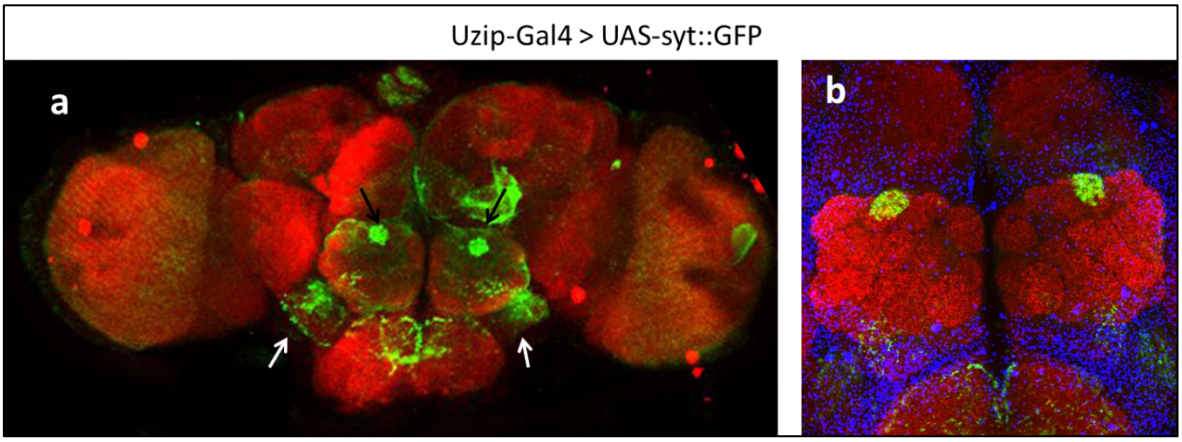

Figure 4.7. *Uzip* expression visualization by pre-synaptic GFP in the adult brain (AC783-Gal4>UAS-mCD8GFP). (a) *Uzip*-expressing pre-synaptic neurons are found in the motor neuron projection centers (white arrows) and on the antennal lobes (black arrows). (b) Pre-synaptic GFP marker sytGFP shows distinct expression on the antennal lobes, most possibly specific to only one glomerulus. α-NCad (red), α-GFP (green), toto3 (blue).

The last three experiments together indicate that also in the adult stage, similar to the larval and pupal stages, glial cells are the main source of Uzip (Figure 4.5). This is consistent with the expression of *Uzip* in the embryonic nervous system as observed by Ding *et al.* (2011). In the adult stage, the most prominent expression is seen in the olfactory system and mushroom bodies (Figure 4.6), suggesting that it could have a role in olfactory system development. It is also detected on the antennal lobe, in a single glomerulus. Therefore, it is expressed in a subtype-specific manner in the ORNs (Figure 4.7). The expression of *Uzip* is also observed in the motor-neuron projection centers (Figure 4.7., white arrows). Since Uzip is a cell adhesion molecule (Ding *et al*., 2011), we hypothesized that it could have a role in the projection of ORNs to the antennal lobe.

4.2. Generation of Uzip Transgenic Lines tagged with Flag::HA and eGFP

Unzipped was identified in an enhancer-trap screen for genes that are expressed in photoreceptor subsets and expression was observed in subsets of neurons and glia. To confirm that the enhancer trap reflects endogenous unzipped expression we set out to determine its expression patterns using different methods. While the generation of an unzipped specific antibody is on its way, I set out to determine the expression of unzipped by tagging the endogenous protein with various tags using BAC recombination technology.

In order to tag *Uzip* protein and express it from its endogenous locus, we made use of homologous recombination and BAC transgenesis technology. We used P[acman] artificial vectors that have been generated from pieces of the genomic DNA of Drosophila and made available through the Pacman-Fly web-site. BAC clones were selected from the PACMAN website according to suggestions mentioned in Venken *et al*. (2007 and 2010). The BAC clone 174H16 from the CH322 library of the P[acman] vectors was ordered from pacmanfly.org. This BAC clone is 22048 bp long and contains about 1.5kb from the upstream of the Uzip gene and about 2.4 kb from the downstream. Therefore, this BAC clone is expected to include all the regulatory regions of the Uzip gene. Individual BAC clones are inserted into the artificial P[acman] vector by restriction-ligation at the BamHI site located at 7617 bp (Figure 4.8)

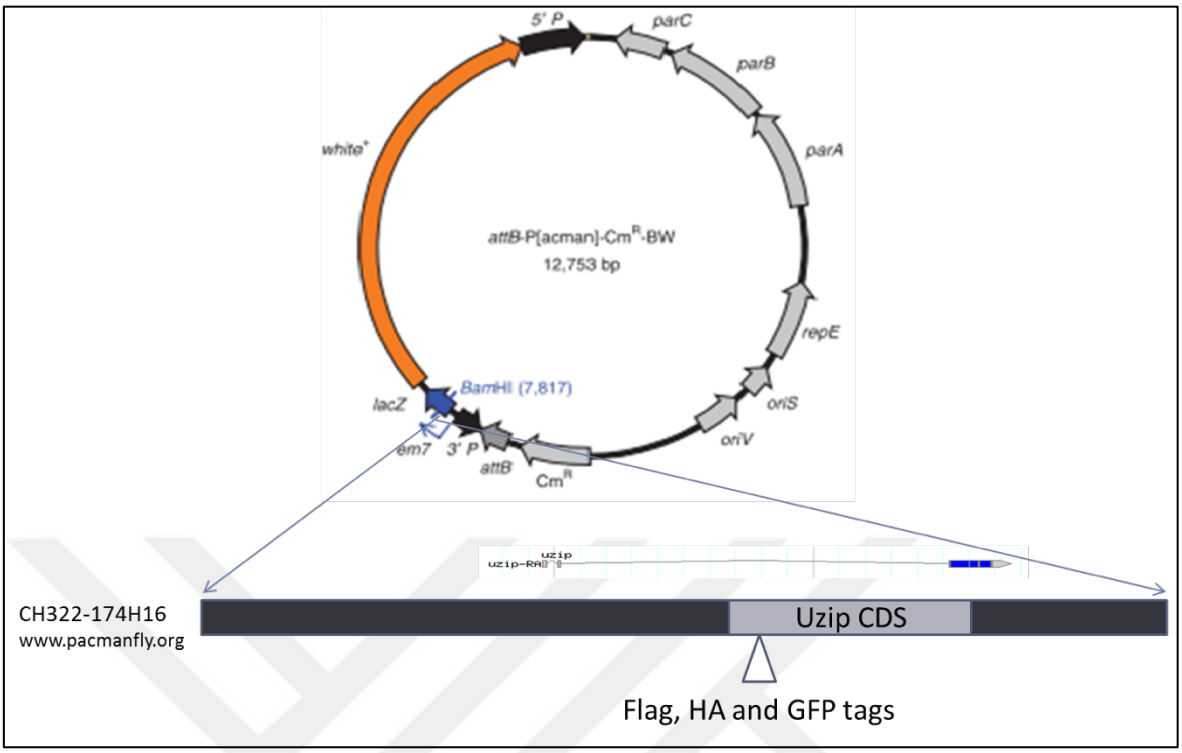

Figure 4.8. Map of the P[acman] plasmid. Individual BAC clones are inserted into the P[acman] plasmids by the restriction-ligation from the BamHI cut-site. The BAC clone CH322-174H16 includes the whole sequence of Uzip gene together with some upstream and downstream regions.

Proteins can be tagged at various positions in the protein. They can be tagged at the N-, or C-terminus or inside the coding region. As unzipped appears to have two isoforms, one secreted and one membrane-bound form, the tagging of both isoforms was intended. In order not to interfere with the proper secretion of unzipped, the tag was introduced after the signal peptide sequence. This should ensure that the protein is localized correctly and the tag will not be removed during cleavage.

4.2.1. Generation of Flag-HA tagged *Uzip* Transgenic Construct

In order to generate the recombination fragment of the Flag::HA-tagged Uzip construct, a three-step PCR was performed (Figure 4.9). In the first step, the upstream homology region including the signal peptide was amplified. A specific oligonucleotide primer was used as the reverse primer (Uzip-FH-overlap_R), which was 60 bases-long, and encoded the Flag polypeptide, the linker and also half of the HA polypeptide coding

sequences at the 5' in order to create overlapping arms for the next round of PCR (See Figure 4.9, PCR1). Meanwhile, a second PCR reaction was perfomed to amplify the downstream homology region. This time, the forward primer was with some of the HA sequence and also a linker after HA (Figure 4.9, PCR1). For both PCR1 and PCR2, the P[acman] plasmid was used as a template. As the last step, products of PCR1 and PCR2 were used together as template, which were expected to overlap and behave as a single template. PCR3 was performed to obtain the fragment that is going to be recombined into the BAC clone.

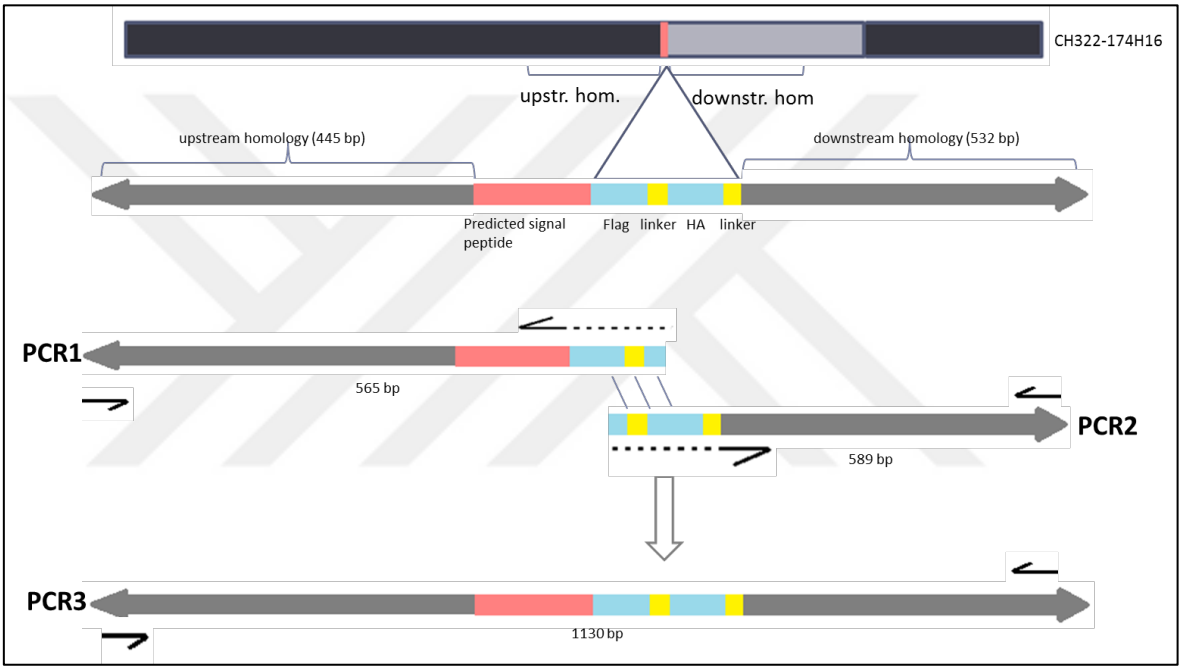

Figure 4.9. Scheme of the preparation of recombination fragment for the generation of Flag::HA tagged Uzip construct.

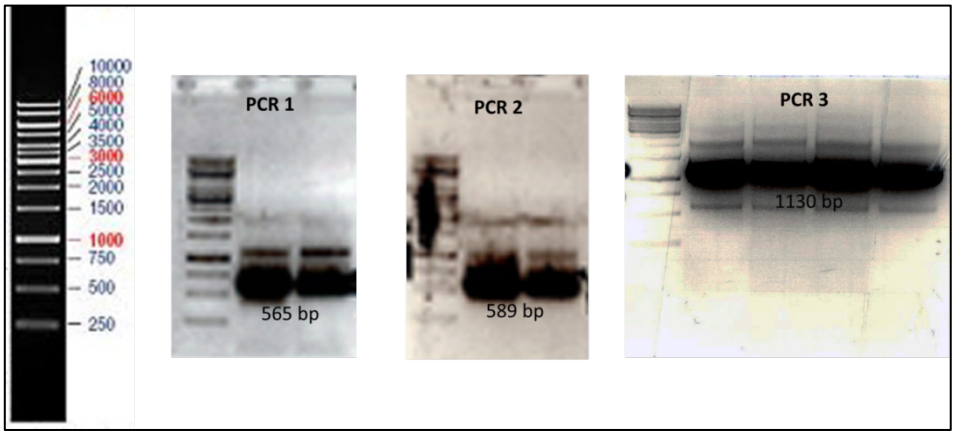

Figure 4.10. Gel photos of the Flag::HA tagged *Uzip* construct.

4.2.2. Generation of Flag-HA-GFP tagged *Uzip* Transgenic Construct

In order to generate the recombination fragment of the Flag::HA::GFP tagged Uzip construct, five step PCR was performed (Figure 4.11). The strategy was the same with the Flag::HA tagged construct. In the first step, the upstream homology region including the signal peptide was amplified. A specific long oligonucleotide primer was used as the reverse primer (Uzip-FH-GFP-overlap_R) which had homology to the HA sequence, GFP coding sequence and a linker that was inserted in between (See Figure 4.11, PCR4). PCR was performed by using the product of PCR3 as a template. Meanwhile, the GFP coding sequence was amplified from an eGFP including plasmid. Products of PCR4 and PCR5 were used as the template of PCR6, in order to obtain the left half of the recombination fragment. PCR7 reaction was perfomed to amplify the downstream homology region. This time, the forward primer with a homology to the GFP coding sequence and also a linker after GFP was added (Figure 4.11, PCR7). As the last step, products of PCR6 and PCR7 were together used as a template in order to obtain the final fragment to be recombined into the BAC clone.

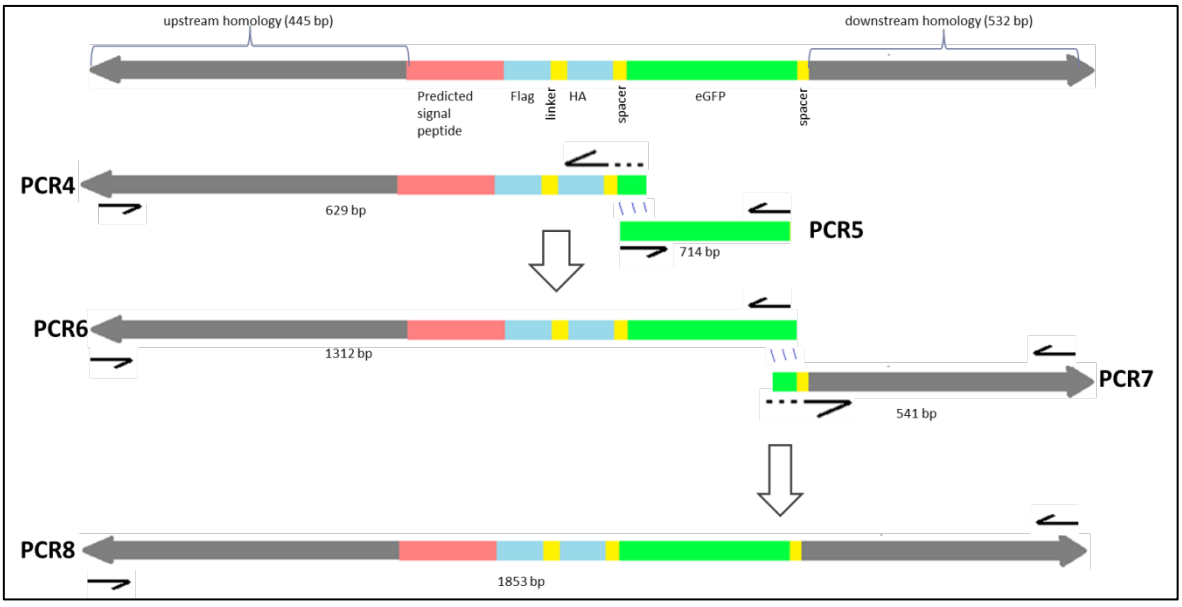

Figure 4.11. Scheme of the preparation of recombination fragment for the generation of Flag::HA::GFP tagged *Uzip* construct.

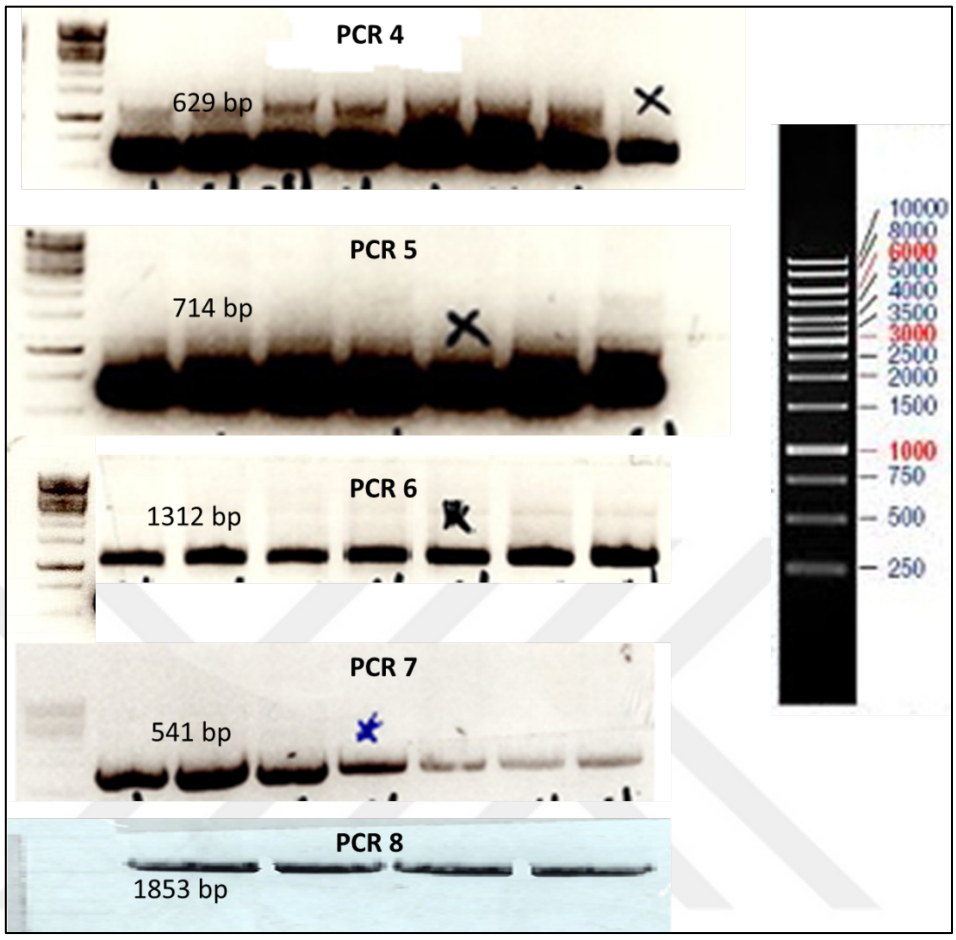

Figure 4.12. Gel photos of Flag::HA::GFP tagged *Uzip* construct.

4.2.3. Analysis of the Flag::HA::Uzip Transgenic Construct

For all the expression studies shown here the enhancer-trap line AC783-Gal4 was used in order to determine the *Uzip* expression pattern. Because of the fact that we didn't have an antibody against *Uzip* in hand, we generated a Flag::HA-tagged transgenic *Uzip* line, which was recombineered on a BAC and thus would show Uzip expression under the control of its endogenous promoter and would reflect the endogenous expression pattern of *Uzip.*

First, a Western blot was performed from the protein extract of *Drosophila* heads. All three lines, which are the progeny of three separate recombinant flies, were used for the analysis. α-HA antibody was used to detect the *Uzip* protein, expressed from the transgenic locus. Two different bands were observed, which resembled the two different forms of endogenous *Uzip* protein. The secreted form at around 65 kD and the membrane-bound form at around 80 kD, respectively (Figure 4.13).

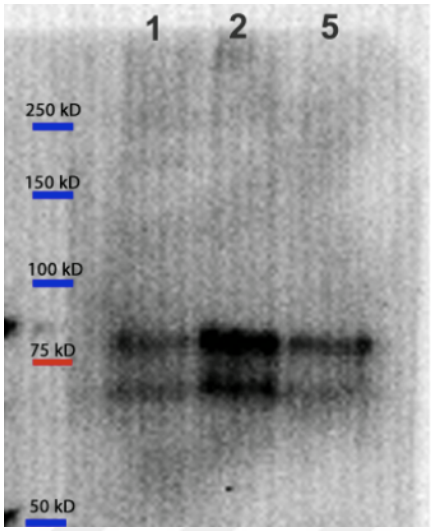

Figure 4.13. Western blot of Flag::HA::Uzip constructs. Each three line of Flag::HA::Uzip genotype express the transgenic Uzip protein as two forms, at ~65 kD and ~80 kD respectively (Protein loading amounts are not equal).

Next, we examined the adult brains of FLAG::HA-tagged Uzip carrying flies through antibody staining. Brains were dissected and stained with an anti-HA antibody (Figure 4.14).

Expression was roughly detected all over the brain, but didn't show a specific pattern. It was localized to the mushroom bodies, supporting previous data obtained through the analysis of the expression of the enhancer-trap line. But neither on the optic lobe, nor on the antennal lobes, a very specific pattern of expression was observed. Only in the medulla and to some extent in the lobula, expression was detected but did not resemble the enhancer-trap line completely. On the other hand, at the antennal lobe periphery and the SOG, expression was detected more specifically than the other regions of the brain.

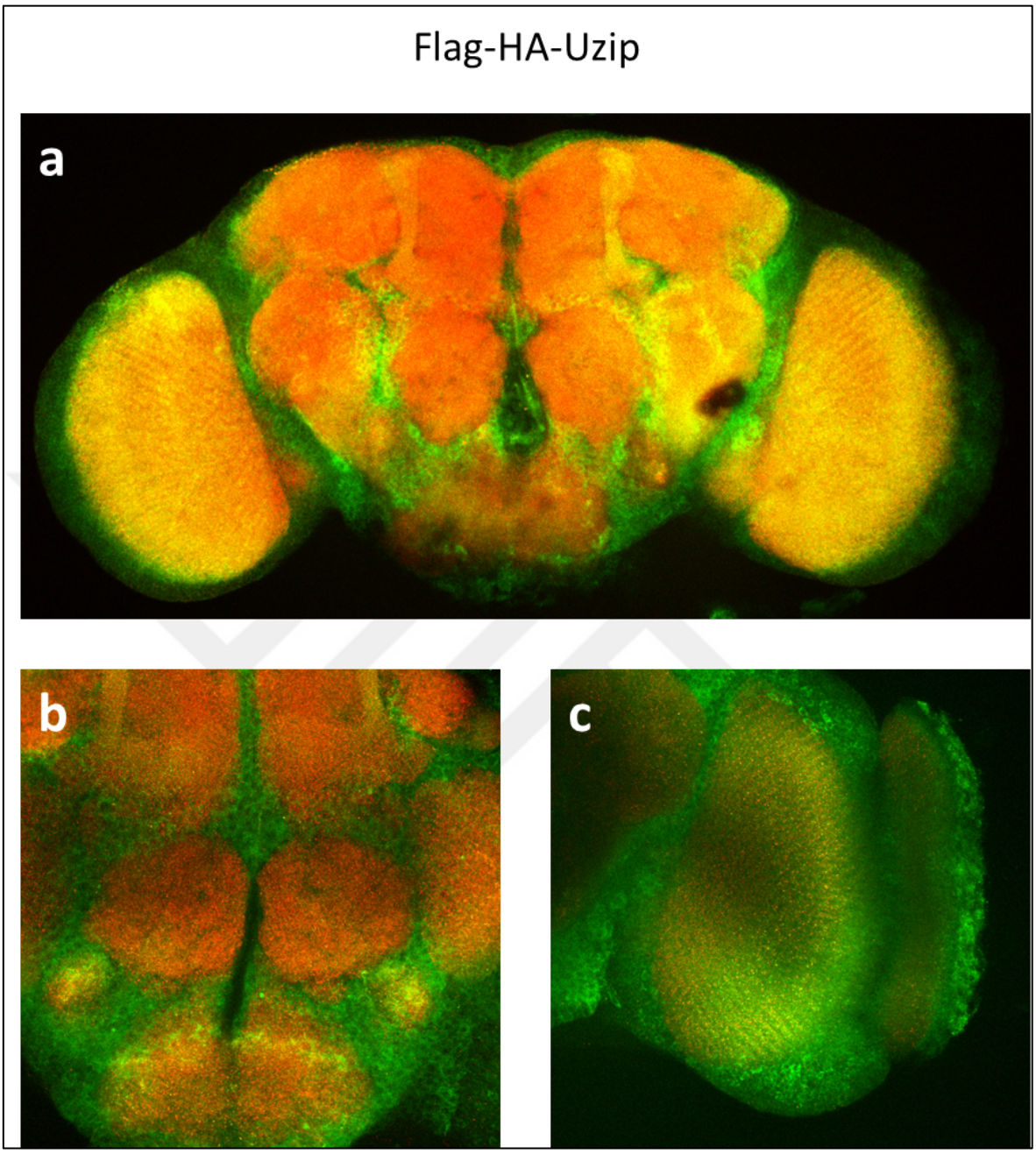

Figure 4.14. Expression analysis of Flag::HA-tagged Uzip constructs using antibody against the HA polypeptide. (a) *Uzip* expression visualized by immunostaining of HA all over the brain, and did not show a specific pattern, except the co-localization with the mushroom bodies. (b) Magnified image of antennal lobes (c) Magnified image of the optic lobe. α-Nc82 (red), α-HA (green).

4.3. Functional Analysis of Uzip in the *Drosophila* Olfactory System

The strong expression of unzipped in the olfactory system led to the hypothesis that unzipped may have a role in guiding ORNs to the antennal lobe. In order to assess its role in olfactory system development several experiments were performed:

(i) a more detailed analysis of unzipped expression in the olfactory system
(ii) analysis of loss-of function alleles of unzipped
(iii) analysis of unzipped function when unzipped is down-regulated by RNAi
(iv) mis-expression of unzipped
(v) cell-specific rescue experiments

4.3.1. Experiments for the Analysis of *Uzip* Expression in the Olfactory System

In order to find out if *Uzip* has a specific role in the development of the *Drosophila* olfactory system, *Uzip* expression was analyzed in the olfactory organs and antennal lobes in more detail. Analysis was started at mid-pupal stages (Figure 4.15), where most connections have been established between peripheral olfactory organs and the antennal lobes and glomeruli have already formed and are easily distinguished.

During the mid-stages of pupal development, Uzip is detected at the antennal lobes (Figure 4.15) and also in the antenna (Figure 4.16). At least some of this expression appears to be neuronal, since *Uzip* co-localizes to some of the individual glomeruli (see the arrows in Figure 4.15b'). *Uzip* is seen also on the antennal nerve (see arrow in Figure 4.15b), where the ORNs projecting from the antenna to the brain fasciculate before entering the antennal lobe. A glomerulus-specific expression of *Uzip* was also observed in the adult brain previously (Figure 4.7b), indicating that only one of the ORN subtypes expresses *Uzip* in the adult stage.

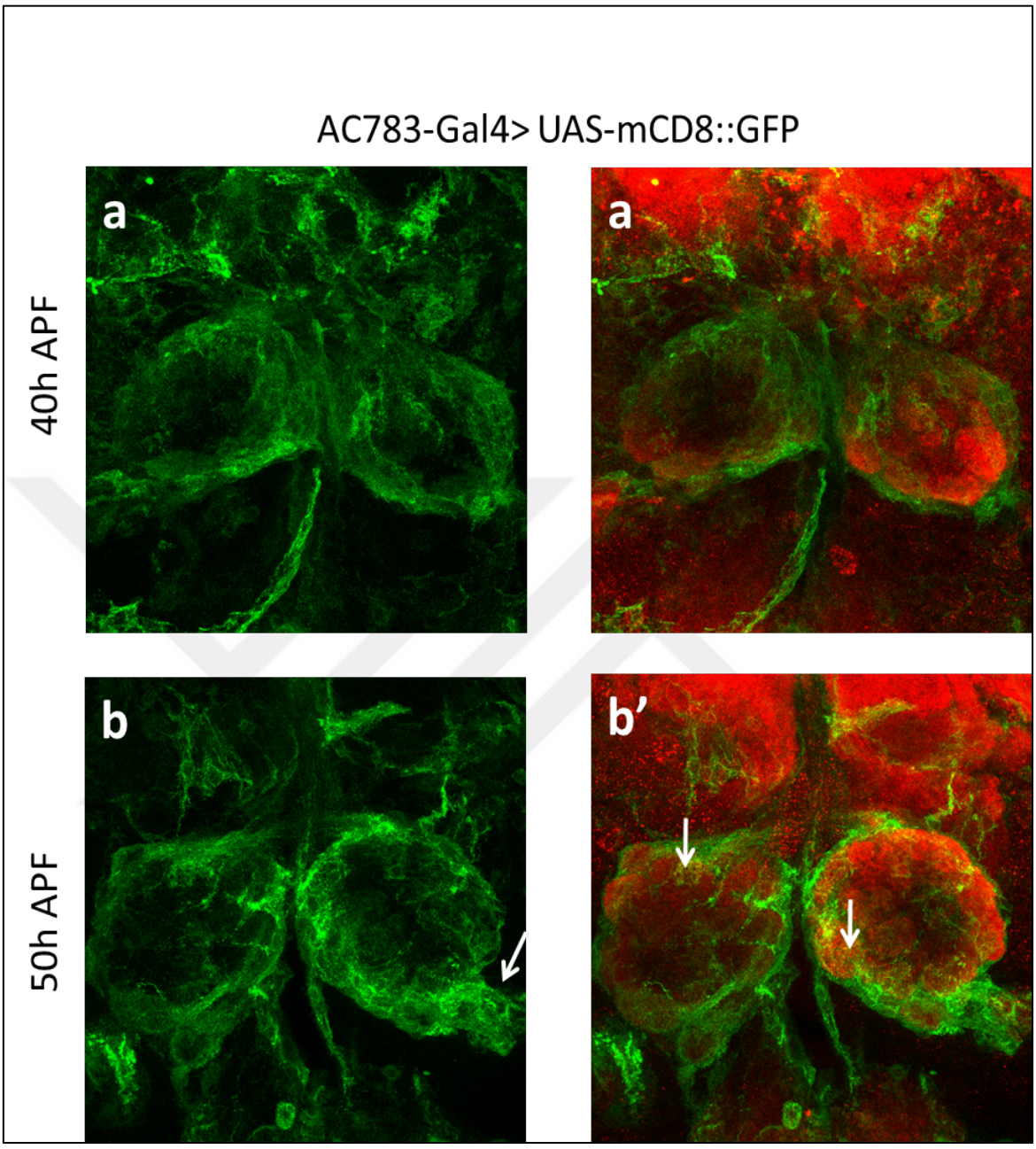

Figure 4.15. *Uzip* expression in the mid-pupal antennal lobes. (a-a') At around 40h APF, Uzip is detected at the outer borders of the antennal lobes and at the midline. (b) At around 50h APF, when the distinct glomeruli are distinguishable, (b') Uzip is detected also specifically on some of the glomeruli (see the arrows). α- Ncad (red), α-GFP (green).

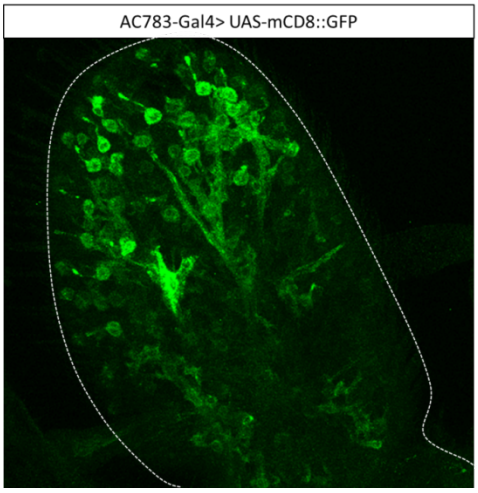

Figure 4.16. Uzip is expressed in the antenna at ~50h of pupal development. α-GFP (green).

Taken together, these results indicate that there is at least one class of ORN expressing *Uzip* during development, and there is another and more diverse source of *Uzip*, most possibly of glial origin. Therefore, to confirm the source of Uzip expression, the FLP-FRT technique (Golic *et al*., 1989) was used, which is a commonly used technique to label subsets of cells by generating individual clones by inducing recombination events in single cells and meanwhile labeling these. The UAS>CD2>CD8::GFP (> stands for FRT) cassette is used in combination with eyeless-Flip (eyFlp), which allows expression of flippase under the control of the eyeless promoter. From the literature, it is known that in the olfactory system, eyeless is expressed only by neurons, but not by glial cells (Callaerts *et al*., 2001). Thus, whereever eyFlp is active, it will cause FRT recombination and flip-out the CD2 sequence that is located between the two FRT sites together with the stop codon that is present right before the second FRT site. Therefore, in neurons, through the activity of eyFlp, expression of CD8::GFP would occur and neurons could be visualized by the GFP marker fused to the promoter of CD8. On the ther hand, in glia, eyFlp would be inactive and CD2 expression would be observed instead of CD8::GFP, thereby labeling the glial cells using an antibody against the CD2 epitope.

Usage of the flip-out technique revealed that *Uzip* is expressed in a ORN subtype-specific manner (Figure 4.17). Besides the antennal ORN class (see the white arrow) that was also observed with the pre-synaptic GFP marker, there was also *Uzip* expression in a

few of the maxillary palp ORN classes (see the blue arrows in Figure 4.16). Glial expression of Uzip was detected by using an antibody against CD2.

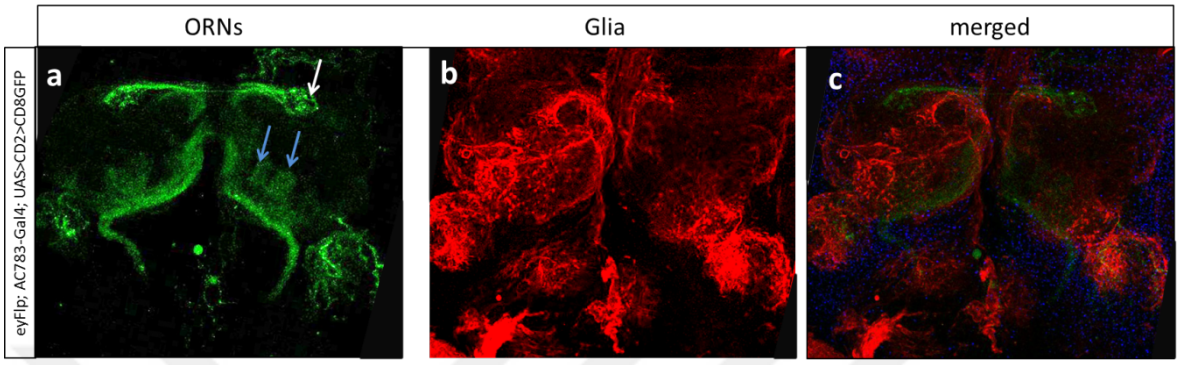

Figure 4.17. Differential labeling of *Uzip* expression in ORNs and glia using the flip-out technique. (a) *Uzip* is expressed in a single subtype of antennal ORNs (white arrow) and also some of the maxillary palp ORNs (blue arrows). (b) *Uzip* is also detected in the glial cell membrane labelled by CD2. (c) Merged image show the whole *Uzip* expression pattern in the antennal lobes. α-GFP (green), α-CD2 (red), toto3 (blue).

After this observation, the expression of Uzip was analyzed in the antenna and maxillary palps of adult *Drosophila* where ORN cell bodies are located. As predicted, Uzip was expressed in a subset of antennal ORNs and some of the maxillary palp ORNs (Figure 4.18).

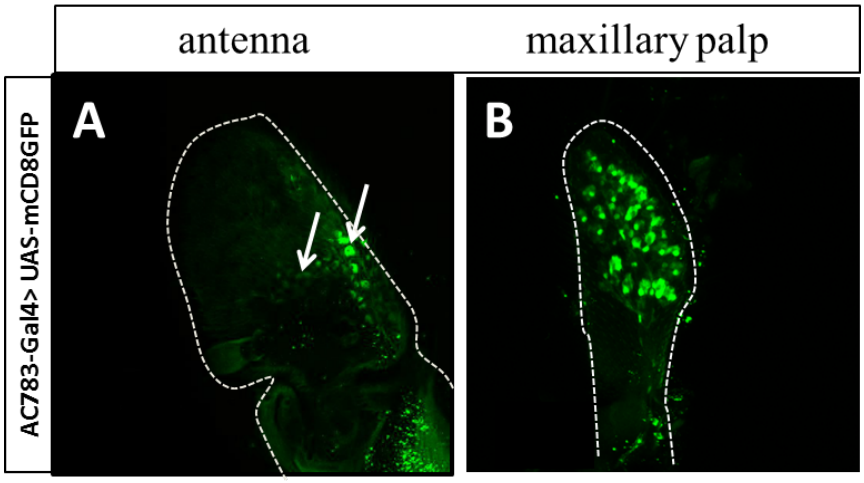

Figure 4.18. Uzip expression in the adult antenna and maxillary palps. α- GFP (green).

In the antenna, Uzip is expressed in a single subset of ORNs, (see the white arrows in Figure 4.18), while a more extensive expression was observed in the maxillary palp. To assess if the observed expression is of neuronal or glial origin, antibody stainings were performed using the relevant markers. Unfortunately, it is not possible to perform conclusive antibody stainings in the antenna, as antibodies cannot penetrate the cuticle. Therefore, analysis was performed in the maxillary palp using the neuronal marker ElaV (Figure 4.19). This analysis showed that expression of Uzip colocalizes with neurons in some instances but not all, indicating that non-neuronal cells also express unzipped.

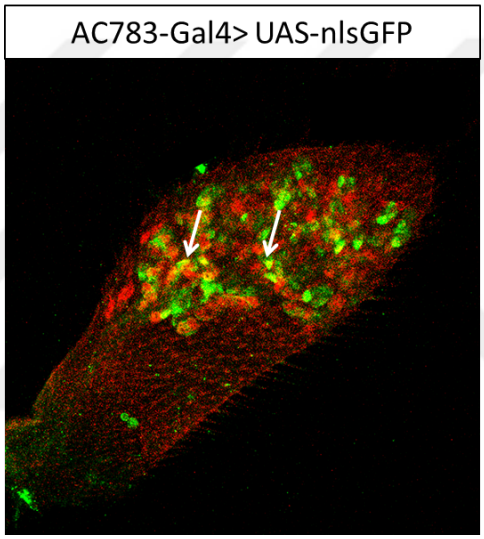

Figure 4.19. Uzip expression in the maxillary palp co-localizes with some of the ORNs (see the white arrows) but not all. α-GFP (green), α-elav (red).

In summary, the results of part 4.3.1 show that *Uzip* is expressed in subsets of ORNs and by glia in the *Drosophila* olfactory system. ORN subsets were observed as only one subset of the antennal ORNs and at least a few of the maxillary palp. *Uzip* expression is also observed in glia wrapping individual glomeruli on the antennal lobes, as well as in antenna and maxillary palps. Taken together, these results strongly indicate a possible role of *Uzip* in the projection and pathfinding of ORNs. To test this hypothesis the projection of ORNs were analyzed in an *Uzip*-deficient background.

4.3.2. Identification of the Antennal ORN Subtype Expressing Uzip

It was previously shown that the expression of the Uzip enhancer-trap line is very specific to a single subset of antennal ORNs (Figure 4.7 and Figure 4.17). Most of the ORN classes are already annotated to their respective glomeruli (Couto *et al*., 2005; Fishilevich *et al*., 2005). From the position of the Uzip glomerulus, we tried to determine the antennal ORN subtype, which strongly expresses *Uzip*. There were two candidates, OR2a and OR56a (Figure 4.20). Since we didn't have properly working OR2a reporter lines, we decided to use OR19a, which is expressed in the same sensillum with OR2a, and whose glomerulus is located right behind the OR2a glomerulus (see the glomerulus map of the antennal lobe in figure 4.20a).

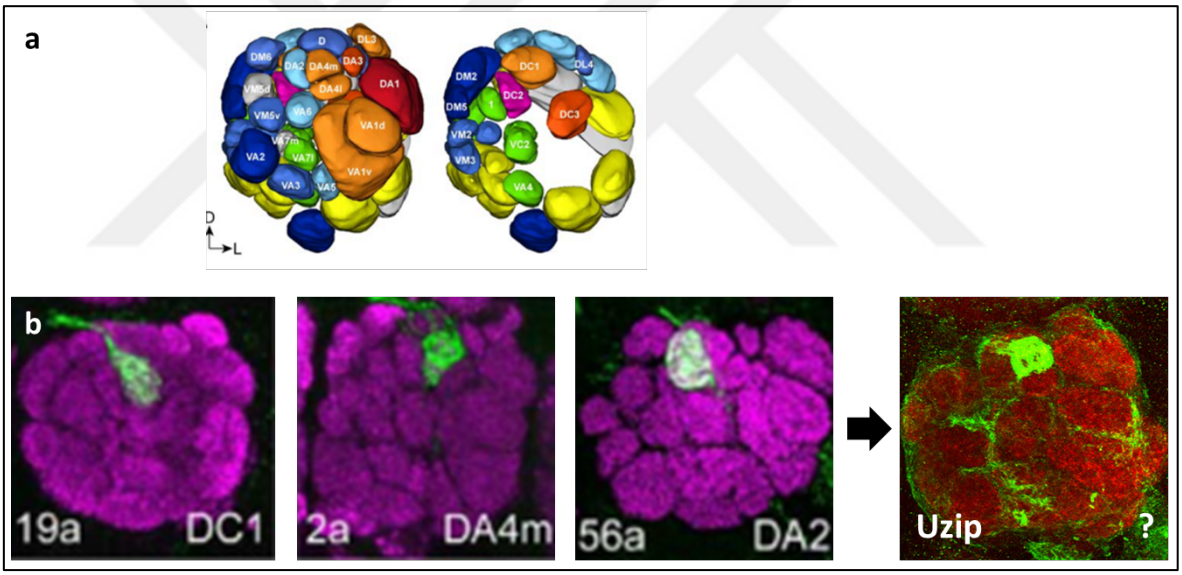

Figure 4.20. Determination of the position of Uzip expressing ORN glomeruli. OR2a and OR19a are the two candidates for the antennal ORN class, expressing *Uzip.* Due to the lack of available OR2a tools, OR19a was used, since the OR19a glomerulus (DC1) is just behind the OR2a (DA4m) glomerulus (a) (Figures taken from Couto *et al*., 2005).

Initially, the relative positions of OR19a and Uzip glomeruli were compared (Figure 4.21a). The position of the Uzip glomerulus, relative to the OR19a glomerulus, was mimicking that of OR2a. Later, the relative positions of the cell bodies of ORNs expressing OR19a and Uzip were compared. Although ORNs of the same sensillum are located next to

each other in the antenna, this was not the case for OR19a and *Uzip* expressing ORN (Figure 4.21b). Therefore, the possibility that OR2a could be expressing *Uzip* was excluded.

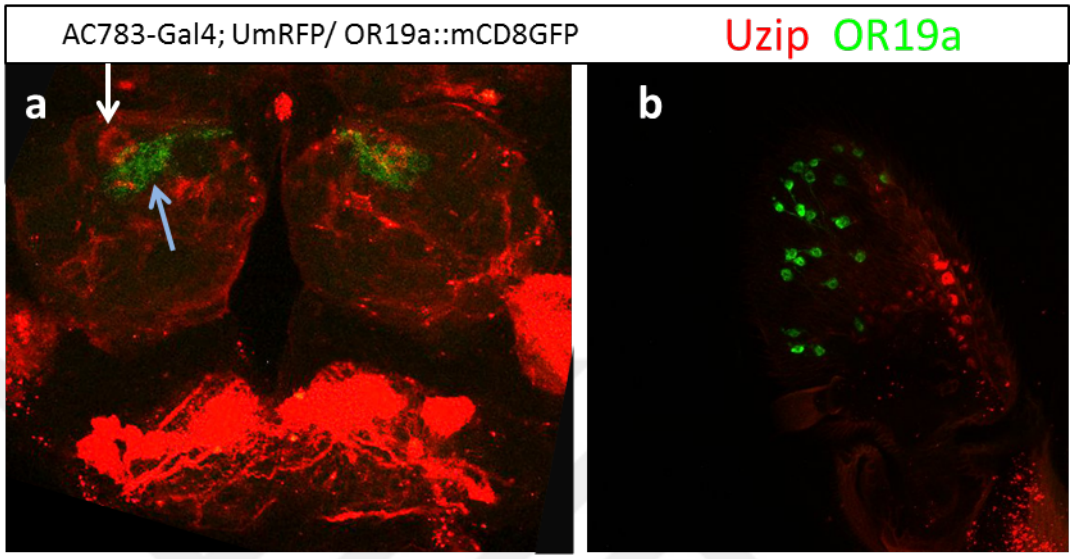

Figure 4.21. Comparison of *Uzip* expression to OR19a expression in brain and antenna. (a) Uzip expressing ORN glomerulus (white arrow) is located right next to the OR19a glomerulus (blue arrow). (b) OR19a and Uzip are expressed at opposite sites in the antennal lobe. Endogenous RFP and GFP expression were visualized using confocal microscopy.

After excluding the possibility that Uzip-expressing ORN might be OR2a, *Uzip* expression was compared to OR56a expression, which was the second candidate (Figure 4.22.). Driving UAS-syt::GFP with AC783-Gal4 and OR56-Gal4 at the same time resulted in two distinct glomeruli, which are next to each other (Figure 4.22a). Also, when the expression patterns in the antenna were compared, they were not similar to each other (Figure 4.22b-c).

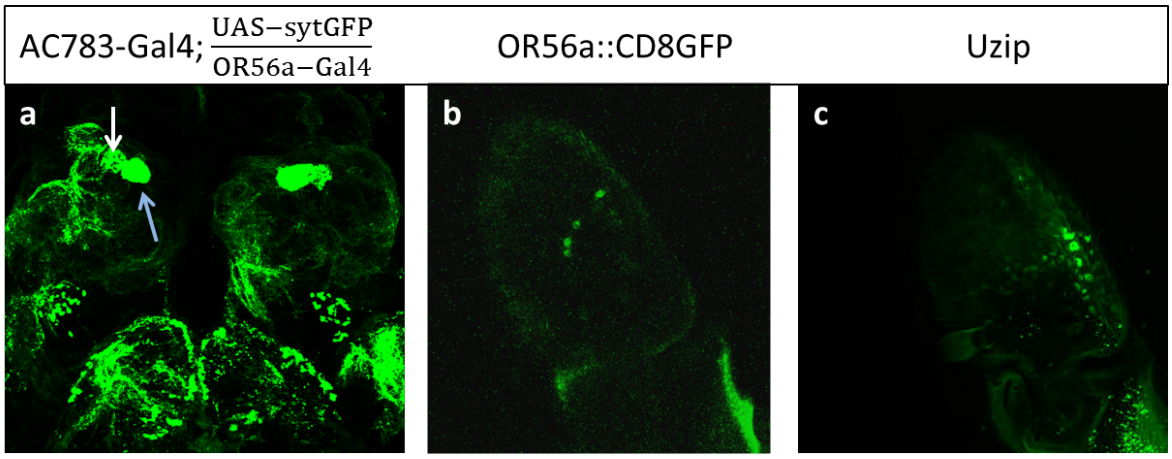

Figure 4.22. Comparison of *Uzip* expression to OR56a expression in the brain and the antenna. (a) Uzip expressing ORN glomerulus (white arrow) is located right next to the OR56a glomerulus (blue arrow). (b-c) OR56a and *Uzip* expression does not colocalize in the antenna. α-GFP (rabbit).

4.3.3. Loss of Function Experiments: Mutant Analysis

In order to uncover the role of *Uzip* in the projection of ORNs to the antennal lobe, we checked the projection pattern of single ORN subtypes, in the *Uzip* mutant background (Figure 4.23). We used the loss of function allele UzipD43 (Ding *et al*., 2011) for the analysis. The mutant was generated by P-element mobilization method by the clear excision of two FRT-sites encovering the *Uzip* coding region.(Ding *et al*., 2011). Three subtypes of antennal ORNs and two subtypes of maxillary palp ORNs were selected for this analysis.

For the analysis of the projection of antennal ORNs, OR22a-Gal4, OR47a-Gal4 and OR47b-Gal4 were used to label the corresponding ORNs. In case of maxillary palp ORNs, OR46a-Gal4 and OR 59c-Gal4 were used.

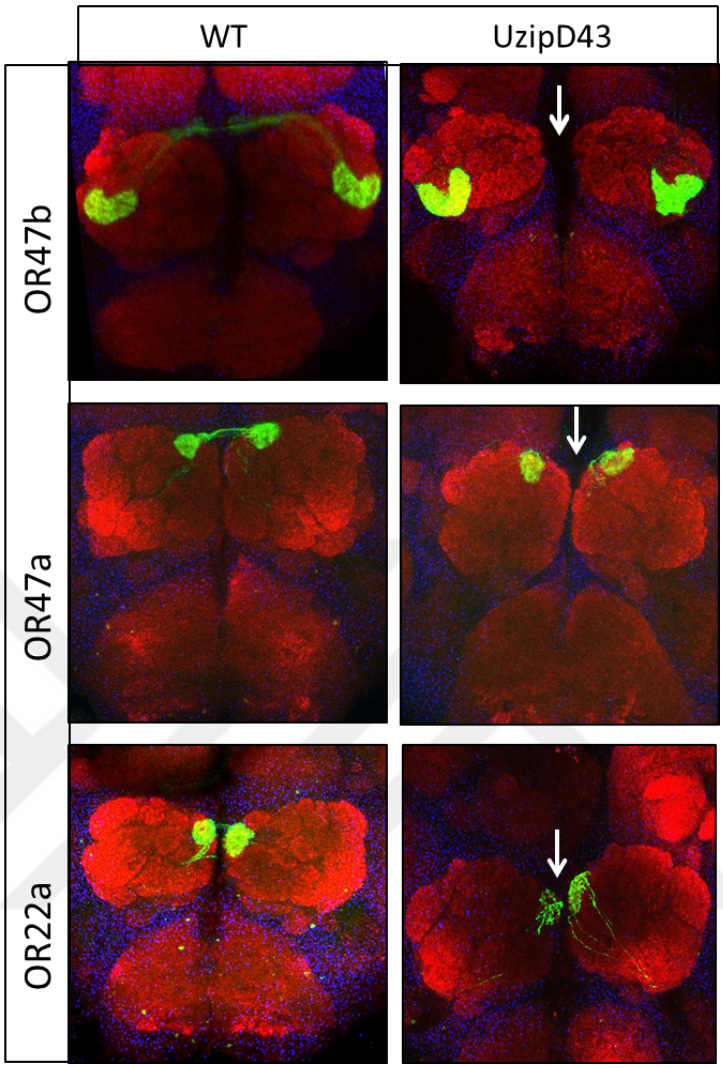

Figure 4.23. Projection of antennal ORNs to the antennal lobe in Uzip mutant background. Although ORNs are able to project to the corresponding glomeruli on the ipsilateral site, they cannot cross the midline to project to the contralateral side (see the white arrows). α-GFP (green), α-NCad (red), toto3 (blue).

In the wild type background ORNs normally converge to form a single glomerulus on the ipsilateral side of the antennal lobe and then project further to the contralateral side, where they contact the corresponding glomerulus (Fig. 4.23, left panel). Reporter lines of OR22a, 47a and 47b were crossed into the Uzip mutant background and expression of GFP was observed after antibody staining against GFP to visualize the particular OR subset, NCad to visualize the neuropil and toto-3 to stain nuclei. The analysis showed that the projection of single subtypes of ORNs to the antennal lobe happened correctly on the

ipsilateral side, however, while they did not project to the contralateral site at all (Figure 4.23).

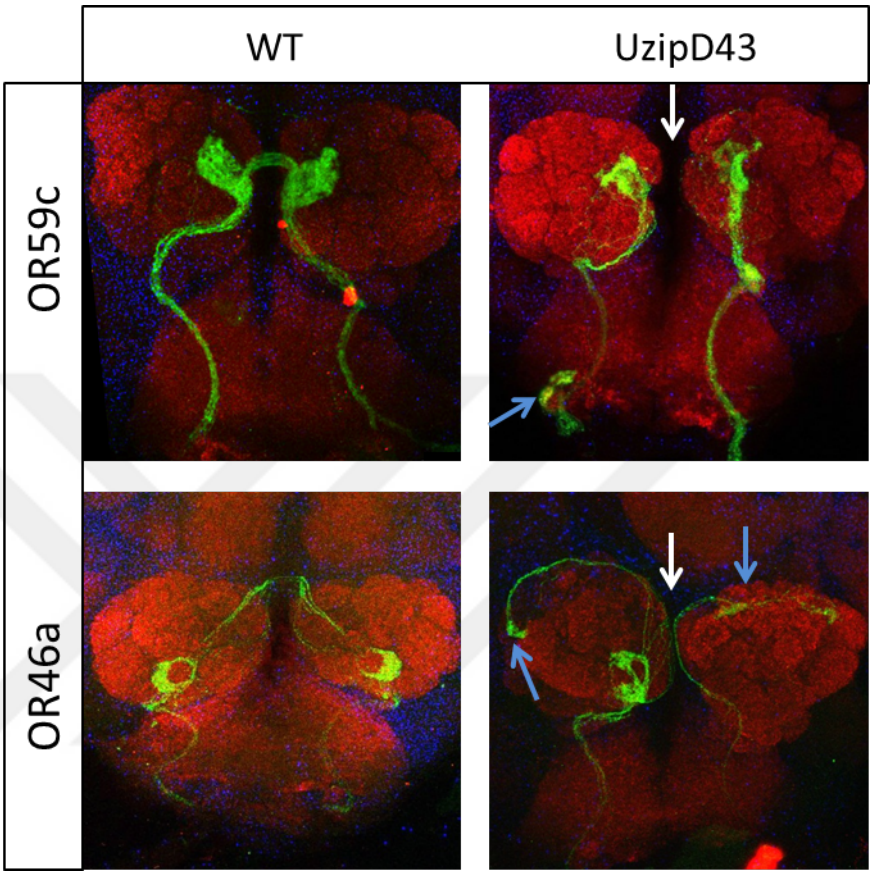

Figure 4.24. Projection of maxillary palp ORNs to the antennal lobe in the background of Uzip loss-of-function. Maxillary palp ORNs target the corresponding glomeruli, but cannot cross the midline to project to the contra-lateral site (white arrows). In addition, some get stuck on the SOG and some ectopic glomerular innervation (blue arrow) was observed. α-GFP (green), α-NCad (red), toto3 (blue).

For the ORN subclasses of the maxillary palp that were analyzed, a similar phenotype was observed. However, in addition to the loss-of-commissure phenotype (Figure 4.24, white arrows), in some instances more severe defects were observed. It was observed that maxillary palp ORNs sometimes cannot cross the suboesophageal ganglion (SOG) to reach the antennal lobe and if they manage to reach it they project to ectopic glomeruli (see blue arrows in Figure 4.24).

In the next round of experiments, Uzip hypomorphs were tested for midline crossing defects (Figure 4.25). These showed similar defects, indicating that not only the presence, but also the level of Uzip protein is important in the projection of ORNs.

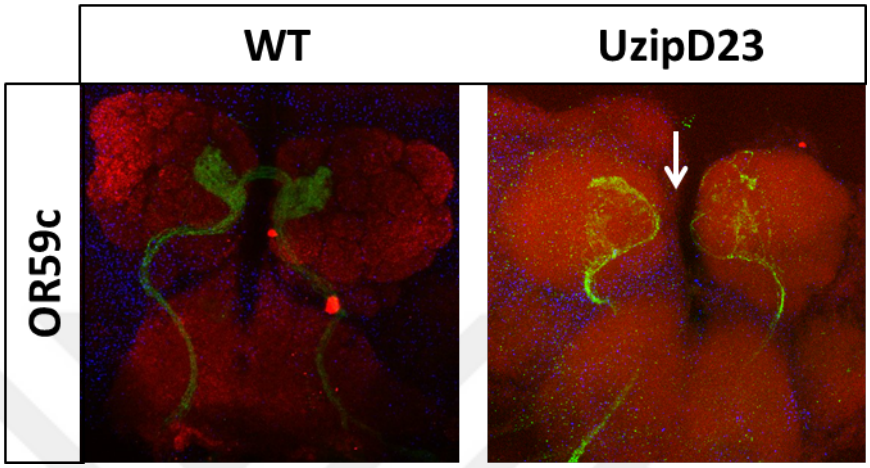

Figure 4.25. Projection of ORNs to the antennal lobe in Uzip hypomorphs (UzipD23). Uzip hypomorphs cannot cross the midline to project to the contra-lateral side (see the white arrow). α-GFP(green), α-NCad (red), toto3 (blue).

4.3.4. Loss of Function Experiments: RNA Interference

In order to understand which expression of Uzip was causing the defects in the projection pattern, Uzip protein levels were down-regulated in a tissue-specific manner. The pan-neuronal driver *elav-Gal4* was used to down-regulate Uzip levels selectively in neurons, and later in glia using the pan-glial driver *repo-Gal4*. In order to down-regulate Uzip protein levels, the RNA interference method was used. The driver causes the expression of double-stranded RNA (dsRNA), which is fused to the UAS sequence. The dsRNA in turn leads to the events resulting in the degradation of the mRNA of the gene of interest (reviewed in Sharp, 1999). Therefore, the protein level is decreased *in vivo*.

Upon down-regulation of Uzip protein levels by RNAi interference in neurons specifically, the number of ORNs that cross the midline decreases (Fig. 4.26, white arrows).

Upon down-regulation of *Uzip* protein levels by RNAi interference specifically in glia, the number of ORNs that cross the midline decreases (Fig. 4.27, white arrow).

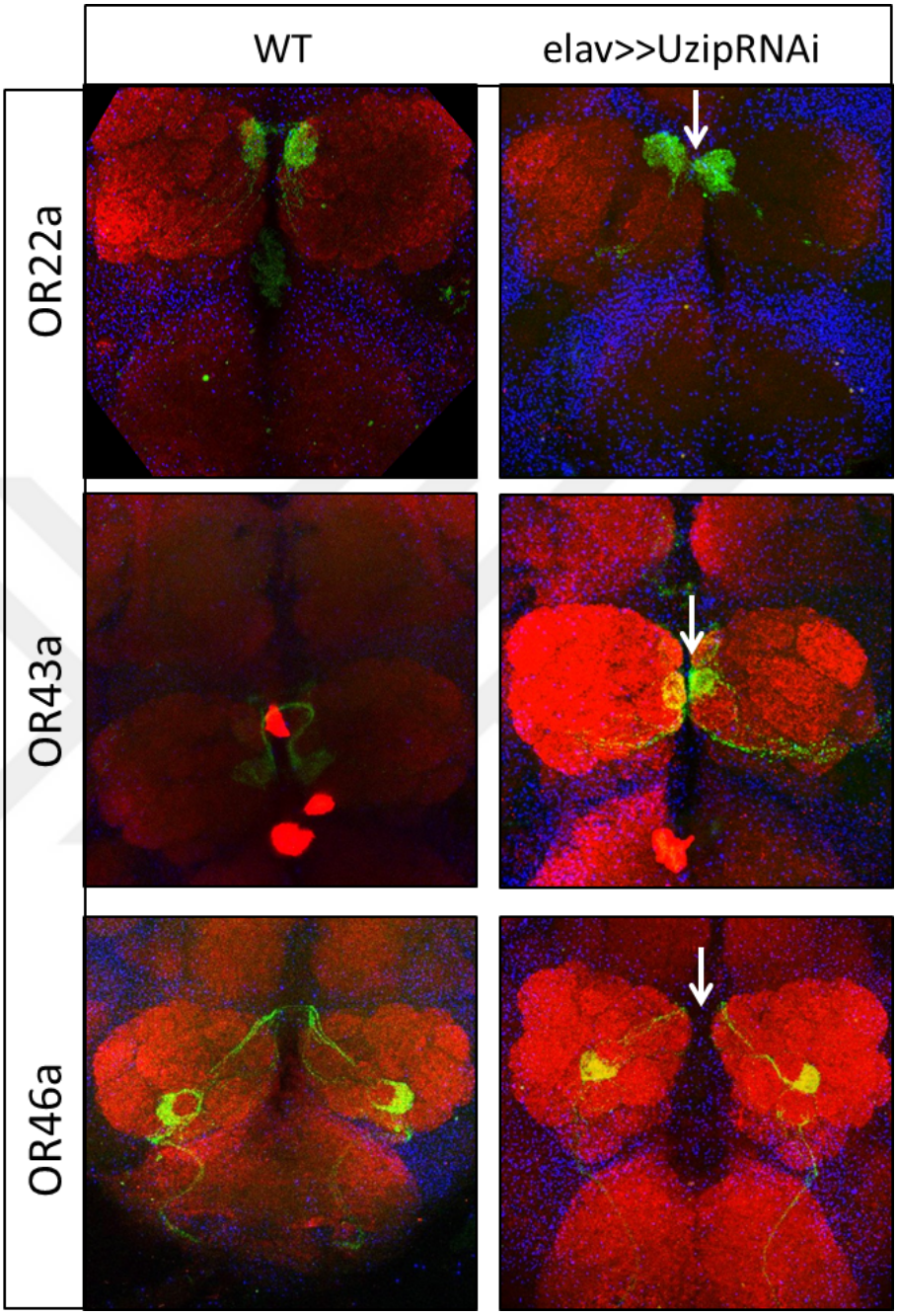

Figure 4.26. Downregulation of Uzip protein levels specifically in neurons. Upon downregulation of Uzip protein levels by RNAi interference, number of ORNs that cross the midline decreases (white arrows). α-GFP (green), α-NCad (red), toto3 (blue).

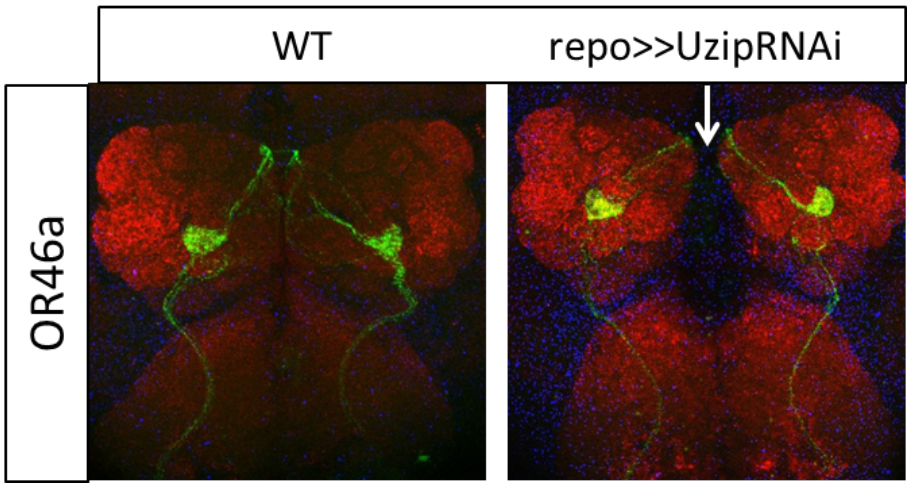

Figure 4.27. Downregulation of *Uzip* protein levels specifically in glia. Upon downregulation of *Uzip* protein levels by RNAi interference, number of ORNs that cross the midline decreases (white arrow). α-GFP (green), α-NCad (red), toto3 (blue).

Taken together these experiments show that the number of ORNs crossing the midline decrease upon either neuronal or glial knockdown, but are never lost completely. To understand how significant the down-regulation by RNAi was, the efficiency was tested by real-time PCR.

For this purpose RNA was extracted from the flies, where expression of RNAi was driven by the *actin*-Gal4 in order to down-regulate the Uzip protein levels everywhere in *Drosophila*. Real-time PCR was performed with Uzip-specific primers and the Uzip mRNA level was compared to wild-type flies. In contrast to our expectation, there was an insignificant increase in the mRNA level, but no decrease (data not shown). Therefore, it was concluded that this RNAi line was not working efficiently. A new RNAi line was ordered from the Bloomington Drosophila Stock Center in order to repeat the knock-down experiments.

4.3.5. Loss-of-Function Experiments: Clonal Analysis

MARCM is a commonly used technique to test the cell-autonomous function of a gene of interest. After the observation of commissural defects in *Uzip* mutants, the question if *Uzip* is necessary in individual ORNs in order to cross the midline was analyzed. *Uzip* homozygous null mutant clones were generated in an otherwise heterozygous animal for the

Uzip mutation (Figure 4.28). eyFlp was used to generate the clones, since it is known that eyFlp is expressed in neurons but not in glia in the olfactory system.

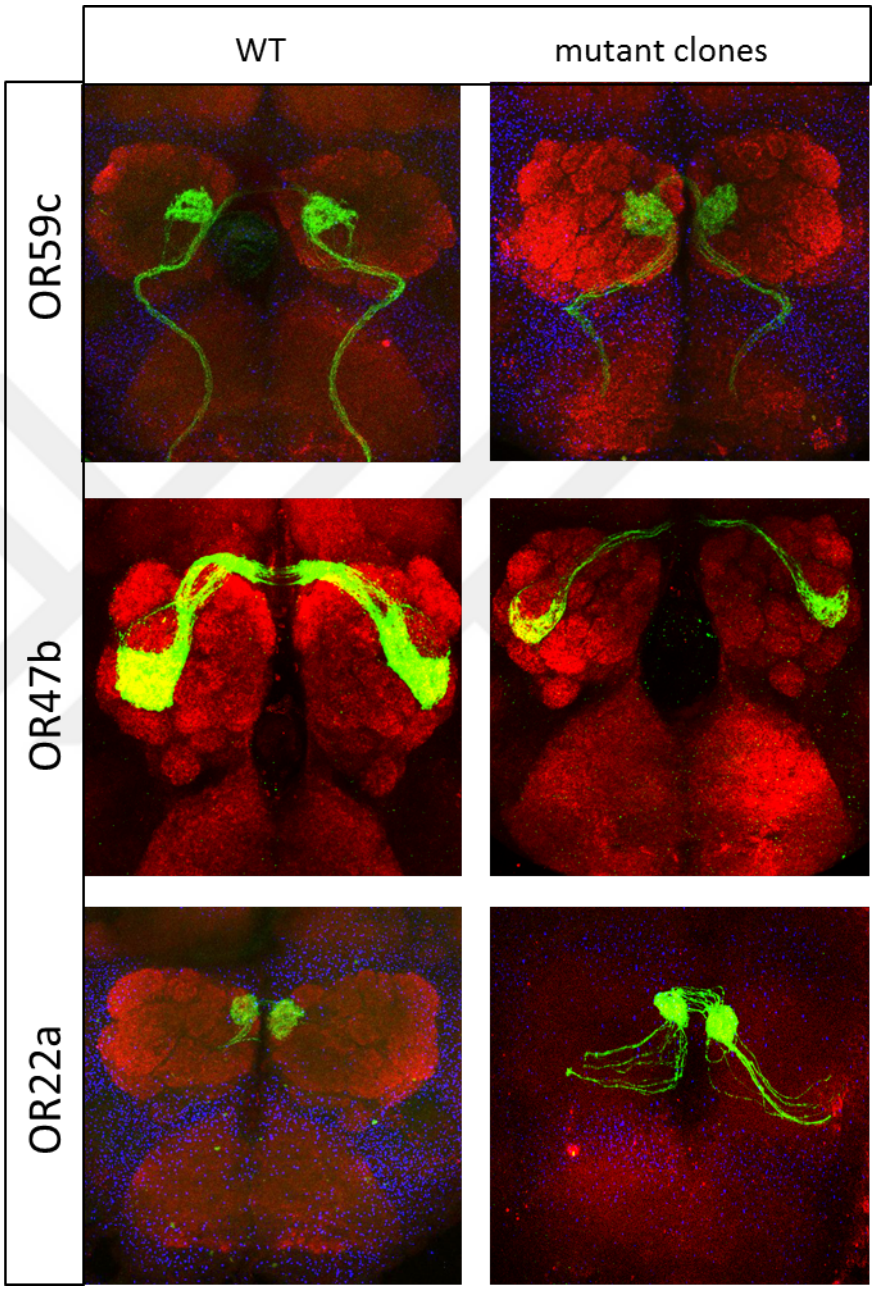

Figure 4.28. MARCM clones of the *Uzip* loss of function allele UzipD43. In MARCM clones of the *Uzip* mutation, ORNs are able to project properly and cross the midline forming the commissure. α-GFP (green), α-NCad (red), toto3 (blue).

MARCM clones were generated and OR classes 22a, 47b, 59c were analyzed. Mutant cells showed no defect in commissure formation. Thus, it was concluded from this experiment that *Uzip* is not necessary in the individual ORNs in order to cross the midline.

4.3.6. Gain of Function Experiments: Mis-expression

For gain-of-function analyses of *Uzip* in glia, the *repo-Gal4* driver was used. *Uzip* expression was driven by repo-Gal4 and using an UAS-*Uzip* transgenic fly line generated by Ding *et al*., 2011 (Figure 4.29). The OR46a reporter line was crossed into this background and analyzed by antibody staining. Neither the projection pattern nor the midline crossing of OR46a neurons seemed to be affected by the mis-expression.

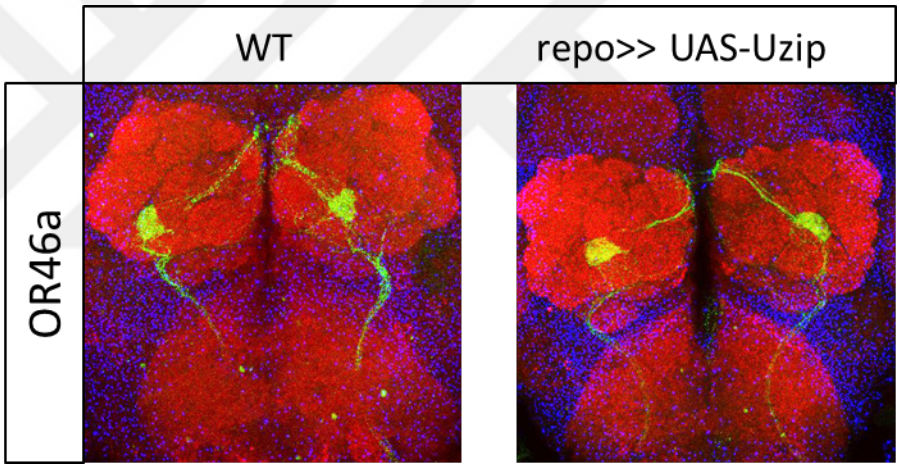

Figure 4.29. Misexpression of *Uzip* in glia does not effect the projection of ORNs. α-GFP (green), α-NCad (red), toto3 (blue).

4.3.7. Gain of Function Experiments: Rescue

To test the functionality of the Flag::HA::Uzip transgenic line and see if it can rescue the mutant phenotype, this line was crossed into the mutant UzipD43 background. Additionally, the reporter constructs for two OR genes were crossed into the same background for analysis. The projection patterns were analyzed by antibody staining against GFP and NCad. While expression of correctly folded protein was observed from this line (see Figure 4.13), no recovery in the mutant phenotype was observed. In this background the OR-reporter lines still displayed the commissural defects (see Figure 4.30).

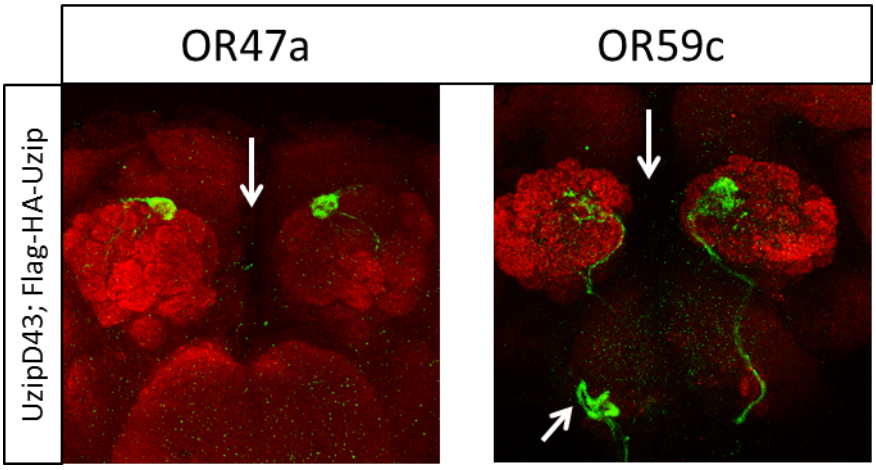

Figure 4.30. Rescue of Uzip loss-of-function phenotype by transgenic Flag-HA-Uzip allele. Defects caused by Uzip loss-of-function are not covered by the introduction of transgenic Uzip construct into the genotype (white arrows). α-GFP (green), α-NCad (red).

In a second experiment, a tissue-specific rescue was performed by driving the expression of Uzip from UAS-Uzip construct in the background of the *Uzip* mutation. Rescue experiments were planned in neurons, in glia, and then simultaneously in both. Unfortunately, due to technical problems, it was not possible to perform all these rescue experiments in the course time of this study. Only glial rescue was performed. But the α-HRP antibody, used for staining all ORN axons, did not give a meaningful pattern (data not shown).

5. DISCUSSION

Even though glia are the prevailing residents of the nervous system, our understanding of their role remains largely unknown. For the longest time they were thought to be only simple supporting cells of the nervous system. Recent studies led to a better understanding of the diverse roles glia have in the development of sensory circuits. It is also reasonable to claim that they may be the main contributors to the complexity, since glial cell number proportionally increases with the complexity of the organims. In humans, 90% of the cells in the nervous system are glia, whereas there are only about 10% in the rather simpler organism, *Drosophila*. On the other hand, despite the differences in the glial ratio between organisms, glial function seems to be highly conserved (reviewed in Freeman and Doherty, 2005).

The role of glia in growth cone guidance has been implicated through several studies. By providing guidance cues to the axonal growth cones, glia play important roles in the regulation of axonal projections. Therefore, glia are the key components of the nervous system, which play critical roles in the formation of the intricate structure of the brain circuitry.

Comparing sensory system structure, the olfactory system constitutes one of the most complex patterns. The sense of smell relies on a large repertoire of olfactory receptors (1200 in mice, 400 in humans, 60 in *Drosophila*) (Ache and Young, 2005). On the other hand, each olfactory sensory neuron expresses only one of these receptors, representing a very complex mechanism of gene regulation. Moreover, olfactory sensory neurons expressing the same receptor converge into the same synaptic subunits in the brain, which is an indication of highly regulated axonal projection mechanisms.

In the framework of this study, we aimed to understand the fuction of a recently identified cell adhesion molecule, Unzipped, in mediating neuron-glia interactions in the development of the *Drosophila* olfactory system. After a detailed analysis of *Unzipped* expression in the nervous system, the role of Unzipped in the proper targeting of ORNs to the brain was investigated.

5.1. Uzip is an R8-Specific Protein in the *Drosophila* Visual System

The *Drosophila* eye is composed of about 800 ommatidia, each of which consists of 8 photoreceptor (PR) cells and 11 supporting cells. These PRs are responsible for the transmission of the visual information to the brain. As the PRs differentiate, bundles of PR cell axons project to temporal layers of the optic ganglion. PR axons reach the specific layers in the optic ganglion and the targeting process finalizes. The R1-R6 cells terminate in the lamina (the first optic ganglion), while the R7 and R8 cells terminate in the M6 and M3 layers of the medulla, respectively (Figure 5.1).

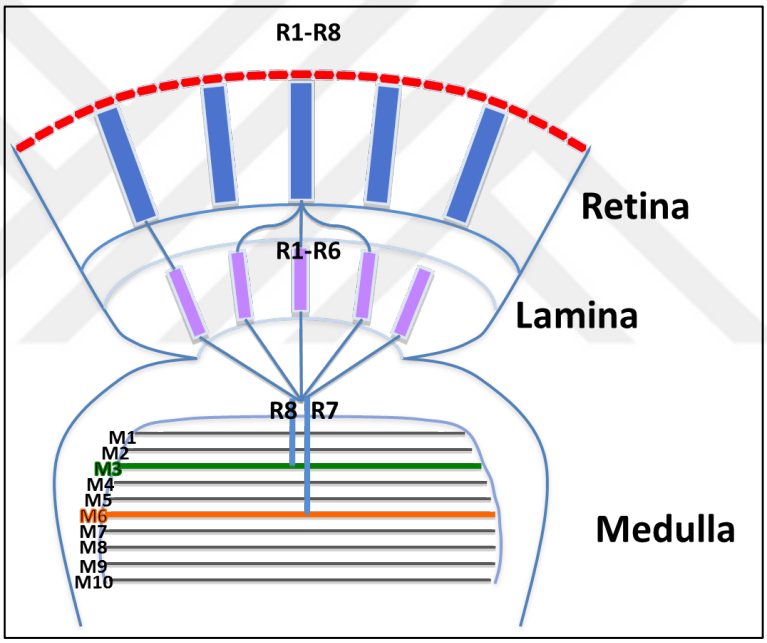

Figure 5.1. Projection of photoreceptor cells to their respective layers in the optic lobe.

Both cell-type specific and broadly expressed molecules function as repellents or attractants in the targeting of photoreceptor axons. These molecules have distinct but also overlapping roles and one of the major questions is how these multiple molecules interact with each other and function harmoniously to regulate the targeting stages of axons (Hadjieconomoue *et al*., 2010). Most of the mechanisms involved in axonal projection and the molecules that guide the photoreceptors to their specific targets in the optic lobe remain to be elucidated. Towards this end, an enhancer-trap screen was performed, to identify R7 and R8-specific genes, which would be the potential candidates to function in the projection

of R7 and R8 cells to their target layers in the optic lobe. One of these proteins, identified in the enhancer-trap screen was Unzipped (Uzip).

In the course of this study, it was shown that Uzip was specifically expressed in R8 cells in the eye imaginal disc, towards the end of larval development (Figure 4.1). Uzip co-localizes with the R8 cells also in the pupal retina. The Uzip protein levels seemed to be higher in the larval stage and decreasing towards the end of pupal development (Figure 4.2). Consistent with this observation, Uzip protein was not detected in the adult retina (data not shown). Although we have seen a neuronal expression, Uzip was also expressed by non-neuronal cells in the eye imaginal disc, which resembles a glial pattern. Co-localization of Uzip with some repo-positive glial cells in the eye imaginal disc was also shown by Ece Terzioğlu-Kara (Figure 5.2). Therefore, Uzip is shown to be expressed in a subset of glial cells in the eye imaginal disc.

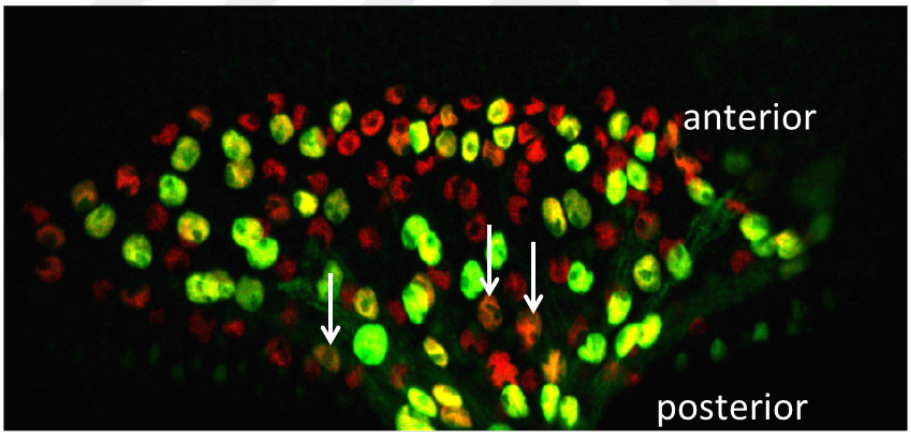

Figure 5.2. Co-expression of Uzip (green) with the glial cell marker repo (red) in the eye imaginal disc.

It is already known that, glial differentiation and migration into the eye imaginal disc occur in a stereotyped manner, and this process is tightly connected to the differentiation and projectional state of photoreceptor neurons. Proper glial migration into the eye imaginal disc is necessary for the projection of photoreceptor axons to the brain. (Ranjarajan *et al.*, 1999) (Figure 1.2). So far, the mechanism how these two processes depend on each other, and the molecules that control this bi-directional regulation remain largely unknown. Uzip was a good candidate to be involved in this process, through its neural-glial expression

pattern and its ability to promote cell-cell adhesion. Therefore, Uzip is a molecular candidate to be involved in regulating neuron-glia interaction in the visual system.

5.2. Uzip is Expressed in the *Drosophila* Olfactory System During Development

While the elucidation of the role of Uzip in the visual system is the topic of other studies conducted in our lab, we wondered if Uzip has a role in the development of other sensory systems. Towards this end, we started a detailed analysis of *Uzip* expression in the *Drosophila* nervous system.

We performed expression analysis studies using several GFP reporter lines. Visualization of the nuclear GFP reporter line showed that Uzip is expressed in a subset of glial cells in whole mount adult brains (Figure 4.5). Use of the membrane-localized GFP reporter, UAS-mCD8::GFP, revealed that *Uzip* expressing cells are mainly localized to antennal lobes and mushroom bodies (Figure 4.6), in addition to the optic lobe (Figure 4.3). It was also detected on a single glomerulus on the antennal lobe, pointing out a single ORN class-specific expression of *Uzip* (Figure 4.7). Taken together, these results suggest that Uzip may have a role in the development of the *Drosophila* olfactory system.

A more detailed analysis of expression specifically in the olfactory system showed that during the pupal stage, Uzip protein was highly expressed around and on the antennal lobes. In support of the initial findings that Uzip is expressed by a specific subset of ORNs (Figure 4.7), Uzip expression was localized to some of the glomeruli in the antennal lobe (Figure 4.15). Moreover, in the pupal antenna, broad expression of Uzip was observed (Figure 4.16). Taken together these results suggest that Uzip is expressed in a subset of ORNs, but perhaps more than one subset, since more than one Uzip-positive glomerulus was observed.

In order to come up with a more explicit answer to the question of which cells express Uzip in the olfactory system, we followed the flip-out strategy in order to label the Uzip-expressing ORNs and glial cells differentially in the adult brains. The UAS-FRT-CD2 stop-FRT-CD8::GFP cassette was driven by the Uzip enhancer trap line, AC783-Gal4. In

addition, eyFlp (eyeless-Flippase) gene was brought to this genetic background, which leads to the exclusion of the CD2 cassette by the recognition of FRT sites on both sides of the CD2 sequence. Hence, wherever eyFlp is expressed, expression of Uzip could be traced by CD8::GFP expression. Wherever eyFlp is not expressed, CD2 expression would reveal the structure of Uzip expressing cells and could be detected by antibody staining with an antibody against CD2.

The results of the flip-out experiments revealed a very interesting pattern of Uzip expression. Unlike any other kind of cell adhesion molecule involved in olfactory system development, expression was limited to a single class of antennal ORNs, and other classes of ORNs likely to be maxillary palp neurons as judged by their glomerular position (Figure 4.17a). But, in comparison to the antennal ORN class, expression of Uzip in these maxillary palp ORN classes was much weaker. This might be the reason why expression in these classes was not observed through syt::GFP reporter earlier. In addition, CD2 expression was detected all over the antennal lobe surface, enwrapping the individual glomeruli, very likely to be a glial pattern (4.17b).

The expression pattern analysis of Uzip was expanded to the adult antenna and maxillary palp. The expression profile in the antenna resembled that of a single subset of ORNs (Figure 3.18a). Although expression was extending towards central positions, which wouldn't fit to single-subset prediction, expression at the more central positions resembled that of glia more than an ORN-specific pattern. The expression profile in the maxillary palp on the other hand, indicated a possible expression in more than one class, maybe in all of the maxillary palp ORNs. To answer this question, Uzip expression was co-labeled with the pan-neuronal marker Elav in the maxillary palp (Figure 3.19). Not all of the Uzip expression co-localized with Elav. The Elav-negative expression pattern most probably belongs to glia.

In summary, detailed analysis of Uzip expression in the olfactory system revealed that Uzip is expressed by a single subset of antennal ORNs and some of the maxillary palp ORNs. In both olfactory organs, it is also expressed in glial cells.

5.3. Problems with Finding the Uzip Expressing Antennal ORN Class

The identification of the specific subclass of ORNs in which Uzip is expressed would enable us to perform loss-of-function and gain-of-function experiments in a class-specific manner and help us to understand the role of Uzip expression in this "single class".

Almost all of the known ORN classes are annotated to their respective glomeruli, and it is possible to identify different glomeruli depending on their position on the antennal lobe (Couto *et al*., 2005; Fishilevich and Vosshall, 2005). Based on the position of the Uzip glomerulus, two ORs were possible: OR2a and OR56a. Since no properly working OR2a tools were available OR19a, which is expressed in the same sensillum with OR2a in the antenna, was used in a comparative manner. Although there is no general rule that applies to all classes, OR19a and OR2a are projecting to neighboring glomeruli, OR19a being behind OR2a (Couto *et al*., 2005). Although the relative position of the Uzip glomerulus to OR19a glomerulus resembled that of OR2a, their locations in the antenna were not close to each other. Therefore, OR2a was excluded from being a candidate. When OR56a expression was compared to Uzip expression both in the antenna and in the antennal lobe, it was clear that OR56a is not the ORN class we were searching for. OR56a axons projected to the neighboring glomeruli, and were not co-expressed in the antenna. Therefore, OR56a was also eliminated. More interestingly, none of the known classes fit to the Uzip expression pattern both in the antenna and the antennal lobe. At this point, the only explanation is that Uzip could be expressed by one of the recently identified antennal ionotropic receptor neurons. These new classes respond to certain odor molecules, which do no activate the classical ORs (Benton *et al*., 2009). And their respective glomeruli are not identified yet.

We didn't pay much attention to the identification of Uzip expressing maxillary palp ORN classes for now, since their loss-of-function phenotype was different than that of the antennal classes (Figure 4.24), which will be discussed in Section 5.6.

5.4. Uzip is Necessary for Midline Crossing of ORNs

Besides some exceptions (OR21a), all ORNs project to both ipsilateral and contralateral sides of the antennal lobe and make synapses with the higher order neurons on both sides (Stocker *et al*., 1990). Upon Uzip loss-of-function, midline-crossing defects were observed in all of the ORN classes analyzed (Figure 4.23 and 4.24). The ORN classes to be analyzed were chosen according to two criteria. One class of each sensillum type was analyzed with the exception of the coeloconic class, the members of which are largely unknown (Figure 5.3). In addition, these classes are basically the ones that are mostly used in ORN projection studies.

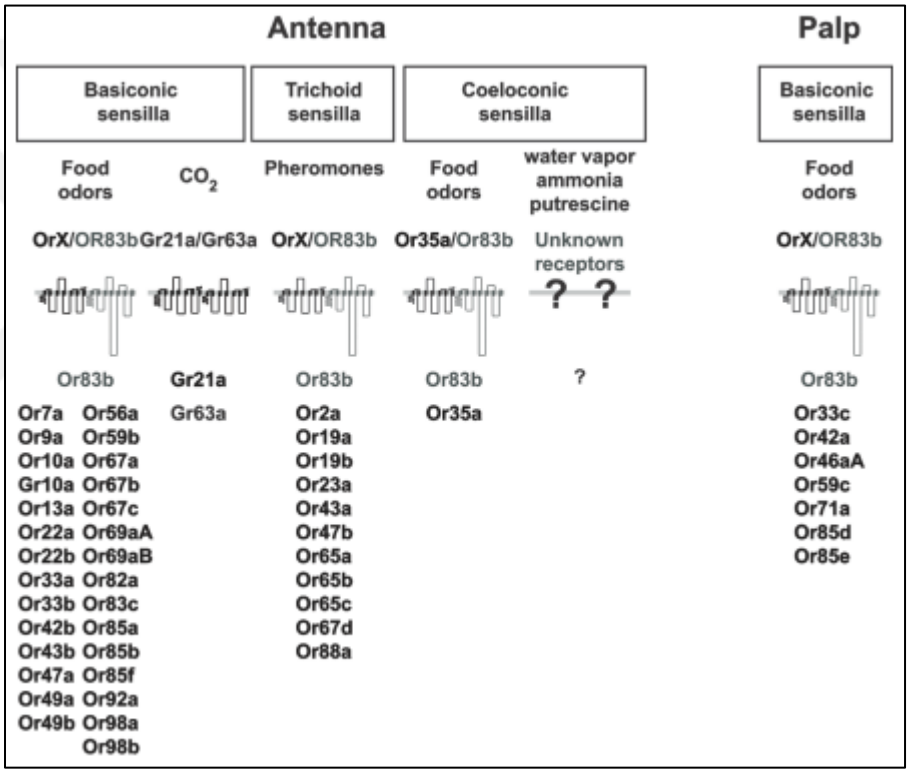

Figure 5.3. Molecular organization of the *Drosophila* olfactory system. At least one ORN subset from each class was chosen to be used in the course of this study, with the exception of coeloconic sensilla classes (Laissue and Voshall, 2008).

Analyses were performed with three antennal and two maxillary palp subsets. Besides the midline-crossing defects observed on all ORNs analyzed (Figure 4.23, 4.24), maxillary palp classes showed an additional type of defect. Some of the ORNs from the same subset were stuck in the SOG, and couldn't reach the antennal lobe, while some others showed mistargeting defects their corresponding glomeruli (Figure 4.24, blue arrows). A hypothesis to explain the mistargeting could be that Uzip may be playing a role in the self-

recognition of maxillary palp ORNs of the same subset, by mediating cell-cell adhesion. Therefore, upon Uzip loss-of-function, this cell-cell communication between the ORNs of the same subset could be disrupted. There might also be a second means of interaction in the SOG, for the decision of passing through the SOG to reach the antennal lobe. This second means of interaction might be between the ORNs and the glia in the SOG, where Uzip is also expressed. When Uzip is lost by the glial cells in the SOG, ORNs are not guided to the antennal lobe.

If we attribute this function to Uzip in the maxillary palp neurons, the single Uzip-positive antennal ORN must have a different role. The situation in the olfactory system and the single OR subclass in the antenna resembles the situation in the visual system where Uzip is expressed by R8 cells and glia. From the literature, it is known that R8 cells are the first photoreceptor neurons to differentiate (Jarman et al., 1994; Tomlinson and Ready, 1987). Therefore, we hypothesize that, R8 cells in the visual system and the Uzip expressing ORN subset in the olfactory system may have pioneering roles in mediating neuron-glia interactions and establish the olfactory circuitry. They may be the first sensory neurons in each system, to interact with glia and receive the guidance cues from them. This is consistent with the findings of Sweeney *et al*. (2006), who show that antennal ORN axons reach and start to pattern the developing antennal lobe before the arrival of maxillary palp axons. Thus, we hypothesize that pioneering properties are acting within the antennal classes only.

Findings of Sweeney *et al*. (2006) fit our observations and help to shape our hypothesis. They have shown that the early-arriving antennal axons have a pioneering role in the projection of maxillary palp axons to the antennal lobe. Here, Sema-1a functions in the antennal axons to make a repulsive interaction with the PlexinA on maxillary palp axons. From this aspect, it can be argued that Uzip may have an interaction with PlexinA as well in order to regulate the projection of maxillary palp axons.

Therefore, our current working hypothesis is that Uzip mediates interaction between neurons and glial cells to support proper axon guidance. Uzip expressing neurons could be pioneering neurons for initial guidance decisions based on glia-derived cues. Uzip, secreted from glia might be localized on pioneering axons by membrane-bound Uzip to

guide the follower axons via heterophilic interaction with a yet unknown partner. The Model is summarized in Figure 5.4.

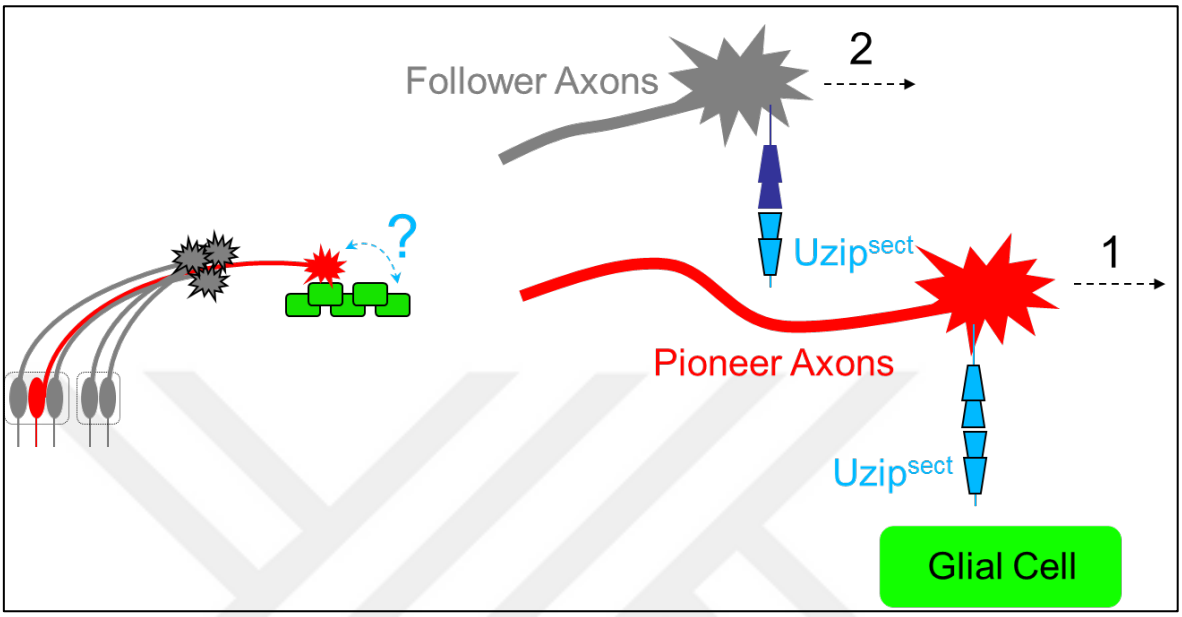

Figure 5.4. Proposed model of the mechanism of Uzip function. Uzip expressing axons may be pioneering axons to mediate the projection of the follower axons. They may be interacting with glia, and the Uzip secreted from glia could be localized on these axons through adhesion. In turn, they could be interacting with the follower axons through Uzip, and turn on other mechanisms through interaction with a yet unknown partner.

5.5. Problems with the Knock-Down Experiments

In order to reveal the role of Uzip in the projection of ORNs, knock-down experiments were performed in a cell-specific manner using Uzip-specific RNAi lines. Our aim was to show that Uzip is required both in neurons and glia to mediate ORN targeting. Unfortunately, no defect in the midline crossing of axons was observed upon knock-down of Uzip in glia and neurons (Figure 4.26, 4.27). Quantitation of the degree of down-regulation of Uzip by RNAi by quantitative RT-PCR was performed (data not shown). Upon knock-down of Uzip in all cells, no significant decrease in the Uzip levels was observed. Therefore, it was concluded that this RNAi line cannot be used for the knock-down experiments. For future experiments, new RNAi lines ordered from VDRC (Vienna Drosophila Stock Center) as well as a recently released TRIP RNAi line generated in Janelia Farms will be used.

5.6. Mis-expression of Uzip in Glial Cells does not Result in any Defect

Gain-of-function experiments were performed by mis-expressing Uzip using the glial driver repo-Gal4. There was no prominent defect observed in the projection pattern of ORNs (Figure 4.29). But these experiments should be performed in a more extensive manner. In addition to mis-expression in neurons, Uzip should be misexpressed both in neurons and glia to see if increase in Uzip levels has any effects on the development of the olfactory system. Mis-expression could also be tried with a more extensively expressed driver, such as actin-Gal4. Thus, the hypothesis of a pioneering role of Uzip expression could be tested more extensively.

5.7. Cell-Specific Rescue of Uzip may Unravel its Role

Perhaps the most important set of experiments, which couldn't be completed in the course of this study, was the cell-specific rescue of Uzip protein. In the background of Uzip loss-of-function, the UAS-Uzip-CFP transgene should be expressed in different cells and the projection of single subsets of ORNs should be traced. This could be the most reliable way to prove our hypothesis. If both glial and neuronal rescue of Uzip wouldn't recover the wild-type phenotype, but rescue in both would, we could rely on the hypothesis. We could say that Uzip mediates a means of neuron-glia interaction in the olfactory system, which is necessary for midline crossing of ORNs.

5.8. Uzip is not necessary in ORNs to Cross the Midline

We performed clonal analysis of the Uzip loss-of-function phenotype in order to check if Uzip is necessary in individual ORNs to cross the midline. We generated MARCM clones by using eyFlp, to ensure that clones are generated only in ORNs. The clones showed no defect in midline crossing (Figure 4.28). Therefore, the ORN classes analyzed in the course of MARCM experiments do not need Uzip on their membranes in order to cross the midline.

This was an expected result considering our hypothesis. But it would be more meaningful to perform MARCM with the Uzip-expressing antennal ORN class, if we could have identified it.

5.9. Problems with the tagged Uzip Transgene

Due to the lack of a properly working antibody against Uzip protein, we decided to tag endogenous expression of Uzip through BAC transgenesis. Two different constructs were prepared: the first one included Flag and HA tags (Figure 4.9), and the second one included eGFP coding sequence in addition to HA and Flag tags (Figure 4.11). The tags were inserted to the N-terminal of the Uzip protein, since Uzip appears to be cleaved at the C-terminus upon secretion (Ding *et al*., 2011). Through this, tagging of both forms of *Uzip* protein was intended. A linker sequence was also inserted before and after each tag, in order not to interfere with protein folding.

Despite all the efforts, recombination with the eGFP including construct was not obtained initially. Several problems were encountered during the selection of the recombinant colonies through 96-well colony PCR. First of all, this selection procedure was quite tedious. In the case of GFP-tagged version especially, it required several rounds of selection to obtain the recombinant single colonies, which ended up being only false-positives. The Flag::HA-tagged construct on the other hand, was successfully injected into the embryos to obtain the transgenic flies.

Flag::HA::Uzip construct was used for immunohistochemistry, although it was initially designed for use in biochemical studies. To detect the HA epitope fused to the Uzip protein, a α-HA antibody was used. However, this antibody appeared to give a high background. Different staining protocols were applied without generating significantly better results. Despite a staining with high background in whole mount adult brains a widely distributed expression around antennal lobes and on mushroom bodies was observed. This expression could reflect the membranous and secreted forms of Uzip. Still a better overlap between the Uzip enhancer trap, as visualized by CD8::GFP, and the HA line was expected. The additional staining could be explained by the detection of a secreted form of Uzip. Expression analysis experiments can be performed later on the GFP-tagged version, which

was successfully obtained very recently and will be sent for injection. In addition, another version of the Uzip transgene can be generated by inserting the tag to the C-terminal end, in order to discriminate between the membrane-bound and the secreted forms.

To test the functionality of the transgenic construct, we performed rescue experiments by adding the Flag::HA::Uzip transgene to the background of the Uzip mutation and analyzing the projection of ORNs. Unfortunately, the midline-crossing defect, caused by Uzip loss-of-function was not recovered by this transgene. We performed Western blot analysis using the α-HA antibody on protein extracts from transgenic flies. Two isoforms of Uzip protein were detected corresponding to ~65kD and ~80kD. Thus, the Uzip transgene is expressed from the BAC transgene and both isoforms can be detected; however, these proteins seem not to be functional *in vivo*. Since we put the tags after the signal peptide sequence, whose sequence was determined only by prediction based on the amino acid sequence, an improper prediction might have occurred. We might have disrupted the protein sequence at a critical position for its function. The rescue experiments have been performed by adding one copy of the BAC transgene and should be repeated using two copies to make sure that the lack of rescue is not due to an expression level problem. Additionally, the same BAC should be used to generate transgenic flies to see if the tagging rendered the protein nonfunctional.

5.10. Which Subsets of Glial Cells Express Uzip?

Even though a co-localization of Uzip with the glial cell marker repo was observed in the brain, and a possible co-localization is predicted to be present in the antenna and maxillary palps, it is not clear which subsets of glia are the main source of Uzip. We observed that at the antennal lobe periphery, Uzip was not co-localized to the glial cell nuclei. However, Uzip is observed in a glia-like pattern on the antennal lobes, enwrapping individual glomeruli. This is in fact the characteristic pattern of neuropil glia, whose cell bodies are located at the antennal lobe periphery and who send their processes into the antennal lobe to wrap the glomeruli. In order to resolve this contradiction, co-localization should be further investigated with a strategy that enables the visualization of both glia and Uzip-expressing cell membranes. At this point, making use of another binary system, LexA::VP16 > LexAOperon is reasonable. Gal4/UAS system could be used to label Uzip

expression whereas LexA::VP16 > LexAOperon could be used for labeling repo expression. Identification of the Uzip expressing glial subset in the visual system in parallel will give more prominent cues about the role of Uzip.

Staining of adult antenna and maxillary palps may be performed using cryostat sections as whole-mount tissues are refractory to antibody penetration. A triple staining of AC783-Gal4>UAS-nlsGFP flies with elav, repo and GFP would give a detailed information about the distribution of Uzip between glia and neurons in these organs.

Moreover, since Uzip has a role in midline crossing, identification of the midline glial cells that express Uzip is crucial. Unfortunately, midline glial cells are not labeled with the glial marker repo. But the driver line 442-Gal4 (also called as drl-Gal4) drives the expression of the Derailed (Drl) gene, which is expressed in the antennal lobe midline during development, specifically in a ring-structure formed by glial cells. This structure is called transient interhemispheric fibrous ring (TIFR), which appears in the late larvae and disappears during the pupal stage. The role of Drl in midline crossing, through mediating Wnt5 signaling was already shown in a previous study (Yao *et al*., 2007).

A more recent study showed the role of another cell adhesion molecule in midline crossing. The Drosophila homolog of L1CAM, neuroglian (Nrg), is expressed in a subset of ORNs and also in the TIFR glia. Nrg functions in the proper development of TIFR, probably by mediating correct changes in cell shapes or adhesion among the TIFR glia. Therefore, upon Nrg loss-of-function, TIFR morphology is disrupted and midline-crossing of ORN axons ceases. However, neither the TIFR structure nor the commissure formation defects were rescued by the expression of UAS-Nrg transgene in the TIFR. Therefore, Nrg was found to be necessary even in another cell type for the proper morphogenesis of TIFR. Nrg may be needed for the adhesion between ORN axons and the TIFR glia to facilitate the extension of the axons over the glial bridge and the subsequent nerve ensheathment (Chen *et al*., 2008).

Taken together, Drl and Nrg could be the possible interaction partners of Uzip. Drl was shown to be regulating Wnt5 signaling (Yao *et al*., 2007). Uzip on the other hand was

also shown to be in interaction with Wnt5 in the embryonic nervous system (Ding *et al*., 2011). Therefore, a possible function of Uzip in this signaling pathway should be considered.

Nrg on the hand, being a cell-adhesion molecule, shares many similarities with Uzip when its expression pattern is analyzed. Both proteins are expressed by ORNs and glia. But still, they are not necessary in ORNs for midline crossing, since mutant ORN clones of both proteins show no defect in midline crossing. Both proteins seem to be functioning through neuron-glia interactions.

Both Drl and Nrg are also shown to be playing a role in the morphogenesis of TIFR. And in the Nrg mutants, ORNs cannot cross the midline, most probably due to the disruption of TIFR morphology. But expression of Nrg only in TIFR is not sufficient for ORNs to cross the midline. Therefore, neuronal-Nrg is also necessary for midline crossing. Perhaps ORN defects seen in the Nrg mutants were due to the degeneration of the TIFR morphology, which might be the case even for Uzip mutants. Nrg and Uzip together might be mediating the adhesion between ORN axons and the TIRF glia to facilitate the extension of the ORN axons over the glial bridge, which is subsequently ensheated by axons.

Although not completely running against our previous hypothesis, this prediction might bring us to another hypothesis that Uzip indeed plays role in the proper formation of glial morphology. Future studies will uncover whether there is an interaction between Nrg and Uzip, and thus may bring new insights into the future studies of the role of Uzip in this project.

REFERENCES

Bao, J., D. Wolpowitz, L.W. Role, and D.A. Talmage, 2003, "Back Signaling by the Nrg-1 Intracellular Domain", *The Journal of Cell Biology*, Vol. 161, No. 6, pp. 1133-1141.

Baumann, P.M., L.A. Oland, and L.P. Tolbert, 1996, "Glial Cells Stabilize Axonal Protoglomeruli in the Developing Olfactory Lobe of the Moth Manduca Sexta", *The Journal of Comparative Neurology*, Vol. 373, No. 1, pp. 118-128.

Bhalerao, S., A. Sen, R. Stocker, and V. Rodrigues, 2003, "Olfactory Neurons Expressing Identified Receptor Genes Project to Subsets of Glomeruli within the Antennal Lobe of Drosophila Melanogaster", *Journal of Neurobiology*, Vol. 54, No. 4, pp. 577-592.

Brand, A.H., and N. Perrimon, 1993, "Targeted Gene Expression as a Means of Altering Cell Fates and Generating Dominant Phenotypes", *Development*, Vol. 118, No. 2, pp. 401-415.

Chen, W., and H. Hing, 2008, "The L1-CAM, Neuroglian, Functions in Glial Cells for Drosophila Antennal Lobe Development", *Developmental Neurobiology*, Vol. 68, No. 8, pp. 1029-1045.

Clyne, P.J., S.J. Certel, M. De Bruyne, L. Zaslavsky, W.A. Johnson, and J.R. Carlson, 1999, "The Odor Specificities of a Subset of Olfactory Receptor Neurons are Governed by Acj6, A POU-Domain Transcription Factor", *Neuron*, Vol. 22, No. 2, pp. 339-347.

Colamarino, S.A., and M. Tessier-Lavigne, 1995, "The Role of the Floor Plate in Axon Guidance", *Annual Review of Neuroscience*, Vol. 18, pp. 497-529.

Cook, G., D. Tannahill, and R. Keynes, 1998, "Axon Guidance to and from Choice Points", *Current Opinion in Neurobiology*, Vol. 8, No. 1, pp. 64-72.

Couto, A., M. Alenius, and B.J. Dickson, 2005, "Molecular, Anatomical, and Functional Organization of the Drosophila Olfactory System", *Current Biology*, Vol. 15, No. 17, pp. 1535-1547.

Ding, Z.Y., Y.H. Wang, Z.K. Luo, H.F. Lee, J. Hwang, C.T. Chien, and M.L. Huang, 2011, "Glial Cell Adhesive Molecule Unzipped Mediates Axon Guidance in Drosophila", *Developmental Dynamics*, Vol. 240, No. 1, pp. 122-134.

Dubin, A.E., and G.L. Harris, 1997, "Voltage-Activated and Odor-Modulated Conductances in Olfactory Neurons of Drosophila Melanogaster", *Journal of Neurobiology*, Vol. 32, No. 1, pp. 123-137.

Duffy, J.B., 2002, "GAL4 System in Drosophila: a Fly Geneticist's Swiss Army Knife", *Genesis*, Vol. 34, No. 1-2, pp. 1-15.

Endo, K., T. Aoki, Y. Yoda, K. Kimura, and C. Hama, 2007, "Notch Signal Organizes the Drosophila Olfactory Circuitry by Diversifying the Sensory Neuronal Lineages", *Nature Neuroscience*, Vol. 10, No. 2, pp. 153-160.

Fischer, J.A., E. Giniger, T. Maniatis, and M. Ptashne, 1988, "GAL4 Activates Transcription in Drosophila", *Nature*, Vol. 332, No. 6167, pp. 853-856.

Fishilevich, E., A.I. Domingos, K. Asahina, F. Naef, L.B. Vosshall, and M. Louis, 2005, "Chemotaxis Behavior Mediated by Single Larval Olfactory Neurons in Drosophila", *Current Biology*, Vol. 15, No. 23, pp. 2086-2096.

Freeman, M.R., and J. Doherty, 2006, "Glial Cell Biology in Drosophila and Vertebrates", *Trends in Neuroscience*, Vol. 29, No. 2, pp. 82-90.

Freeman, M.R., J. Delrow, J. Kim, E. Johnson, and C.Q. Doe, 2003, "Unwrapping Glial Biology: Gcm Target Genes Regulating Glial Development, Diversification, and Function", *Neuron*, Vol. 38, No. 4, pp. 567-580.

Groth, A.C., E.C. Olivares, B. Thyagarajan, and M.P. Calos, 2000, "A Phage Integrase Directs Efficient Site-Specific Integration in Human Cells", *Proceedings of National Academy of Sciences*, Vol. 97, No. 11, pp. 5995-6000.

Hallem, E.A., and J.R. Carlson, 2004, "The Spatial Code for Odors is Changed by Conditioning", *Neuron*, Vol. 42, No. 3, pp. 359-361.

Hildebrand, J.G., and G.M. Shepherd, 1997, "Mechanisms of Olfactory Discrimination: Converging Evidence for Common Principles Across Phyla", *Annual Review of Neuroscience*, Vol. 20, pp. 595-631.

Hummel, T., and S.L. Zipursky, 2004, "Afferent Induction of Olfactory Glomeruli Requires N-Cadherin", *Neuron*, Vol. 42, No. 1, pp. 77-88.

Hummel, T., K. Schimmelpfeng, and C. Klambt, 1999, "Commissure Formation in the Embryonic CNS of Drosophila", *Developmental Biology*, Vol. 209, No. 2, pp. 381-398.

Hummel, T., M.L. Vasconcelos, J.C. Clemens, Y. Fishilevich, L.B. Vosshall, and S.L. Zipursky, 2003, "Axonal Targeting of Olfactory Receptor Neurons in Drosophila is Controlled by Dscam", *Neuron*, Vol. 37, No. 2, pp. 221-331.

Hummel, T., S. Attix, D. Gunning, and S.L. Zipursky, 2002, "Temporal Control of Glial Cell Migration in the Drosophila Eye Requires Gilgamesh, Hedgehog, and Eye Specification Genes", *Neuron*, Vol. 33, No. 2, pp. 193-203.

Jarman, A.P., E.H. Grell, L. Ackerman, L.Y. Jan, and Y.N. Jan, 1994, "Atonal is the Proneural Gene for Drosophila Photoreceptors", *Nature*, Vol. 369, No. 6479, pp. 398-400.

Jefferis, G.S., R.M. Vyas, D. Berdnik, A. Ramaekers, R.F. Stocker, N.K. Tanaka, K. Ito, and L. Luo, 2004, "Developmental Origin of Wiring Specificity in the Olfactory System of Drosophila", *Development*, Vol. 131, No. 1, pp. 117-130.

Jessen, K.R., 2004, "Glial Cells", *The International Journal of Biochemistry and Cell Biology*, Vol. 36, No. 10, pp. 1861-1867.

Jessen, K.R., and R. Mirsky, 2002, "Signals That Determine Schwann Cell Identity", *Journal Anatomy*, Vol. 200, No. 4, pp. 367-376.

Jhaveri, D., A. Sen, and V. Rodrigues, 2000, "Mechanisms Underlying Olfactory Neuronal Connectivity in Drosophila-the Atonal Lineage Organizes the Periphery While Sensory Neurons and Glia Pattern the Olfactory Lobe", *Developmental Biology*, Vol. 226, No. 1, pp. 73-87.

Jhaveri, D., and V. Rodrigues, 2002, "Sensory Neurons of the Atonal Lineage Pioneer the Formation of Glomeruli within the Adult Drosophila Olfactory Lobe", *Development*, Vol. 129, No. 5, pp. 1251-1260.

Klambt, C., and C.S. Goodman, 1991, "The Diversity and Pattern of Glia During Axon Pathway Formation in the Drosophila Embryo", *Glia*, Vol. 4, No. 2, pp. 205-213.

Klambt, C., J.R. Jacobs, and C.S. Goodman, 1991, "The Midline of the Drosophila Central Nervous System: a Model for the Genetic Analysis of Cell Fate, Cell Migration, and Growth Cone Guidance", *Cell*, Vol. 64, No. 4, pp. 801-815.

Kretzschmar, D., and G.O. Pflugfelder, 2002, "Glia in Development, Function, and Neurodegeneration of the Adult Insect Brain", *Brain Research Bulletin*, Vol. 57, No. 1, pp. 121-131.

Laissue, P.P., C. Reiter, P.R. Hiesinger, S. Halter, K.F. Fischbach, and R.F. Stocker, 1999, "Three-Dimensional Reconstruction of the Antennal Lobe in Drosophila Melanogaster", *The Journal of Comparative Neurology*, Vol. 405, No. 4, pp. 543-552.

Leiserson, W.M., E.W. Harkins, and H. Keshishian, 2000, "Fray, a Drosophila Serine/Threonine Kinase Homologous to Mammalian PASK, is Required for Axonal Ensheathment", *Neuron*, Vol. 28, No. 3, pp. 793-806.

Mombaerts, P., 2001, "How Smell Develops", *Nature Neuroscience*, Vol. 4 Suppl, pp. 1192-1198.

Oland, L.A., H.G. Marrero, and I. Burger, 1999, "Glial Cells in the Developing and Adult Olfactory Lobe of the Moth Manduca Sexta", *Cell and Tissue Research*, Vol. 297, No. 3, pp. 527-545.

Oland, L.A., J.P. Biebelhausen, and L.P. Tolbert, 2008, "Glial Investment of the Adult and Developing Antennal Lobe of Drosophila", *The Journal of Comparative Neurology*, Vol. 509, No. 5, pp. 526-550.

Oland, L.A., L.P. Tolbert, and K.L. Mossman, 1988, "Radiation-Induced Reduction of the Glial Population During Development Disrupts the Formation of Olfactory Glomeruli in an Insect", *The Journal of Neuroscience*, Vol. 8, No. 1, pp. 353-367.

Olivares, E.C., R.P. Hollis, T.W. Chalberg, L. Meuse, M.A. Kay, and M.P. Calos, 2002, "Site-Specific Genomic Integration Produces Therapeutic Factor IX Levels in Mice", *Nature Biotechnology*, Vol. 20, No. 11, pp. 1124-1128.

Peng, H.B., J.F. Yang, Z. Dai, C.W. Lee, H.W. Hung, Z.H. Feng, and C.P. Ko, 2003, "Differential Effects of Neurotrophins and Schwann Cell-Derived Signals on Neuronal Survival/Growth and Synaptogenesis", *The Journal of Neuroscience*, Vol. 23, No. 12, pp. 5050-5060.

Pereanu, W., D. Shy, and V. Hartenstein, 2005, "Morphogenesis and Proliferation of the Larval Brain Glia in Drosophila", *Developmental Biology*, Vol. 283, No. 1, pp. 191-203.

Peters, A., K. Josephson, and S.L. Vincent, 1991, "Effects of Aging on the Neuroglial Cells and Pericytes within Area 17 of the Rhesus Monkey Cerebral Cortex", *The Anatomical Record*, Vol. 229, No. 3, pp. 384-398.

Rangarajan, R., Q. Gong, and U. Gaul, 1999, "Migration and Function of Glia in the Developing Drosophila Eye", *Development*, Vol. 126, No. 15, pp. 3285-3292.

Ray, K., and V. Rodrigues, 1995, "Cellular Events During Development of the Olfactory Sense Organs in Drosophila Melanogaster", *Developmental Biology*, Vol. 167, No. 2, pp. 426-438.

Reddy, L.V., S. Koirala, Y. Sugiura, A.A. Herrera, and C.P. Ko, 2003, "Glial Cells Maintain Synaptic Structure and Function and Promote Development of the Neuromuscular Junction in Vivo", *Neuron*, Vol. 40, No. 3, pp. 563-580.

Ressler, K.J., S.L. Sullivan, and L.B. Buck, 1993, "A Zonal Organization of Odorant Receptor Gene Expression in the Olfactory Epithelium", *Cell*, Vol. 73, No. 3, pp. 597-609.

Rossler, W., L.A. Oland, M.R. Higgins, J.G. Hildebrand, and L.P. Tolbert, 1999, "Development of A Glia-Rich Axon-Sorting Zone in the Olfactory Pathway of the Moth Manduca Sexta", *The Journal of Neuroscience*, Vol. 19, No. 22, pp. 9865-9877.

Rubin, G.M., and A.C. Spradling, 1982, "Genetic Transformation of Drosophila with Transposable Element Vectors", *Science*, Vol. 218, No. 4570, pp. 348-353.

Ryder, E., and S. Russell, 2003, "Transposable Elements as Tools for Genomics and Genetics in Drosophila", *Briefings in Functional Genomics and Proteomics*, Vol. 2, No. 1, pp. 57-71.

Sakurai, M., T. Aoki, S. Yoshikawa, L.A. Santschi, H. Saito, K. Endo, K. Ishikawa, K. Kimura, K. Ito, J.B. Thomas, and C. Hama, 2009, "Differentially Expressed Drl and Drl-2 Play Opposing Roles in Wnt5 Signaling During Drosophila Olfactory System Development", *The Journal of Neuroscience*, Vol. 29, No. 15, pp. 4972-4980.

Shanbhag, S.R., B. Muller, and R.A. Steinbrecht, 2000, "Atlas of Olfactory Organs of Drosophila Melanogaster 2. Internal Organization and Cellular Architecture of Olfactory Sensilla", *Arthropod Structure & Development*, Vol. 29, No. 3, pp. 211-229.

Sharp, P.A., 1999, "RNAi and Double-Strand RNA", *Genes & Development*, Vol. 13, pp. 139-141.

Song, H., C.F. Stevens, and F.H. Gage, 2002, "Astroglia Induce Neurogenesis from Adult Neural Stem Cells", *Nature*, Vol. 417, No. 6884, pp. 39-44.

Sonnenfeld, M.J., and J.R. Jacobs, 1995, "Macrophages and Glia Participate in the Removal of Apoptotic Neurons from the Drosophila Embryonic Nervous System", *The Journal of Comperative Neurology*, Vol. 359, No. 4, pp. 644-652.

Spindler, S.R., I. Ortiz, S. Fung, S. Takashima, and V. Hartenstein, 2009, "Drosophila Cortex and Neuropile Glia Influence Secondary Axon Tract Growth, Pathfinding, and Fasciculation in the Developing Larval Brain", *Developmental Biology*, Vol. 334, No. 2, pp. 355-368.

Stocker, R.F., M.C. Lienhard, A. Borst, and K.F. Fischbach, 1990, "Neuronal Architecture of the Antennal Lobe in Drosophila Melanogaster", *Cell and Tissue Research*, Vol. 262, No. 1, pp. 9-34.

Stoeckli, E.T., and L.T. Landmesser, 1998, "Axon Guidance at Choice Points", *Current Opinion in Neurobiology*, Vol. 8, No. 1, pp. 73-79.

Stowers, R.S., and T.L. Schwarz, 1999, "A Genetic Method for Generating Drosophila Eyes Composed Exclusively of Mitotic Clones of a Single Genotype", *Genetics*, Vol. 152, No. 4, pp. 1631-1639.

Sweeney, L.B., A. Couto, Y.H. Chou, D. Berdnik, B.J. Dickson, L. Luo, and T. Komiyama, 2007, "Temporal Target Restriction of Olfactory Receptor Neurons by Semaphorin-1a/Plexina-Mediated Axon-Axon Interactions", *Neuron*, Vol. 53, No. 2, pp. 185-200.

Sweeney, L.B., A. Couto, Y.H. Chou, D. Berdnik, B.J. Dickson, L. Luo, and T. Komiyama, 2007, "Temporal Target Restriction of Olfactory Receptor Neurons by Semaphorin-1a/Plexina-Mediated Axon-Axon Interactions", *Neuron*, Vol. 53, No. 2, pp. 185-200.

Tessier-Lavigne, M., and M. Placzek, 1991, "Target Attraction: are Developing Axons Guided by Chemotropism?", *Trends in Neuroscience*, Vol. 14, No. 7, pp. 303-310.

Thyagarajan, B., E.C. Olivares, R.P. Hollis, D.S. Ginsburg, and M.P. Calos, 2001, "Site-Specific Genomic Integration in Mammalian Cells Mediated by Phage Phic31 Integrase", *Molecular Cell Biology*, Vol. 21, No. 12, pp. 3926-3934.

Tomlinson, A., and D.F. Ready, 1987, "Neuronal Differentiation in Drosophila Ommatidium", *Developmental Biology*, Vol. 120, No. 2, pp. 366-376.

Tucker, E.S., and L.P. Tolbert, 2003, "Reciprocal Interactions Between Olfactory Receptor Axons and Olfactory Nerve Glia Cultured from the Developing Moth Manduca Sexta", *Developmental Biology*, Vol. 260, No. 1, pp. 9-30.

Tucker, E.S., L.A. Oland, and L.P. Tolbert, 2004, "In Vitro Analyses of Interactions Between Olfactory Receptor Growth Cones and Glial Cells That Mediate Axon Sorting and Glomerulus Formation", *The Journal of Comparative Neurology*, Vol. 472, No. 4, pp. 478-495.

Ullian, E.M., B.T. Harris, A. Wu, J.R. Chan, and B.A. Barres, 2004, "Schwann Cells and Astrocytes Induce Synapse Formation by Spinal Motor Neurons in Culture", *Molecular and Cellular Neuroscience*, Vol. 25, No. 2, pp. 241-251.

Vassar, R., J. Ngai, and R. Axel, 1993, "Spatial Segregation of Odorant Receptor Expression in the Mammalian Olfactory Epithelium", *Cell*, Vol. 74, No. 2, pp. 309-318.

Vosshall, L.B., and R.F. Stocker, 2007, "Molecular Architecture of Smell and Taste in Drosophila", *Annual Review of Neuroscience*, Vol. 30, pp. 505-533.

Vosshall, L.B., H. Amrein, P.S. Morozov, A. Rzhetsky, and R. Axel, 1999, "A Spatial Map of Olfactory Receptor Expression in the Drosophila Antenna", *Cell*, Vol. 96, No. 5, pp. 725-736.

Walz, W., 2002, "Chloride/Anion Channels in Glial Cell Membranes", *Glia*, Vol. 40, No. 1, pp. 1-10.

Webster, N., J.R. Jin, S. Green, M. Hollis, and P. Chambon, 1988, "The Yeast UASG is A Transcriptional Enhancer in Human HeLa Cells in the Presence of the GAL4 Trans-Activator", *Cell*, Vol. 52, No. 2, pp. 169-178.

Yao, Y., Y. Wu, C. Yin, R. Ozawa, T. Aigaki, R.R. Wouda, J.N. Noordermeer, L.G. Fradkin, and H. Hing, 2007, "Antagonistic Roles of Wnt5 and the Drl Receptor in Patterning the Drosophila Antennal Lobe", *Nature Neuroscience*, Vol. 10, pp. 1423-1432.